REPORT BY THE UNIVERSITY OF WASHINGTON

Renewable Energy Opportunities for Haleakala National Park: Kipahulu District

March 2006

Prepared for:

University National Park Energy Partnership Program
and
National Park Service

Prepared by:

Keith Boyd Fackler and Phillip C. Malte
Department of Mechanical Engineering
University of Washington
Seattle, Washington 98195-2600
Phone: 206.543.6851
Email: malte@u.washington.edu

Renewable Energy Opportunities for Haleakala National Park: Kipahulu District

Keith Boyd Fackler and Phillip C. Malte
Department of Mechanical Engineering
University of Washington
Seattle, Washington 98195-2600

Executive Summary

This report is based on the Masters of Science (Mechanical Engineering) Thesis of Mr. Fackler completed March 2006. The report covers a comprehensive study of electrical energy options for the Kipahulu district of Haleakala National Park, a remote area not connected to commercial grid electricity. Kipahulu is located on the southeastern flank of Maui, where approximately 800,000 visitors come annually to camp on the beaches, bath in the pools of Ohe'o, and hike in the numerous trails throughout the lush Hawaiian jungle.

Currently National Park facilities at Kipahulu include a Visitor Center (which doubles as a ranger station), a parking area, restrooms, a campground, and a small maintenance center. In the near future, the National Park Service has major plans to expand their current facilities at Kipahulu. These plans have been divided into two different locales: 1) facilities on the south side of Hwy 31 near the Visitor Center, and 2) facilities on the north side of the highway.

The facility changes in plan for the south site include:

- The existing Visitor Center will be moved and expanded to add more room for the ranger station.
- New restrooms will be built.
- An entry station will be built.
- A new parking area will be developed.
- The historical house of Charles Lindbergh has been moved to the area and will serve as a cultural center and provide office space for park employees.

Future plans for the north site include:

- Construction of three new 1500 sq. ft homes for park employees.
- Construction of a new maintenance center.

It is the goal of this study to develop the engineering design and economic analysis for the use of renewable power generation at Kipahulu. Solar PV with

the added possibility of small scale hydropower is about the only way that the National Park Service can obtain electricity in an environmentally acceptable manner for the new facilities planned for Kipahulu. In addition, this installation will provide an excellent opportunity to showcase solar energy in the National Parks.

Both current and projected loads at Kipahulu have been accounted and the peak power demand and daily energy consumption for the area are found to be 20.2 kW and 112 kWh, respectively. While both the north and south sites at Kipahulu could be serviced by a centralized PV generator located at the north site, it is decided to split up the generating capacity for each site in order to minimize the cost and complexity of electrical distribution. In addition, this approach provides an opportunity for the National Park Service to showcase solar energy at the south site, where most of the tourists will visit.

The projected peak power demand and daily energy consumption for each site are 7.2 kW and 47.5 kWh for the south site, and 13 kW and 64.5 kWh for the north site. Since many of the buildings have not been constructed as of yet, a detailed load profile is unavailable. The load profile has been estimated as constant throughout the year using available appliance and lighting usage information and discussing electrical requirements with park employees. All projected loads are assumed to be independent of season and are designated to involve as energy efficient appliances and lighting as possible. Once the actual loads are known, it is recommended that these loads be compared with those predicted in order to determine the extent that the electrical generator must be augmented or reduced.

Much of this study focuses on the potential for solar PV to meet the electrical needs of Kipahulu. Although Kipahulu is located on the cusp of one of the wettest rainforests in the U.S., prior installations and solar data indicate that there is significant solar potential at the site with a peak daily solar energy potential of 6.47 kWh/m^2 occurring in September, a low daily energy potential of 5.07 kWh/m^2 occurring in November, and a yearly average daily energy potential of 5.79 kWh/m^2. The incident daily solar energy is calculated assuming that the collectors are oriented due south at an optimal yearly tilt angle of 20º. The daily incident solar energy can be increased by optimizing the tilt angle throughout the year; however, it is decided that the increase in energy is minor compared to the added maintenance and equipment issues that would result from varying the tilt of such a large array.

In addition to solar energy, the potential of harnessing micro-hydro power from Palikea stream is explored for this study. Palikea stream is located directly northwest of Kipahulu and currently flows though two dams that were used for irrigation purposes in the past. Both dams are slightly weathered; however, they are both in good enough shape to accommodate the installation of a micro-hydro

intake weir. The dams are located at 1546 feet and 546 feet in elevation, and Kipahulu sits at approximately 150 feet above sea level. The upper dam has a large head potential of over 1,300 feet; however, there is an available flow rate of only 13 gpm with 92% annual reliability. Both low reliable flow and huge capital cost for long runs of penstock lead to the decision of neglecting the upper dam and focusing on the lower dam for the installation. Analysis shows that a flow rate of 200 gpm can be channeled off the lower dam with over 97% annual reliability, providing 2.4 kW of continuous power generation feeding into battery banks at the north and south sites. This is only about 10% of the peak demand; however, if the turbines are running 24 hours a day, nearly 58 kWh of electricity can be generated daily, which can supply over 50% of the daily consumption projected for Kipahulu. Utilizing this resource can reduce the size of a solar array considerably, in addition to potentially increasing system reliability by utilizing two complementary resources.

In order to have available energy at night and during extended periods of cloudy weather, it is necessary to design and apply a storage system. Batteries are not required in grid-tie systems, where excess electricity is fed into the grid during periods where production exceeds usage and electricity is drawn from the grid when production falls short of usage. For stand-alone, off-grid PV systems, or PV-hybrid systems, a battery bank is required to sustain the load during periods of low production, and it must be sized in such a way as to maintain the load for an extended period of time without being recharged. Although there are many different types of batteries, still the most common and economical method to store large amounts of electrical energy for PV applications is the lead-acid battery bank. The battery bank designed for each respective site is composed of flooded lead acid batteries and is sized to accommodate the effects of charging/discharging, temperature, and system efficiencies. A 48 volt battery bank is selected for each site with capacities of 4,625 and 3,650 amp hours for the north and south sites, respectively. The battery banks are designed to provide more than two days of autonomous electrical supply without the aid of any external renewable or propane-fired generator.

Once the load, consumption, and resource potential for Kipahulu are defined, the solar and hydro generator components are selected. Although there are many different companies that manufacture products that can harness power from these resources, the particular components and models are selected due to cost, functionality, efficiency, and reliability considerations. It should be noted that any of the particular brands and products that are referenced in the report could be replaced by a component from a different company with similar specifications, cost, and reliability.

While the solar array for the north site can be ground mounted with electrical conditioning equipment housed in the planned maintenance facility, it is recommended that the array for the south site be mounted on an awning

structure to provide a showcase for solar electricity, shady place to eat lunch and a building to protect the battery bank and power conditioning equipment. The Maintenance Department at Haleakala National Park has quoted a cost of approximately $75,000 to build such a structure. While this cost is larger than originally anticipated, it is still recommended to build the structure in order to provide the benefits notes above.

After defining electricity consumption and demand, assessing energy resource potential, and selecting appropriate equipment to harness the energy, an economic analysis is performed in order to determine the optimum system configuration for Kipahulu. The four system configurations that are analyzed are as follows:

1. Solar PV with backup propane-fired gensets.
2. Solar PV with micro-hydro and backup propane-fired gensets
3. Propane-fired gensets only
4. Grid Extension.

The battery bank and inverter size for configurations 1 and 2 are determined from the electrical demand and consumption of each site. The optimum array size for configurations 1 and 2 are determined by comparing the higher initial capital cost of a larger array with the higher maintenance and operational cost resulting from decreasing the array size and running the gensets more often. While both configurations 1 and 2 include backup gensets, the gensets are the sole electrical generator for configuration 3. For additional comparison, the cost of extending the grid five miles south from outside Hana to Kipahulu has been obtained from the Maui Electric Company. The fuel cost for genset operation for configurations 1 through 3 is assumed to be constant over the 20 year lifetime of the system and is quoted at $3.75 per gallon from the Utilities Gas Company in Kahului. The cost of electricity purchased from Maui Electric for configuration 4 is $0.27 per kWh and is also assumed constant over the life cycle of the system.

Each configuration is sized to meet the total projected electrical demand and consumption of Kipahulu. The optimum system arrangement is determined within each configuration, and the optimum arrangements from each of the configurations are compared amongst each other in regards to total capital cost, life cycle cost, annualized life cycle cost, reliability and cost of electricity.

Shown in the below table, the two renewable options have significantly lower life cycle costs than gensets only or grid extension. The renewable options also have a lower capital cost than a grid extension, assuming that the park service would incur the entire cost of extending the grid. It is no surprise that the gensets only system has by far the lowest capital cost. However, the capital cost is far overshadowed by the high fuel, maintenance, and replacement costs that would result from installing this system.

A comparison of the four respective system configurations.

Configuration	Installed Capital Cost	Life Cycle Cost	Annualized Life Cycle Cost	Cost of Electricity ($/kWh)
PV without hydro	**$284,482**	**$368,870**	**$36,342**	**$0.73**
PV with hydro	**$259,348**	**$336,660**	**$33,831**	**$0.68**
Gensets only	**$18,490**	**$576,769**	**$49,096**	**$0.99**
Grid	**$711,000**	**$844,384**	**$69,873**	**$1.71**

It is now a question of which renewable system to install: PV with hydro or PV without hydro. The PV system with hydro has the lowest capital and life cycle cost by about $30,000 in each configuration. This being said, it is only about a 10% improvement, and may not be worth the additional system complexity. There will be greater maintenance and installation needs to overcome with the hydro system; however, the hydro resource is an excellent complement to the solar, with low solar irradiation usually being compensated by high stream flow availability and vice versa. If there were no backup genset, the PV/hydro combination would certainly be a better choice than solar PV alone.

In closing, solar PV systems with and without hydro have lower life cycle costs than both gensets only and grid extension. The PV system without hydro is slightly more expensive, but it may prove to be less hassle in both maintenance and installation. Adding hydro to the system will slightly decrease both capital and life cycle costs, and will most certainly increase the availability of renewable energy; thus decreasing backup genset run time. The National Park Service is encouraged to select the system with which they feel the most comfortable. It is our recommendation that if there is sufficient available help for system maintenance, the solar PV with hydro would be the better choice; however, the PV without hydro is a lower hassle investment.

Table of Contents

List of Figures

Figure Number Page

List of Tables

Table Number Page

Acknowledgements

The author would like to express extreme gratitude to all of the people whose expertise, support, and direction helped in the accomplishment of the study. We would like to thank Dr. Jamie Winebrake and the University National Park Energy Partnership Program (UNPEPP) for the financial support of the study. Special thanks also go to Joe Dunstan and Steve Butterworth of the National Park Service Columbia Cascades Support Office. In addition, the warm hospitality and practical knowledge of Frank Baublits and everyone at Haleakala National Park is deeply appreciated. Special thanks go to Jim Fuller of Mount Ranier National Park for providing access to a practical system example at the White River Ranger Station. In addition, David Love of SunWize Technologies has been an excellent resource in practical solar engineering knowledge. Lastly, the author would like to thank my Master's committee, Professors Phil Malte, Mark Damborg, and Chris Stipe for providing knowledge and guidance vital to the completion of this report.

Introduction

More than 1500 years ago, Polynesians migrated in double hulled canoes to the lush Kipahulu valley on the southeastern flank of Maui shown in Figure 1. They brought with them agriculture and livestock and utilized the bountiful natural resources that the Kipahulu jungle has to offer.

First established as a portion of Hawaii Volcanoes National Park in 1916, Haleakala National Park was founded as a separate entity in September 1960. The Kipahulu Valley was added to Hawaii Volcanoes National Park a few years before Haleakala split off in March of 1951 with the coastal areas of Ohe'o and Puhilele added to the park in 1969 and 1998, respectively. Currently the Kipahulu area receives about 800,000 visitors per year, who come to soak in the beautiful seven pools of Ohe'o, or visit one of the many spectacular water falls in the lush Kipahulu rainforest.

In order to maintain trails, guide tourists, and manage plants and wildlife in the Kipahulu area, the current National Park service facilities at Kipahulu include a Visitor Center (which doubles as a ranger station), a parking area, restrooms, a campground, and a small maintenance center. In the near future, the National Park Service has major plans to expand their current facilities at Kipahulu. These plans have been divided into two different locales: 1) facilities on the south side of Hwy 31 near the visitor center, and 2) facilities on the north side of the highway. Throughout the remainder of this study, the two sites will be referred to as the south and north site, respectively.

The facility changes in plan for the south site include:

- The existing Visitor Center will be moved and expanded to add more room for the ranger station.

- New restrooms will be built.
- An entry station will be built.
- A new parking area will be developed.
- The historical house of Charles Lindbergh has been moved to the area and will serve as a cultural center and provide office space for park employees.

Future plans for the north site include:

- Construction of three new 1500 sq. ft homes for park employees.
- Construction of a new maintenance center.

Although a lot has changed since the first Hawaiian settlers, one aspect of life that still remains constant is the lack of grid electricity. The Maui Electric Company is the sole provider of grid electricity on the island. Shown below in Figure 1, the grid ends approximately where the maintained road ends, which is about 5 miles North of Kipahulu in Hana. Currently electrical power for the visitor center is provided by a small 800 watt pole mounted PV array. Water for the area is provided by a 1.8 kW PV-powered pumping system, located about a half mile north of Hwy 31. Both solar electric systems seem to be operating as expected, but with the addition of the before mentioned facilities and improving the existing buildings will warrant an increased electrical production.

It is the goal of this study to develop the engineering design and economic analysis for the use of renewable power generation at Kipahulu. Solar PV with the added possibility of small scale hydropower is about the only way that the National Park Service can obtain electricity in an environmentally acceptable manner for the new facilities planned for Kipahulu. In addition, this installation will provide an excellent opportunity to showcase solar energy in the National Parks.

Figure 1: A map of Maui showing the location of Kipahulu.[1]

As mentioned, this study will explore various solutions to the future electrical demand at Kipahulu. The focus of the report will be to design an off-grid solar PV generator that is potentially augmented by stream hydropower. In addition to renewable generation, the possibilities of either extending the grid or using a fossil fuel fired generator will also be briefly explored.

The outline for this report is as follows:

1. The electrical demand and consumption are assessed.
2. The available solar and hydro resources are identified and assessed.
3. Based on peak load, consumption, and solar/hydro resource potential, the vital components of each of these generators are explored and selected.
4. An economic analysis is conducted in order to determine the most cost effective combination of renewable power generation, which is compared both

with the possibility of extending the grid as well as employing the more traditional method of generating off-grid power, the fuel fired generator.

1. Site Assessment

1.1 Existing and projected electrical demand and consumption

In order to properly design a renewable power generation system, the site location, weather, topography, and most importantly the peak demand and consumption must be carefully assessed in order to properly size the system. The actual projected electrical loads have not changed much since the site assessment three years ago by Mr. Harold Post of Sandia National Laboratories.[2] The load requirements are calculated by counting existing loads as well as gathering feedback from both park rangers and the park maintenance department to determine future loads. There are two separate sites that need to be evaluated as explained above. The south site includes a visitor center/ranger station, two restrooms, an entrance station and the Charles Lindbergh house, which will be converted into a cultural center on the first floor with park offices on the second floor. A new maintenance facility as well as three National Park Service houses will be located at the north site. A detailed topographical map shown below in Figure 2 outlines the approximate locations of each site.

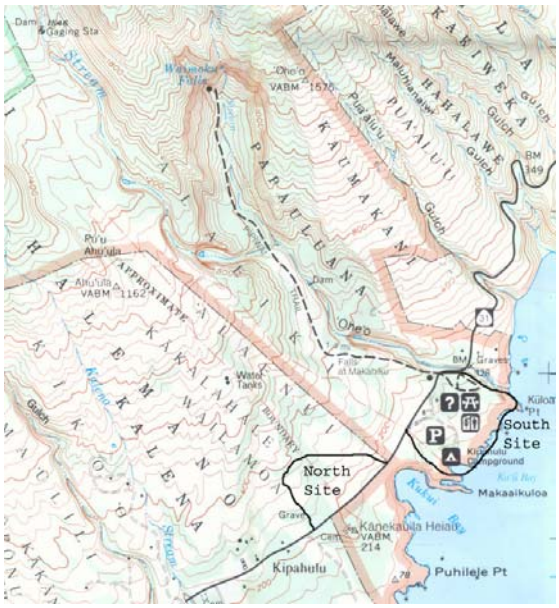

Figure 2: A Layout of the two proposed system sites.[3]

Electrical load breakdowns for each site (ie, south and north sides of the highway) are shown in Tables 1 and 2 depicting maximum power demand, daily energy consumption, and basic appliances (both existing and projected) for each building. A detailed breakdown of each individual demand is displayed in Appendix A.

Table 1: South site projected and existing peak demand and average daily consumption.

Facility	Loads	Peak Demand (kW)	Daily Energy Consumption (kWh)
Visitor Center	o **4 lights** o **4 computers** o **2 printers** o **2 ceiling fans** o **1 refrigerator** o **1 TV/ VCR** o **1 Microwave** o **Miscellaneous**	1.61	9.33
Restrooms	o **4 exhaust fans** o **8 lights**	0.36	3.12
Entrance Station	o **3 lights** o **1 computer** o **1 AC unit** o **Miscellaneous**	1.41	14.04
Lindbergh House	o **10 lights** o **3 computers** o **1 printers** o **1 copy machine** o **1 AC unit** o **2 ceiling fans** o **1 refrigerator** o **1 microwave** o **Miscellaneous**	3.785	21.06

Table 2: North projected and existing peak demand and average daily consumption.

Facility	Loads	Peak Demand (kW)	Daily Energy Consumption (kWh)
Maintenance Facility	o **12 lights** o **4 ceiling fans** o **1 microwave** o **1 refrigerator** o **1 AC well pump** o **1 table saw** o **1 computer** o **1 air compressor**	6.22	25.22
3 NPS Houses	o **30 lights** o **15 ceiling fans** o **3 microwaves** o **3 refrigerators** o **3 TV/ VCR** o **3 washers/ dryers** o **Miscellaneous**	6.83	39.27

The peak demand for the entire area comes out to be approximately 20.2 kW with a daily consumption of 112 kWh. The peak demand and consumption for the south site are 7.17 kW and 47.5 kWh, respectively. The peak demand and consumption for the north site are 13 kW and 64.5 kWh, respectively.

In addition to the two sites mentioned above, the before mentioned PV powered pumping system has been in successful operation since 1996, but there is a plan to augment the two existing 6,000 gallon water tanks with an additional 80,000 gallon tank in order to compensate the increased water use due to the future installation of flush toilets; however, this work has been commissioned elsewhere and is not of concern to this study.

1.2 Load Profile

Although the park is open 24 hours a day, the hours of operation for the buildings located in the south site are 8:00 AM to 5:00 PM; however, park rangers occasionally occupy the premises after these hours and the restrooms are open 24 hours for people to use that are staying at Kipahulu campground. For the north site, work begins at the maintenance facility around 7:00 AM and ends around 5:00 PM, and the houses will have variable power consumption throughout the day in accordance to park employees' schedules. Since the actual load profile will not be known exactly until the buildings are constructed and occupied, it is assumed for this study that most of the electrical consumption will occur during day light hours at the south site with consumption occurring both day and night at the north site. Since temperature and daylight hours do not vary significantly throughout the year in Maui and there is no real off-season for park visitors, it is also assumed that these loads are seasonally constant.

2. Solar Assessment

2.1 Solar Irradiation Data

After defining the electrical load of a system, the solar resource must be evaluated in order to select the proper number and type of modules needed for the array as well as the size of the battery bank. The National Solar Radiation Data Base[4] has 30 years of solar radiation and meteorological data spanning 1961 through 1990 for 237 sites in the U.S., Guam, and Puerto Rico. Amongst the information, they have daily statistical data and hourly data throughout the 30 years and a Typical Meteorological Year file, TMY2, which represents a typical year containing weather data that has been statistically derived from the thirty year long data set. Unfortunately, Kipahulu is not included in the database's archives; however, data for Kahului is found.

Kahului is located at the north end of the isthmus that separates the two mountainous halves of Maui (ie, east and west Maui), and Kipahulu is located on the southeastern flank of Haleakala (ie, east Maui). It doesn't initially appear logical to use this data in order to assess the Kipahulu solar resource; especially because Kipahulu is on the cusp one of the wettest rainforests in the United States. However, there is evidence that the Kahului solar data may be sufficient for this application. According to Mr. Hal Post from the Sandia National Laboratory, the PV water pumping equipment was designed using the Kahului data and appears to be operating as expected.[5] In addition, we have obtained a solar map of Maui from Maui Electric Company, shown in Figure 3 that indicates a correlation between average daily solar energy received at Kahului and Kipahulu.

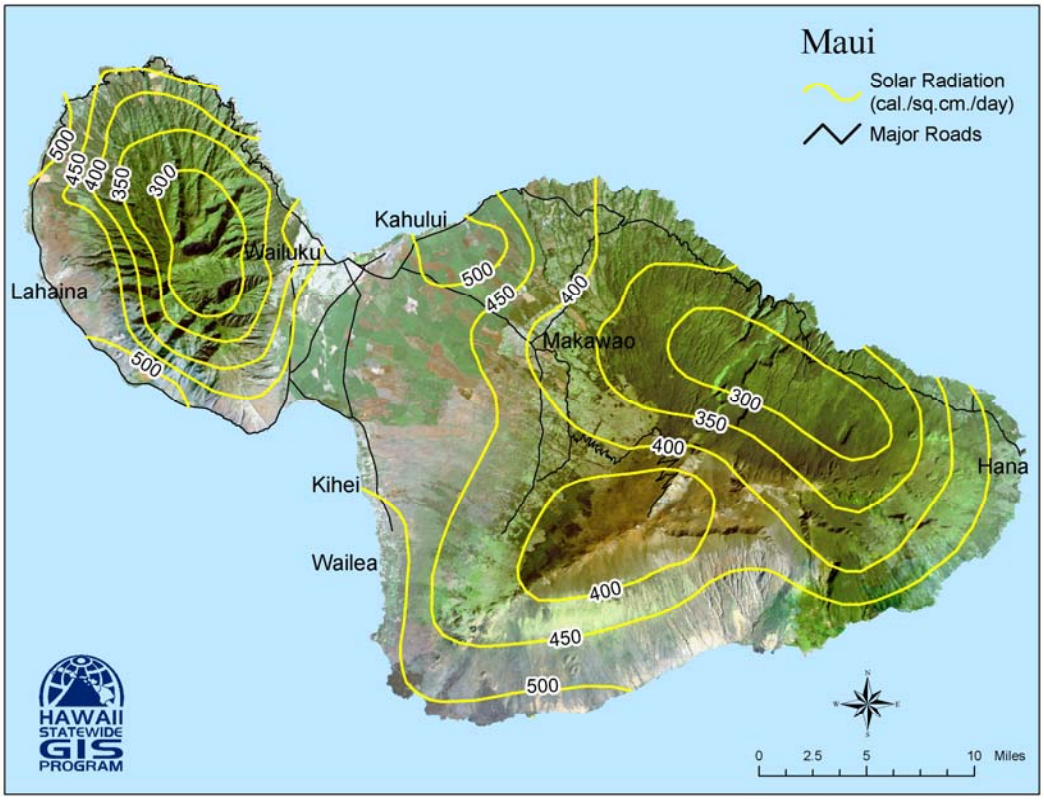

Figure 3: Solar Radiation Map of Maui.[6]

Shown in Figure 3, both Kahului and Kipahulu (about 10 miles on the coast west, southwest of Hana) appear to be located in the same region of energy incidence. The set of units that the map uses is a Langley, or a cal/cm^2-day, which is an average daily solar energy per unit area of horizontal ground. Both Kahului and Kipahulu are located in zone 450, which corresponds to a total absorbed energy of about 5.2 kWh/m^2-day, which is a more common unit. The map was prepared by the State of Hawaii in order to be a useful guide in sizing solar thermal systems. According to Herman Goldman from Maui Electric, it is quite accurate in areas where sugar cane grows; however, they warn that it may not be specific enough for other applications such as sizing PV systems.[7] Even if the map lacks resolution, both Kahului and Kipahulu fall into the same zone and the existing solar water pumps were designed with the Kahului data; thus, the TMY2 data from Kahului are used to size the PV system.

2.2 Solar Angles

In order to optimize the tilt of an array to gather the maximum amount of solar irradiation, knowledge must be gathered about the intensity of the sun and the path it takes around that site throughout the year. There are many angular relations that are important to calculating the incident radiation on a surface. Some of these angles are shown below in Figure 4.

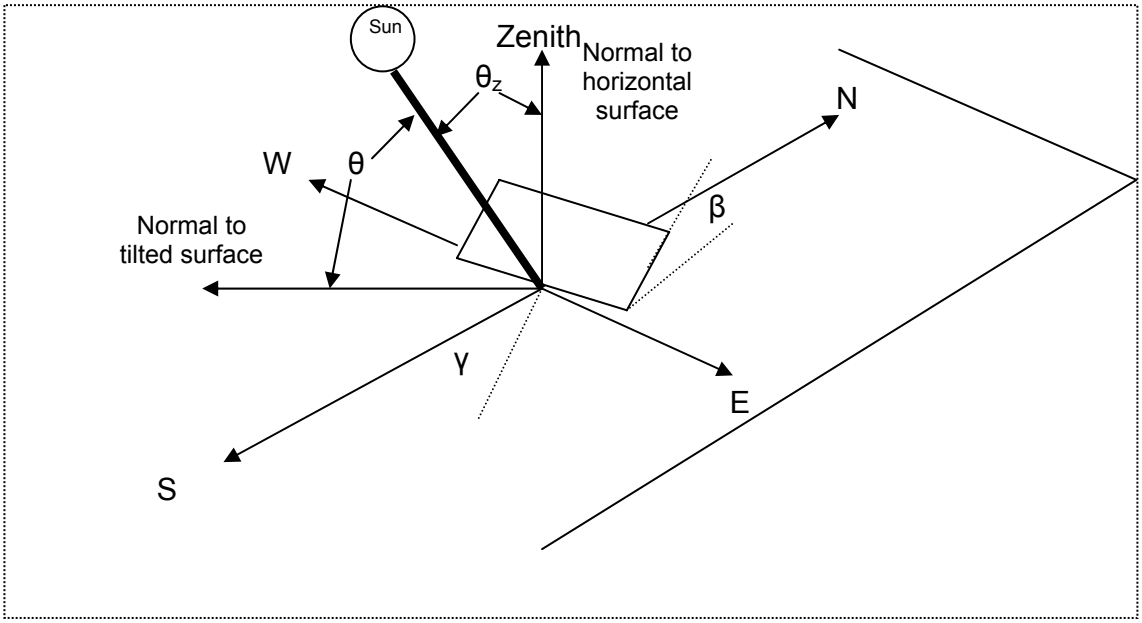

Figure 4: Solar diagram depicting γ, β, θ, and θz.[8]

The basic definitions of the important angles are as follows:

- The latitude angle is the observer's angular location on the globe north or south of the equator.
- The declination angle is the tilt of the earth's axis of rotation varying from minus 23.45º during the winter solstice and positive 23.45º during the summer solstice.
- The hour angle is the angular displacement of the sun with respect to the local meridian. The sun rotates 15º per hour; thus the hour angle is

negative in the morning, positive in the afternoon, and equal to zero at solar noon.

- The tilt angle is the angle between the collector and the horizontal plane of the surface in question as shown above in Figure 4.
- The incidence angle is the angle between the beam radiation of the sun and the normal to the tilted surface upon which the radiation is incident. .
- The surface azimuth angle is the angle between the projection of the collector on a horizontal surface and the local meridian. It is equal to zero due south, positive to the west, and negative to the east. For optimum design purposes, the collectors will be oriented due south (assuming southern sun).
- The zenith angle is the angle between a line perpendicular to the horizontal surface and the position of the sun.

Mathematical equations and more detailed definitions for each of the angles are displayed in Appendix B.

2.2 Solar Irradiation Incident on a Collector

The angular path of the sun is determined by calculating the before mentioned angles throughout the day. The total solar radiation incident on a surface is composed of three basic components, direct beam, diffuse, and reflected radiation. Direct beam radiation is the radiation received by the sun that has not been scattered by clouds or the atmosphere. Diffuse radiation is beam radiation that has been scattered by the atmosphere. Reflected radiation is total solar radiation (the sum of diffuse and beam radiation) that has been reflected back onto the tilted surface. Note that there will be no reflected component on a horizontal surface. If the sky is assumed to be isotropic, diffuse and reflected radiation are received uniformly from all directions.

Basic solar irradiation models assume that the sky is isotropic for purposes of calculating the diffuse component of irradiation. Although modeling the diffuse radiation as isotropic is approximately correct, it gives slightly lower estimations due to the fact that diffuse radiation is not completely isotropic. Instead, it is composed of three parts:

1. The isotropic part is diffuse radiation received uniformly from the entire sky.
2. Circumsolar diffuse results from forward scattering of radiation around the sun.
3. Horizon brightening refers to diffuse radiation concentrated near the horizon.[9]

Each of these diffuse components, along with a ground reflected component and direct beam component are depicted below in Figure 5. Note that the circumsolar diffuse radiation is coming from the same direction as the beam radiation.

Modeling solar irradiation with the inclusion of the non-isotropic components is referred to as the HDKR model, named after the scientists that derived it. Although the isotropic model is the simplest, the HDKR model produces results that are closer in agreement to measured values; thus it will be used to predict solar radiation incident on a tilted collector for this study.

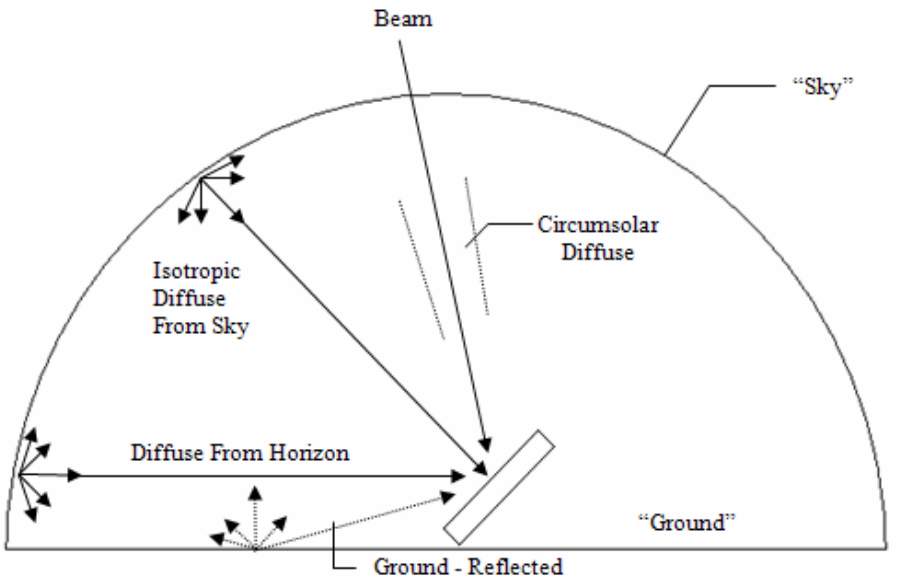

Figure 5: Beam, diffuse, and reflected solar radiation on a tilted surface.[10]

All of the mathematical equations used in the HDKR model are also included in Appendix B.

2.3 Tilt Angle Optimization

Once the latitude of the site is known and values for direct, beam, and total solar radiation are collected from the National Solar Radiation Data Base, the hourly solar irradiation on the tilted collector is calculated, and the tilt of the collector is optimized. Since the tabulated data for irradiation is given per hour, the daily, monthly and yearly solar energies are calculated by simply adding up the hourly values. The optimal tilt angle is then determined by the angle that maximizes daily, hourly, or yearly energy. Shown below in Figure 6 is the daily available solar energy in Wh/m^2-day on June 21st for a collector positioned at the yearly optimal angle, at the monthly optimal angle for June, and at the daily optimal angle for June, 21.

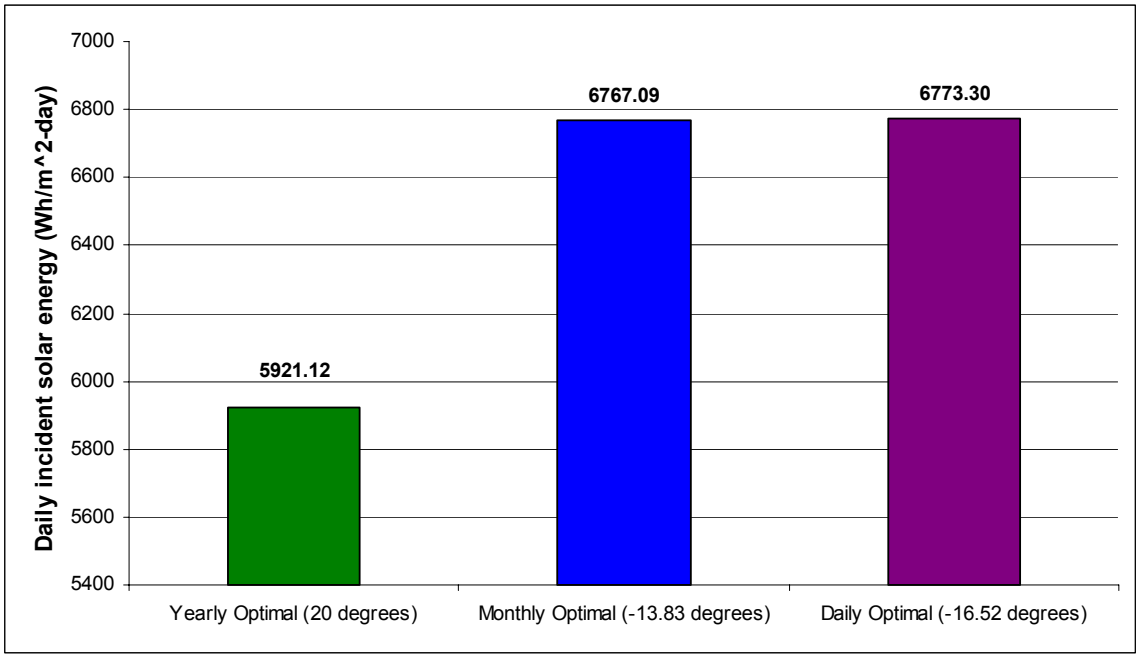

Figure 6: Incident solar energy at Kipahulu on June 21, optimized for the day, month, and year.

As shown in Figure 6, the yearly optimal tilt angle is found to be 20º, while the optimal tilt angles for the month of June, and June 21st are -13.83º and -16.52º, respectively. At first glance, it appears strange that the optimal tilt angle for June and June 21st is negative, meaning the panel is tilted towards the north. This is the case due to the fact that the sun is actually in the northern hemisphere during the summer months, and Kipahulu is located south of the Tropic of Cancer. A collector pointed towards the north will actually see more sun in the summer than a flat collector. One other point to take note of is the fact that there is a significant increase in incident energy going from a yearly tilt angle to a monthly tilt; however, there is barely any increase going from an optimal monthly tilt angle to an optimal daily tilt. This point will be explored further below.

A rule of thumb to optimize a solar array to obtain the maximum amount of solar irradiation per year is to face the modules at an azimuth of true south (in the northern hemisphere) at a tilt angle equal to the latitude where the array is located, which has been found to be the case since Kipahulu is located at latitude

of 20.66º. As shown above, the optimal tilt angle for the year will not be equal to the optimal tilt angle per season or per month. The optimal tilt will become steeper in the winter and flatter in the summer. The only issue with changing the tilt angle is that it must be changed either mechanically or manually, both of which increase installation and maintenance costs of the system. The tilt of the collectors is optimized for changes twice, four times, and twelve times per year and the results are shown in Figure 7.

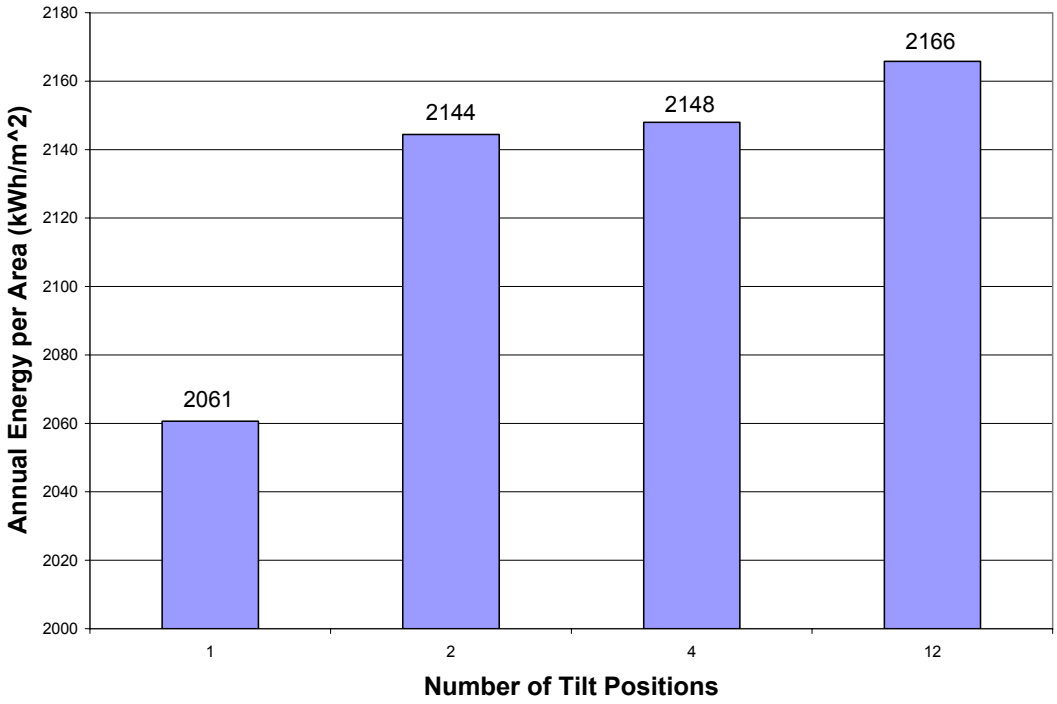

Figure 7: Annual energy with respect to the number of tilt optimization positions.

As shown in Figure 7, changing the tilt twice increases annual solar energy by about 4% or 83 kWh/m^2, changing the tilt four times increases the energy by about 4.2% or 87 kWh/m^2, and changing the tilt by month increases the collected solar energy about 5.2% or 105 kWh/m^2. It does not appear that varying the array throughout the year to increase energy collection potential by 4 to 5% will offset the added costs for maintenance and installation; thus an optimal yearly tilt of 20 degrees is used for the remainder of the design.

Once the optimal tilt angle is determined, the average daily peak sun hours can be calculated. The number of average daily peak sun hours, refers to the amount of time during a day where the sun is effectively at full intensity of 1,000 W/m^2. For example, a day could contain 8 hours of light with hourly irradiance ranging from 200 W/m^2 to 800 W/m^2. In order to calculate the number of peak sun hours, simply add up the individual daily energy to obtain Wh/m^2 and divide this number by 1,000 W/m^2 to obtain peak sun hours. The average monthly peak sun hours and yearly peak sun hours are shown below in Figure 8.

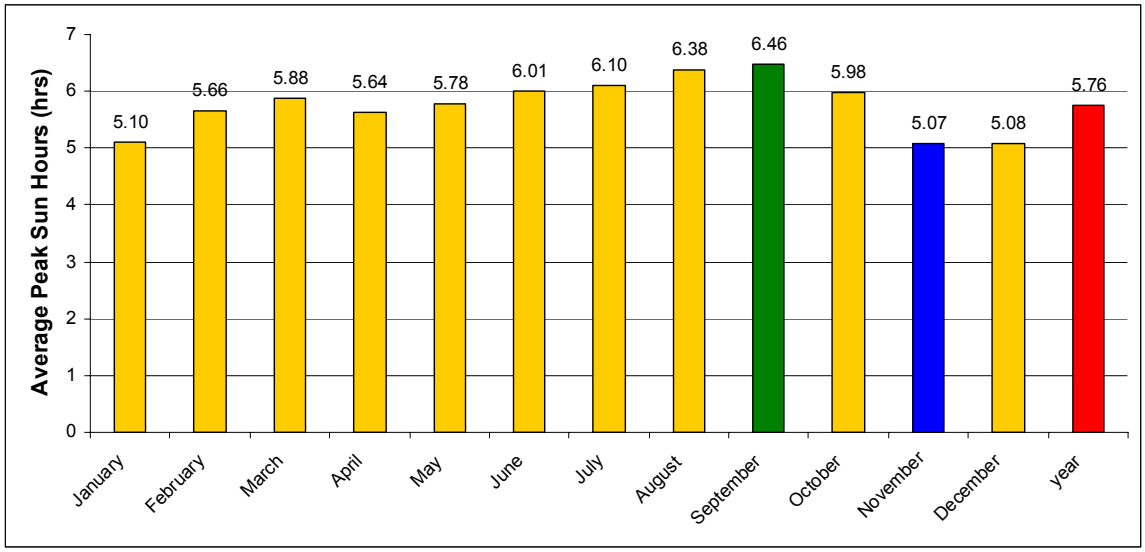

Figure 8: Average daily peak sun hours per month on a collector with an optimal yearly tilt of 20 degrees located at Kipahulu.

As shown above in Figure 8, September has the highest average peak sun hours per day of 6.46, while November has the lowest of 5.07 hours, followed closely by December and January. Over the year, the variation in daily incident sun hours is small at the optimal annual tilt angle, varying from about 5.0 to 6.5. These numbers will become important later while determining the desired system reliability and selecting an appropriate sized battery bank.

If the system is designed for the worst case scenario (supplying all required energy in November), the estimated panel area is estimated to be 78 m^2 and 106

m^2 for the south and north sites, respectively. This crude calculation is made using the daily energy consumption for each respective site found in Tables 1 and 2, assuming 12% system efficiency, and the average daily sun hours at the optimal yearly tilt for November of 5.07 sun hours per day, or 5.07 kWh/m^2-day, as shown in Equation 2.1.

$$A = \frac{E_{consumption}}{S * \eta} \qquad \textbf{Equation 2.1}$$

where,

- A is the estimated panel area
- $E_{consumption}$ is the daily energy consumption for each site in kWh/day
- S is the average daily incoming solar energy per in kWh/m^2-day
- η is the assumed system efficiency.

Obviously, if higher system efficiency is assumed, or the system was designed to provide sufficient energy generation for one of the summer months instead of November, the estimated panel area would be less. Later in this study actual daily solar radiation is calculated using hourly insolation data for each day and actual panel efficiency.

3. Hydropower Assessment

3.1 Dam Locations

There are two existing dams on Palikea stream that were used for irrigation purposes nearly half a century ago shown in Figures 9 and 10.

Figure 9: The upper dam located at 1546 feet above sea level.

As shown above in Figure 9, the upper dam is weathered, as is the irrigation penstock shown in the left corner of the photograph. A medium to large scale hydroelectric project would probably warrant the construction of a new dam; however, due to the small scale of flow that we are dealing with, a new dam would hardly be worth the effort or cost.

Figure 10: The lower dam located at 483 feet above sea level.

The lower dam shown in Figure 10 is in slightly better shape than that of the upper dam. It is far closer to road access, and may prove to be easier and cheaper for installing a micro-hydroelectric system. The only drawback for the lower dam is that it is situated quite close to a popular hiking trail.

It would probably be both expensive and environmentally intrusive to construct new dams for hydroelectric purposes in the national park. Since these dams are already in existence and are located outside of the park boundaries, it is recommended to consider these dam locations for the purposes of this study.

Shown below in Figure 11 are the locations of the two dams on Palikea Stream: the lower dam, located at 483 feet above sea level and the upper dam, located at 1546 feet in elevation.

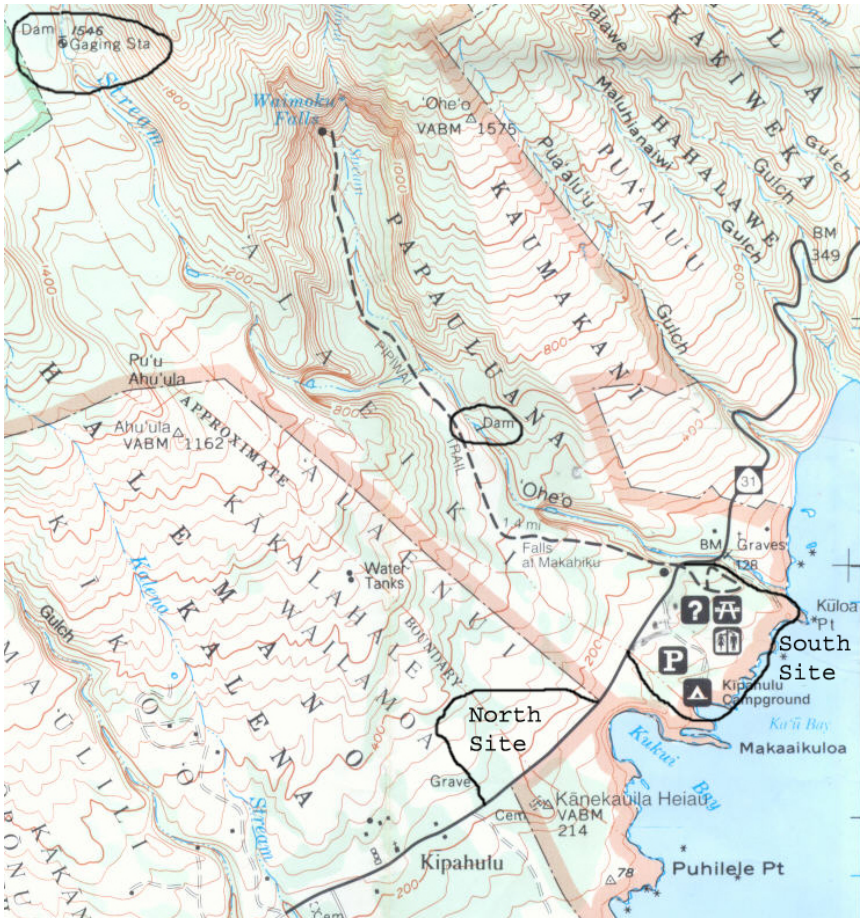

Figure 11: The locations of two the two dams on Palikea stream.

The lower dam is relatively low in elevation and is situated about 20 feet north of a popular hiking trail to Waimoku Falls; in contrast, the upper dam currently can be accessed via a 3 mile jeep trail, then about a mile hike. The distance and lack of road could be problematic; however, it has about 1,000 feet more head than the lower dam, so it should not be counted out yet.

The USGS compiled daily stream flow data between 3/1/1927 and 8/18/1983 for a gauging station located below the upper dam, and additionally has about 16 years of data between 1/7/1988 and 3/9/2004 for the lower dam. Energy potentials for both the upper and lower dams are analyzed below.

3.2 Hydropower Potential

In order to properly size a turbine or even determine if there exists enough energy to install a micro-hydro system, the hydropower potential must be evaluated. This power potential, P_{kW}, is a function of stream flow rate and the head, as shown in Equation 3.1.

$$P_{kW} = \frac{Q\gamma H\eta * 0.746}{550}$$ **Equation: 3.1**[11]

where,

- P_{kW} is power output, kW
- Q is flow rate, ft^3/s
- γ is the specific weight of water, 62.37 lb/ft^3 @ 60ºF
- H is available head, ft – the net head after frictional losses have been subtracted
- η is plant efficiency in decimal form
- 550 is the conversion factor, number of ft-lb/s in 1 hp
- 0.746 is the conversion factor, number of kW in 1 hp

Although efficiencies of 80 to 90% are common in large turbines, efficiencies of 40 to 60% are common to the micro-hydro world. Since the dams have already been constructed, the head for each site is set; thus, the limiting factor will be flow rate. (A common way to estimate micro-hydro power potential is to multiply flow rate in gpm by head in feet, dividing by 10 gives power in watts, which assumes 53% efficiency.[12] GPS measurements indicate that the north and south sites are located at approximately 248 feet and 137 feet above sea level with head potentials of 1,298 and 346 feet, respectively.

It is highly unlikely that the entire 1,298 feet of head can be used for a micro-hydro installation for the north site. First off, the 1,298 feet of head is run over 4 miles. The friction loss alone would warrant the need to install a penstock with an extremely large diameter. In addition, Schedule 80 PVC pipe has a maximum

rated pressure of 160 psi. Assuming that the static fluid pressure will be the highest pressure in the system, the static head limit to pipe that is rated at 160 psi is approximately 369 feet as shown below in Equation 3.2.

$$AllowableHead = \frac{160lbs}{in^2} * \frac{144in^2}{ft^2} * \frac{ft^3}{62.4lbs} = 369.2\,feet \qquad \textbf{Equation: 3.2}$$

Long runs of steel penstock can be extremely expensive, as shown later in Chapter 7; thus, for energy potential analysis, gross heads of 369 and 346 feet are used for the north and south sites, respectively.

3.3 Stream Flow Analysis

3.3.1 Upper dam

The USGS hydrologic data for the upper dam is highly variable ranging from zero flow to a maximum flow rate of about 3500 cfs. As shown in Figure 12, the average daily flow per year is also highly variable with obvious trends between dry and wet years; however, the mean daily flow rate remains about 58 cfs with a relatively low standard deviation of about 19 cfs. A flow rate of 39 cfs is more than adequate to run a micro-turbine; however there are many days where this flow rate is not met as discussed below.

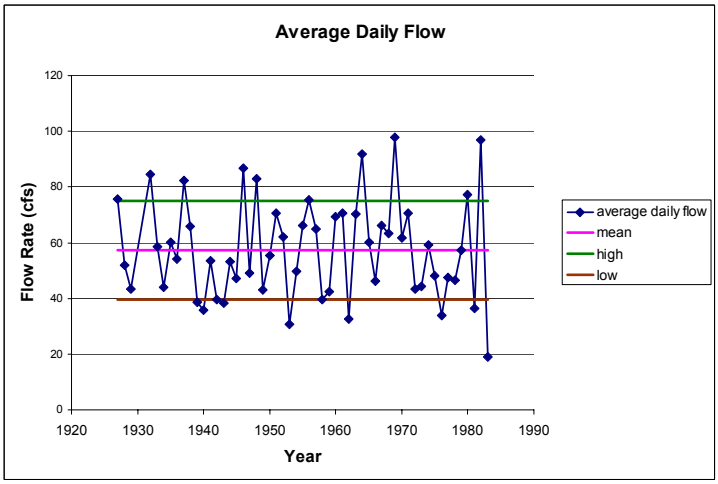

Figure 12: Mean and standard deviation annual flow rates for the upper dam.

By normalizing both average stream flow rate and daily solar energy by their respective maximum values, one can see how the energy potential for each of these resources compares with one another throughout the seasons. Coupling the above USGS hydrologic data with NRSDB solar irradiation data falling on a horizontal collector from Kahului, it is shown in Figure 13 that stream flow peaks in the winter and the daily solar energy peaks in the summer. This result is not surprising, which points to the possibility of a hydro system picking up the slack of the PV system during the winter, and vice versa in the summer.

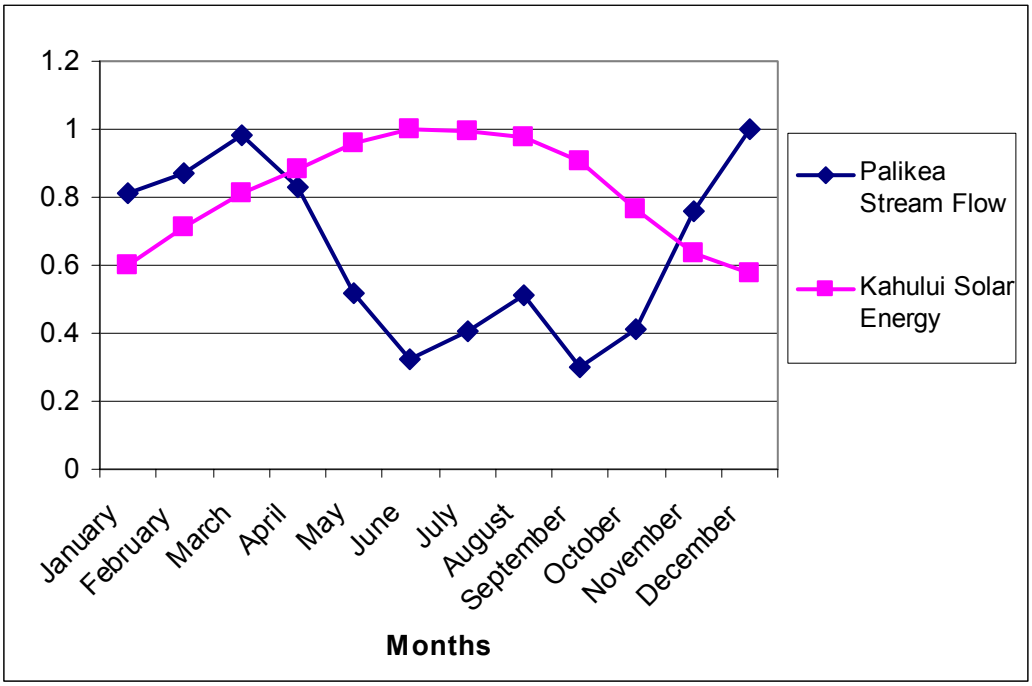

Figure 13: Normalized average daily stream flow vs. average daily solar energy per month.

What this graph fails to show is the number of days that have little or no flow, which could prove to be critical to the reliability of any size system. These low flow days have been determined on average per month and are shown Figure 14.

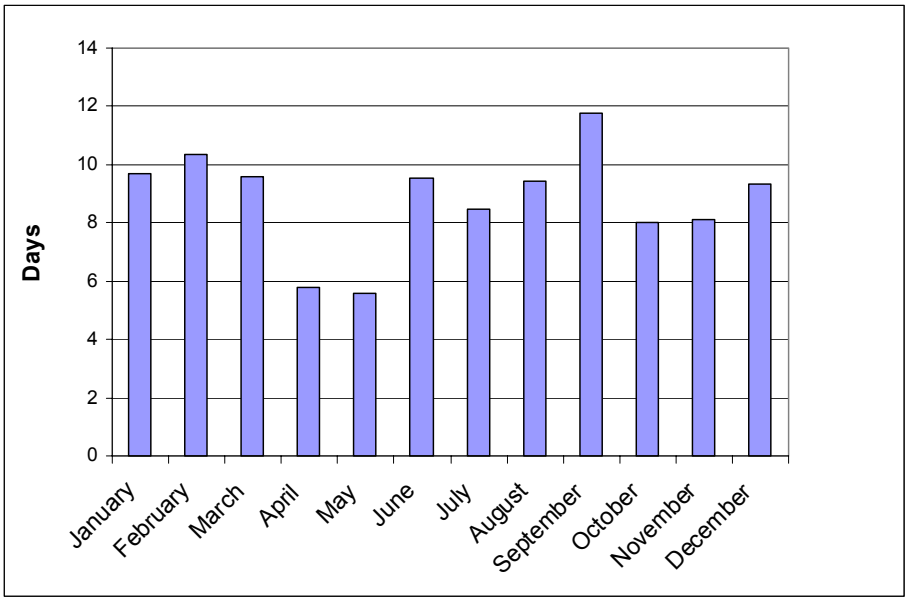

Figure 14: Average Number of low flow days per month.

These results appear troubling, especially since there are 7 months out of the year when there is an average of more than 9 low flow days. Due to the fact that it is very difficult to gain useful information to size a hydro system on mean flow, especially for a site with such a high variability in flow regime, a flow duration curve has been developed to evaluate the availability of stream flow with respect to all of the other flow data that has been collected.

As discussed above, in order to incorporate micro-hydro into this site, significant issues must be addressed to account for the large fluctuations in daily flow. Since there are many days that have little to no flow on the cfs (cubic feet per second) scale, it has been decided to focus the study on a small class of turbines, which operate with flow rates on a gpm (gallon per minute) scale. Shown below in Figure 15 is a monthly flow duration curve generated from the approximate 56 years of flow data taken at Palikea stream by the USGS. A flow duration curve, FDC, is a plot of flow versus the percent of time the flow can be expected to be exceeded. References to flow duration curves are usually made as Q_{20}, Q_{50}, Q_{95} etc. corresponding to flow values at an indicated percentage point.[13] Typically, systems that have an automatic flow control valve should be

designed around Q_{50}; however, installing automatic flow control is quite expensive and is often times an unavailable accessory in a small scale turbine. In order to minimize the cost involved in adding automatic flow control, or the maintenance required to open and close valves by hand, it is decided to operate at a FDC point of Q_{90}, which corresponds to flow rates between 10 and 80 gpm for every month.

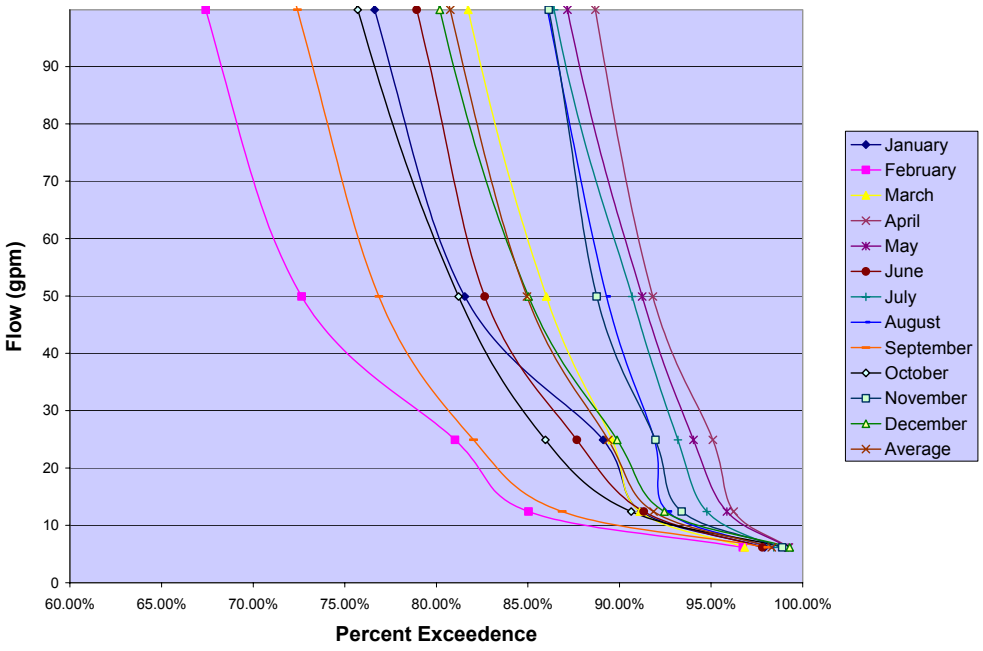

Figure 15: A monthly flow duration curve for the upper dam.[14]

There is a possibility that valves can be open and closed dependent on the month. For example, as shown in Figure 15, the FDC for April shows that it can sustain a flow rate of about 80 gpm with 90% reliability, while February and September can only sustain a flow rate of about 10 gpm with 90% reliability. While designing the system to operate at an elevated flow rate could allow for almost an 800% increase in power potential for April and significant increases in power potential for the other months of the year, varying the flow through the use of control valves will still require a certain level of human maintenance to ensure everything is operating properly. Although there are many shapes and sizes of micro-hydro turbines, there are very few that will tolerate such a small flow rate.

Although there is a high probability that solar resource will pick up the slack during periods of low flow, it is still necessary to manually open and close flow control valves on the turbine. Thus, it is decided to design the system around the worst case, which means operating at a flow rate corresponding to Q_{90}, or 10 gpm. Employing Equation 3.1, using a plant efficiency of 53%, and a maximum head of 369 feet, the micro-hydro power potential is approximately 368 watts, which is not a significant amount of power for this site. If a steel pipe is utilized, which can operate at much higher pressures, it would be possible to utilize the entire head of 1298 feet giving a power potential of 1.29 kW, which is better but still not large for meeting the site electricity demand. This being said, it is decided to focus the hydroelectric design around the lower dam, which has significantly higher flow potential as discussed below.

3.3.2 Lower dam

The USGS has compiled about ten years of flow data from the lower dam. Shown below in Figure 16 is a flow duration curve generated from this data. Due to the fact that there is not as much head to utilize from the lower dam, it is important that there are relatively large flow rates with high reliability. Every month except May has a flow rate above 100 gpm with 95% reliability and for every month discharges of 200 gpm can be achieved with 90% reliability, both of which are more than adequate flow rates for most micro-hydro turbines on the market.

With a flow rate of 200 gpm, a plant efficiency of 53%, and 346 feet of head, Equation 3.1 gives a power potential of approximately 6.9 kW. This is a significant amount of power, and can provide nearly 165 kWh of energy per day to both sites, which could potentially eliminate the need for any solar array. As implied above, it may not be economically feasible to utilize the upper dam to

power the north site; however, power from the lower dam could easily be transported to both sites and effectively utilized. Component selection followed by an economic analysis is given in Chapters 7 and 8 in order to fully explore the prospect of exploiting this resource.

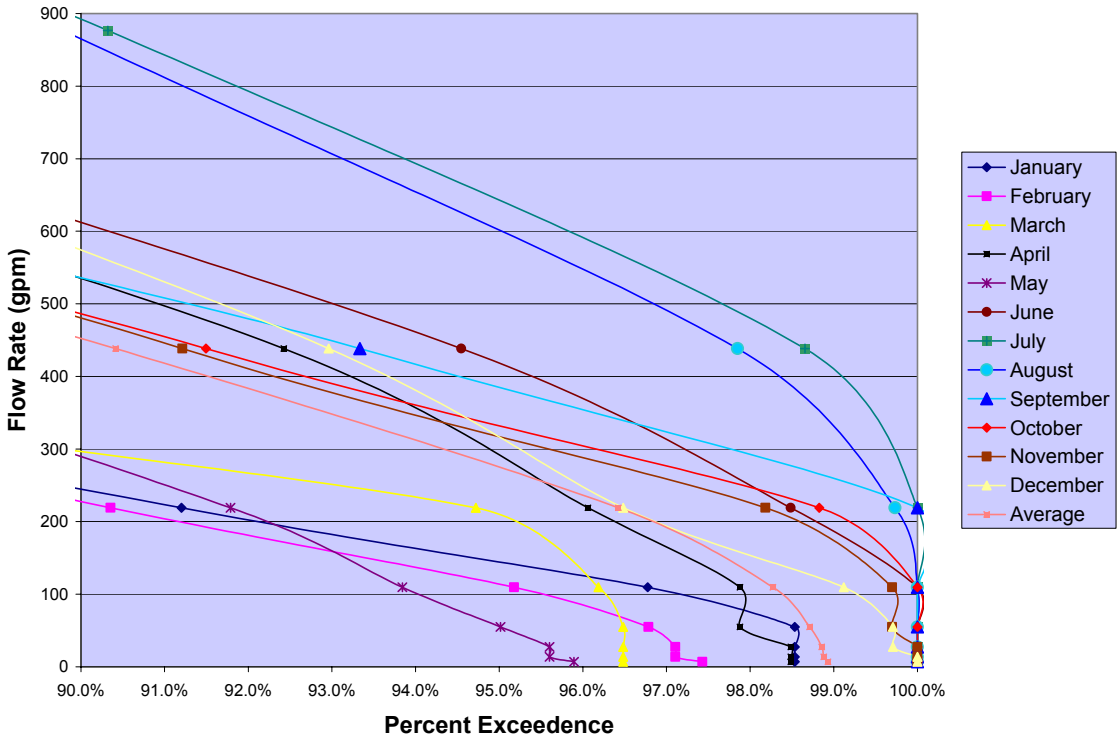

Figure 16: A monthly flow duration curve for the lower dam.[15]

It should be noted that the curves in Figure 16 appear to have different slopes than those in Figure 15; however, this is actually not the case as we are looking at a much narrower domain from 90 to 100% exceedence in Figure 16, whereas the domain in Figure 15 goes from 60 to 100% exceedence.

4. Energy Storage

4.1 Introduction

In order to have available energy at night and during extended periods of cloudy weather, it is necessary to design and apply a storage system. Batteries are not required in grid-tie systems, where excess electricity is fed into the grid during periods where production exceeds usage and electricity is drawn from the grid when production falls short of usage. For stand-alone, off-grid PV systems, or PV-hybrid systems, a battery bank is required to sustain the load during periods of low production, and it must be sized in such a way as to maintain a load for an extended period of time without being recharged. Although there are many different types of batteries as well as alternative storage techniques such as making hydrogen for use in a fuel cell or pumping water up hill to be run through a turbine later, still the most common and economical method to store large amounts of electrical energy for PV applications is the lead-acid battery bank.[16] The basic chemistry behind the lead acid battery is detailed in Appendix C.

4.2 Charging and Discharging Considerations

There are many different types of lead-acid batteries. Depending on the application, these batteries may be optimized for shallow or deep discharge. The battery capacity is defined as the number of amp-hours that can be removed from a battery at a specified discharge rate.

It is common to refer to a battery's depth of discharge, DOD, or state of charge, SOC, when speaking of charging and discharging. The depth of discharge of a battery is simply the percentage of amp-hours that are removed during discharge in relation to the total capacity of the battery, and a batteries' state of charge is

the percentage of amp-hours that are left in a battery in comparison to its total capacity; thus DOD + SOC will equal unity.[17] Shallow cycle, starting, lighting, and ignition, SLI, batteries are primarily used to start automobile engines. These batteries are designed to supply a large current for a brief time period in order to start an engine; however, they have a very poor cycle life if the batteries are discharged to more than 75% DOD, having only 20 or so deep discharge cycles before the battery is damaged.[18] Lead-acid batteries that are optimized for PV applications are deep discharge and can be cycled down to 80% DOD, or 20% SOC, although they often last longer if they are not cycled down so far.

The rate at which lead acid batteries are discharged is important to consider. Charging and discharging rates are typically referred to as C/x, where C is the capacity of the battery in amp hours, and x is time in hours. For example, if a battery with 100 amp-hours of capacity is discharged by a 10 amp load; then the battery will be completely discharged in 10 hours at a rate of C/10. It is well documented that the battery becomes discharged more quickly at a high discharge rate due to the fact that acid circulation into the pores of the plates and water dispersion out of theses pores is too slow to sustain the reaction; consequently, only the outermost layer of the plate surface is available to take place in this reaction and a large percentage of the active material and electrolyte are left unutilized.[19] The affect discharge rate has on total capacity is depicted below in Figure 17. Note that far less capacity is available at high discharge rates.

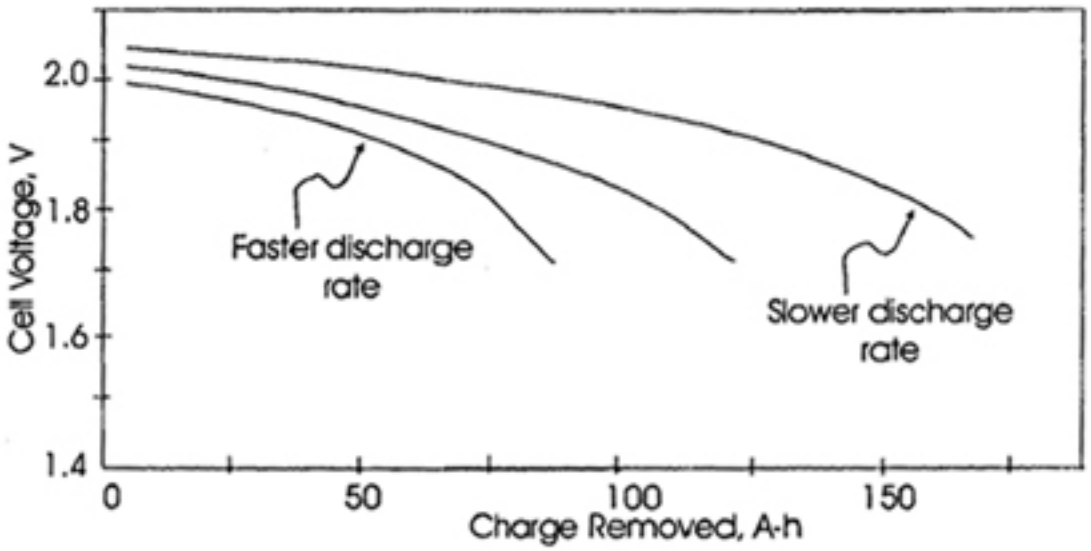

Figure 17: The effect of discharge rate on available energy from the lead-acid battery.[20]

The other main discharging consideration is that the battery should never be discharged to 100% DOD, due to the fact that lead sulfate can build up on the electrodes to a point where the effective surface area of the electrodes is diminished, leading to a reduced capacity.[21]. In addition, plate buckling can occur due to the accumulation of more lead sulfate on the electrodes; thus, occupying more space than that of the original active material.[22]

In addition to discharging considerations, the rate at which batteries are charged should also be considered. Shown below in Figure 18 is the effect that charging rate has on the voltage and state of charge profile of a typical lead acid battery. Note that the recommended end of charge voltage and end of discharge voltage are 1.7 and 2.65 volts per cell, respectively. Also note that in region A, efficient charging occurs, in region B end of charge is approaching and gassing begins, and in region C excessive gassing takes place.[23] The battery should never be allowed to be operate in region C due to the fact that there is extreme electrolyte loss and damage to active material on the plates; however, an equalization charge (region B) should be performed occasionally to stir up electrolyte and

prevent sulfation, which refers to a circumstance where large sulfate crystals grow in place of small crystals typically present during discharge. These larger crystals are formed when a partially charged battery remains dormant for any length of time, or it remains at a partial state of charge for a number of days without an equalization charge.[24]

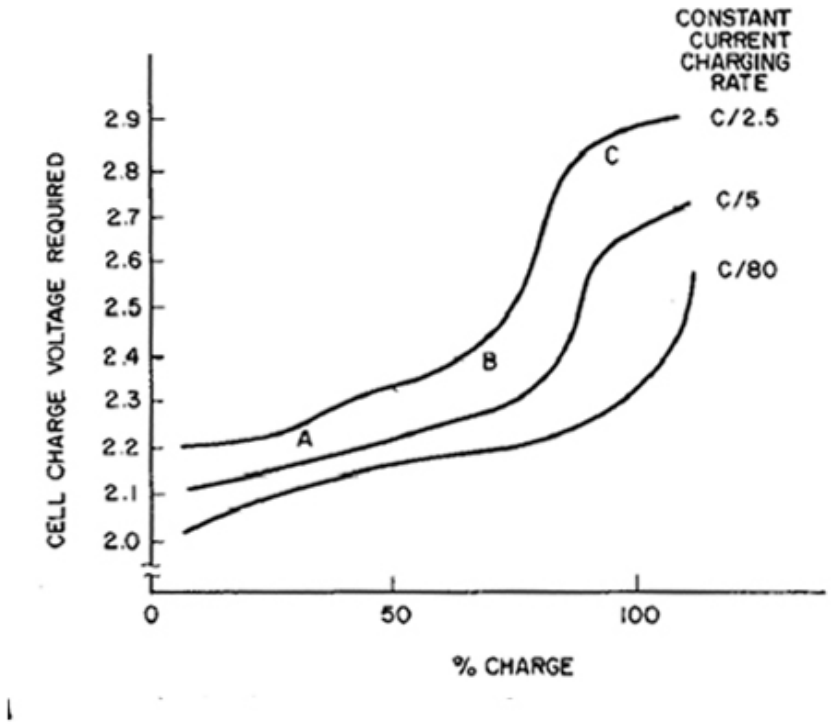

Figure 18: Charge voltage characteristic of the lead-acid battery.[25]

Charging efficiency can be defined as the amount of charge gained in a battery divided by the energy put into charging it. Essentially, charging efficiency is proportional to the slope of the curve in Figure 18; a relatively shallow slope indicates that a large voltage increase is not necessary to raise the SOC of the battery; however, a steep slope corresponds to a large voltage increase with respect to battery SOC. Also shown in Figure 18, battery charging efficiency is relatively high during a low state of charge; however, as the battery state of charge moves closer to 100%, this efficiency drops off quickly with nominal battery charging efficiencies ranging at low states of charge of around 85% to close to 50% at a high state of charge.[26] Although battery banks in PV systems

are usually designed for a maximum DOD of 50%, they often operate near 20 to 30% DOD.[27]

By increasing the size of the battery bank one can achieve a system with a higher availability; however, this also causes the battery bank to operate closer to full charge. This being said, when charging the batteries closer to full SOC, more energy must be put into the battery to achieve the same charging rates as experienced during low SOC. As explained above, if the battery is allowed to lay dormant for a couple of days, or at a partial state of charge, battery capacity decreases each cycle due to electrolyte stratification and sulfation. This degradation will continue until the battery has been equalized; however, if the charging source is too small, C/40 or less, the battery may not be able to achieve an equalizing charge, and the battery will continue to degrade due to reasons explained above.[28]

In order to prevent the loss of capacity and promote battery longevity, it is important to design a battery bank that is large enough to provide a reasonably high reliability and a charging source that can at least supply a high enough charging current to equalize the batteries every so often, which should be able to charge at charging rates between C/20 and C/10.[29] These considerations will be taken into effect in Chapters 5 and 6 where the array and genset are selected.

4.3 System Availability and Battery Bank Size

When designing the size of a battery bank, the required system availability should be taken into consideration. Critical loads such as microwave repeaters and medical refrigerators may need to have 99% availability, while non critical loads such as residences and office buildings can get by with 95% availability. Obviously as required system availability increases, so does required battery storage and overall system cost, with system cost sharply increasing as system

availability approaches 100% as shown below in Figure 19. Note that the solar resource of the site is also a factor with high system availability being more expensive to achieve in Burlington, Vermont, which has a low solar resource in comparison to Albuquerque, New Mexico.

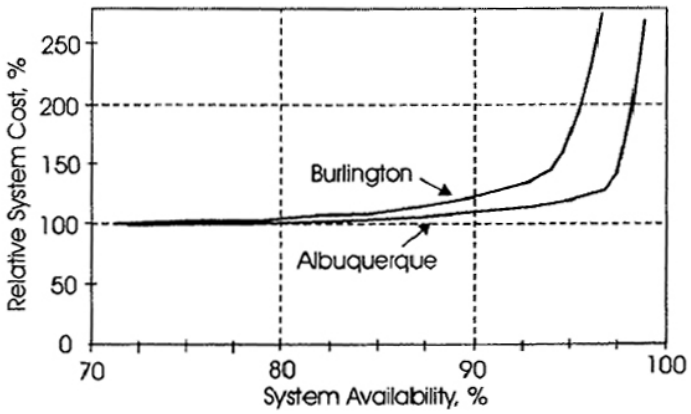

Figure 19: System Cost vs. Availability for two sites with different solar resources.[30]

As shown above in Figure 19, solar resource plays an important role when determining availability. Sandia National Laboratories has developed correlations to determine the required days of autonomy, or battery storage capacity, to achieve 99 and 95% availability as shown below in Equations 4.1 and 4.2.

$$D_{crit} = -1.9 * T_{\min} + 18.3$$ **Equation 4.1[31]**

$$D_{non} = -0.48 * T_{\min} + 4.58$$ **Equation 4.2[32]**

where,

- D_{crit} is number of storage days required for critical availability.
- D_{non} is number of storage days required for non-critical availability.
- T_{min} is the minimum average peak sun hours over the year as determined in Chapter 2.

Since this system is not a critical application, it is decided to use Equation 4.2 to determine the required days of autonomy. With the minimum number of peak sun hours of 5.07 at the yearly optimal tilt occurring in November, the battery

bank should be able to deliver 2.15 days of autonomous electricity to achieve 95% system reliability.

4.4 Other Sizing Considerations

In addition to required days of autonomy and amp-hour usage per day, other factors must also be taken into account such as wire losses, inverter efficiency, battery charging/discharging efficiency, battery temperature, maximum depth of discharge, and maximum charging/discharging rate.

Since all of the DC energy produced in a day must first be converted to AC, the required daily usage must be divided by the inverter efficiency. In all electrical distribution systems, there will be some voltage drop and a corresponding power loss. The National Electrical Code requires that voltage drop be less than 5%, with well designed systems having voltage drops in the area of about 2%. Assuming that the load current remains nearly constant, the power losses will also correspond to 2%; thus the daily energy requirement must also be divided by 0.98.[33] In addition to wire and inverter losses, charging and discharging a battery bank is not 100% efficient as detailed above. If the battery bank is not charged or discharged at a higher rate than it is rated for; then a charging/discharging efficiency of 90% can be assumed and the maximum daily usage should also be divided by a factor of 0.9.[34] Taking into account inverter efficiency, wire loss, and battery charging/discharging inefficiencies, the corrected daily loads are obtained by Equations 4.3 and 4.4 for the north and south sites, respectively.

$$CorrectedAmpHoursNorth = \frac{64.5 * 1000}{48 * 0.93 * 0.98 * 0.90} = 1638 \qquad \textbf{Equation 4.3}$$

$$CorrectedAmpHoursSouth = \frac{47.5*1000}{48*0.93*0.98*0.90} = 1206$$ **Equation 4.4**

Note that respective daily energy consumption in kWh calculated in Chapter 1 has been changed to amp-hours by dividing by the battery voltage and multiplying by 1000 watts per kW. Also inverter efficiency is assumed to be 93%, which is the efficiency of the selected inverter, explained in Chapter 6.

Due to slower chemical reactions at lower temperatures, the capacity of the lead acid battery decreases about 1% per 1 ºC drop in temperature.[35] As shown below in Figure 20, a 100% capacity is seen around temperatures of 25 ºC, and capacity can go to virtually zero at -40 ºC.

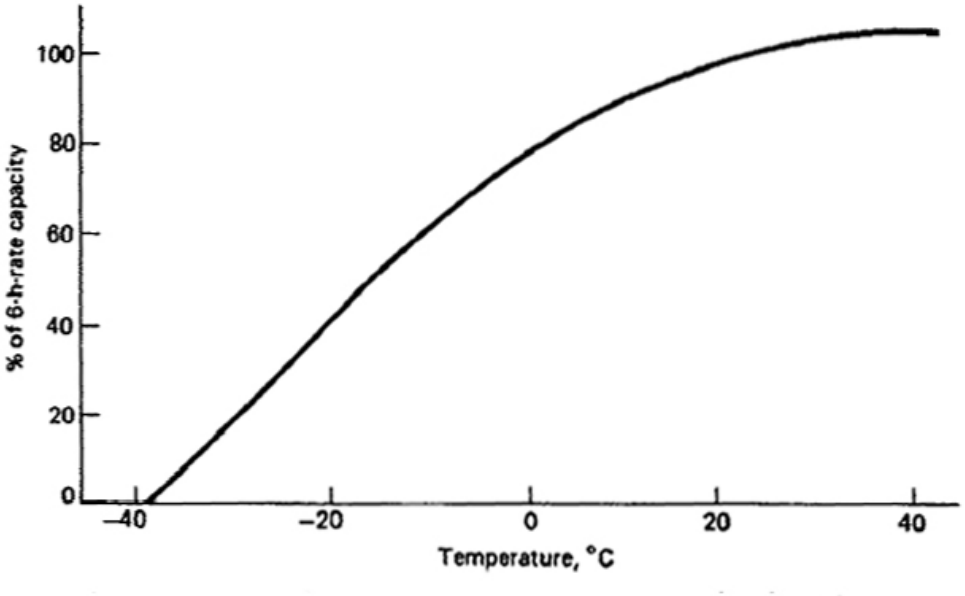

Figure 20: The effect of temperature on capacity of a lead-acid battery.[36]

The capacity of the battery will obviously be decreased by cold temperatures. A temperature compensation correlation has been developed and is given below in Equation 4.5.

$$D_T = 0.00575 * T + 0.54$$ **Equation 4.5**[37]

where,

- D_T is the temperature duration factor in decimal form
- T is temperature in degrees F

The average ambient temperature for Kipahulu is 75.2 ºF; thus D_T is evaluated as 0.97.

In addition to temperature compensation a battery bank must be further increased if there is a maximum charging or discharging current that is larger than the maximum current a battery is rated for and lasts 10 minutes or longer, as given by Equation 4.6.

$$D_{ch} = \frac{I_{rated}}{I_{\max}}$$ **Equation 4.6**[38]

where,

- D_{ch} is the charge/discharge derating factor
- I_{rated} is the maximum current the battery is rated at
- I_{max} is the maximum expected load, or charging current that will be present for 10 minutes, or longer.

There are no load currents in this application that will draw a huge amount of current for any duration of time, and all of the charging sources will be properly sized; thus D_{ch} is set to unity.

As mentioned above, the maximum allowable depth of discharge for a deep cycle lead-acid acid battery is 80%. Using the corrected energy consumption from Equations 4.3 and 4.4, the charging/discharging and temperature compensation factors, and an 80% depth of discharge, the required capacity of the battery bank is determined by Equation 4.7.

$$BatteryCapacity = \left(\frac{Ah}{day}\right) * \left(\frac{D_{non}}{D_T D_{ch} DOD}\right)$$ **Equation 4.7**[39]

where,

- $BatteryCapacity$ is the required battery capacity in amp-hours
- $\left(\frac{Ah}{day}\right)$ is the corrected daily energy consumption in amp-hours
- D_{non} is the number of storage days for 95% system availability
- D_T is the temperature compensation factor
- D_{ch} is the excessive charging/discharging duration factor
- DOD is depth of discharge

When Equation 4.7 is applied to each respective site, the required battery capacities come out to be 4,538 amp-hours and 3,341 amp-hours for the north and south sites, respectively. The actual battery bank will be selected in Chapter 5.

5. Solar Component Selection

5.1 Introduction

There are two basic types of solar photovoltaic systems: stand-alone and grid-tied. The major difference is that stand-alone power systems are not connected to the grid; thus, a battery bank and charge controllers are necessary. A grid-tied system has the solar array directly tied to the grid through an inverter, which sends electricity to the grid when production exceeds demand and pulls electricity from the grid when demand exceeds production. A grid tied system is more cost effective, since no storage or charge control is needed, coupled with the fact that in many states there is net metering, where the local utility buys electricity back from the system when it produces more than the household consumes. Unfortunately, the grid needs to be present at the site in order to tie to it, which is extremely expensive for sites that are located a significant distance from the grid. Since the buildings at Kipahulu are not currently connected to the grid, a stand-alone system will be designed for each site, south and north of the highway. Later in Chapter 8, the life cycle cost of extending the grid to Kipahulu is compared to that of a stand-alone PV system.

The basic components of a stand-alone solar photovoltaic system are shown in Figure 21. Note that a stand-alone PV system could power only DC loads, this would cut out the need for an inverter. A DC system would reduce cost; however, DC powered devices are few and far between and nearly all of the existing and projected building loads will be AC powered. Thus, an inverter will be included in the system design.

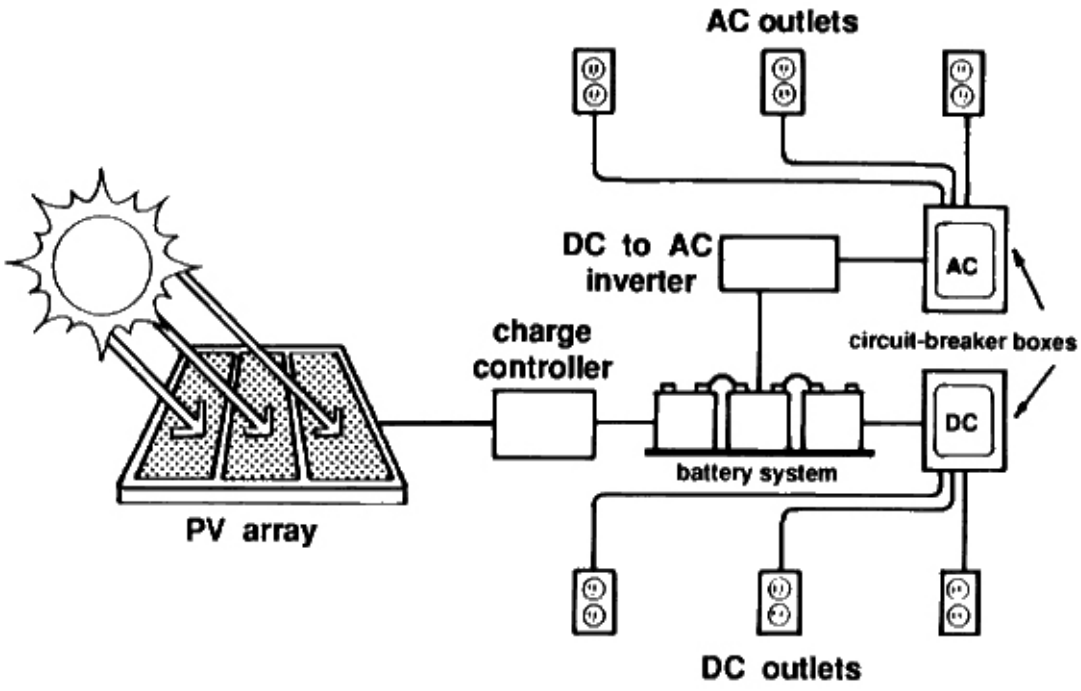

Figure 21: A diagram of the basic components of a stand-alone PV system.[40]

As shown above in Figure 21, the basic components for a stand-alone PV system are the array of solar modules, the charge controller, the battery bank, the inverter, conducting cable, and over-current protection. Not shown in the above figure are array racks, ground fault protection, back up generator, and other electrical components that will be covered later in Chapter 6.

5.2 Modules

The essential component of a stand-alone photovoltaic system is the solar module, which is also known as the PV panel, and is defined as a number of PV cells connected in series and parallel. Each PV cell has a voltage and current corresponding to its design and incident sunlight. A module made up of PV cells will have a voltage equal to the number of cells wired in series, and a current equal to the number of series strings wired in parallel. Although understanding the specific electronics behind the solar cell is not the goal of this report, a brief

explanation is given below to grasp the basics. The interested reader is encouraged to explore the electrical physics by themselves.

The equivalent circuit for a cell, module, or array is shown in Figure 22, where the current-voltage relationships are given by Equations 5.1 through 5.3.

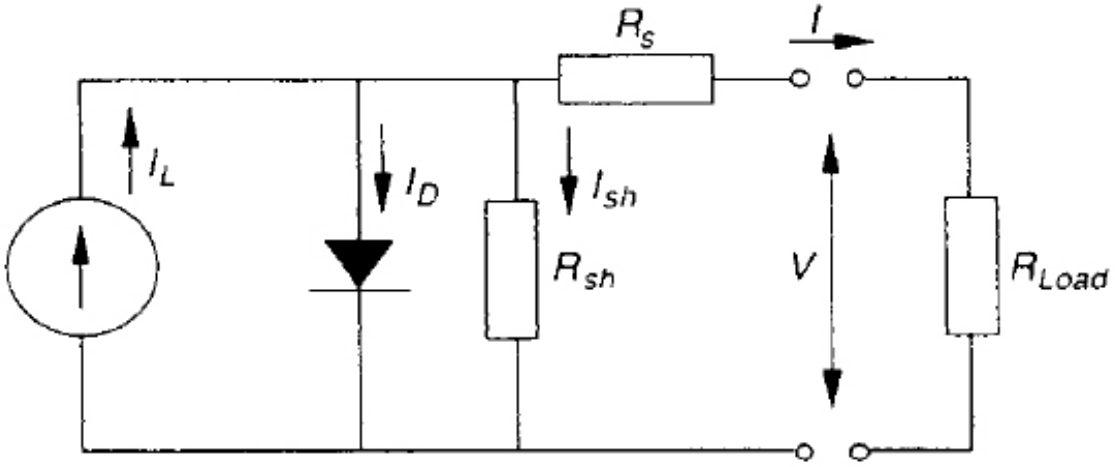

Figure 22: The equivalent circuit of a PV cell.[41]

$$I = I_L - I_D - I_{sh}$$ **Equation 5.1[42]**

$$I_D = I_0\left(\exp\left[\frac{V + IR_s}{a}\right] - 1\right)$$ **Equation 5.2[43]**

$$I_{sh} = \frac{V + IR_s}{R_{sh}}$$ **Equation 5.3[44]**

where,

- o I is the load current
- o I_L is the solar generated current
- o I_D is the diode current given
- o I_{sh} is the shunt current
- o I_0 is the diode reverse saturation current
- o R_s is the series resistance
- o R_{sh} is the shunt resistance
- o a is a curve fitting parameter

Power can be determined from the product of load current, I, and voltage, V shown in Equation 5.4.

$$P = IV \qquad \textbf{Equation 5.4}$$

Shown in Figure 23, are the current/voltage characteristics for a given module depicting both a current-voltage curve and a power-voltage curve.

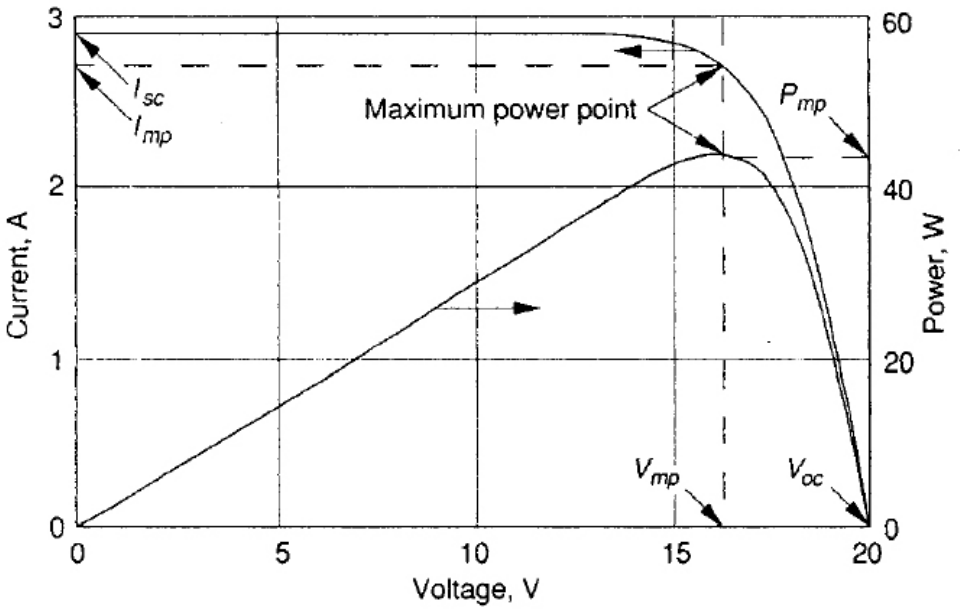

Figure 23: Standard I-V and P-V curves for a PV module.[45]

Notice that at zero voltage, the current is at a maximum known as the short circuit current, I_{sc}, and at zero current, the voltage is at a maximum known as the open circuit voltage, V_{oc}. As the voltage increases, the diode current, I_D, becomes more of a factor, decreasing the load current, I, which eventually brings the curve down to V_{oc}. There is a certain point in the graph, where the load current and voltage produce a maximum amount of power, P_{mp}, which is referred to as the maximum power point, where I_{mp} and V_{mp} refer to the current and voltage corresponding to the maximum power point.

The curves in Figure 23 are specific to a fixed cell temperature and solar irradiance, due to the fact that all of the variables in Equations 5.1 to 5.3 are functions of cell temperature and the light current, I_L, is both a function of cell temperature and solar irradiance.[46]

Module manufacturers provide values for I_{sc}, V_{oc}, I_{mp}, P_{mp}, and V_{mp} based on standard test conditions, STC. Traditionally STC correspond to a solar irradiance of 1,000 W/m^2, an ambient temperature of 25 ºC, and an air mass ratio, AM, of 1.5. The air mass ratio is a function of both site altitude and sun elevation angle, providing a relative measurement of the path length solar irradiance must travel through the atmosphere.[47]

Many researchers have developed complicated correlations that can be used to calculate the cell operating characteristics in Equations 5.1 through 5.3. One could calculate the I-V and P-V curves for any module on the market; however PV module manufacturers have made it convenient by publishing temperature coefficients that relate V_{oc}, I_{sc}, and P_{mp} at STC to their values at elevated cell temperatures. Once the cell operating temperature, T_c, is calculated, all other operating parameters can be determined. The cell operating temperature, T_c, can be estimated by Equation 5.5.

$$T_c = T_A + \left(\frac{NOCT - 20}{0.8} \right) G \qquad \textbf{Equation 5.5}^{48}$$

where,

- T_c is the cell operating temperature in ºC
- T_A is the ambient temperature in ºC
- G is the solar irradiance in kW/m^2
- NOCT is the nominal operating cell temperature, which is the cell temperature when it operates at an irradiance of 800 W/m^2, an ambient

temperature of 20 ºC, an AM value of 1.5, and a wind speed of 1 m/s or less.[49]

Module manufacturers also provide the NOCT for their products; thus, cell temperature can be calculated by Equation 5.5, ambient temperature data, and local irradiance data. The P_{mp} of the module can than be calculated by use of the cell operating temperature and given temperature coefficients. Knowledge of the temperature compensated power point gives a PV designer an idea of the highest power that the module can output, given a cell temperature and irradiance. If a maximum power point tracking controller is used; then, the designer can bank on producing this maximum output, as will be explained in more detail later in the coming charge controller section.

The efficiency of any power generator is the energy out of the generator divided by the energy into the generator. The efficiency of a solar module is defined by Equation 5.6.

$$\eta_{module} = \frac{P_{module}}{G * A_{module}} \qquad \textbf{Equation 5.6}$$

where,

- η_{module} is the module efficiency
- P_{module} is the electrical output of the module
- G is the local solar irradiance on the tilted collector in W/m^2
- A is the module area in m^2.

The efficiency of the module is based on how well it can convert incident solar irradiation with respect to the physical area it encompasses; thus, a module with the same rated output but higher efficiency than another will cover a smaller area. The maximum efficiency is obtained by applying Equation 5.6 using P_{module} and G equal to the maximum rated output of the module and 1,000 W/m^2, respectively.

As the solar modules are the most critical components of the installation, they are also the hardest to procure (at least at present because of the shortage of PV-grade silicon and the high demand for PV). The other system components such as the charge controllers, inverters, fuses, breakers, wiring, and batteries can be obtained almost immediately; however, the modules must be ordered far in advance. For example, if Sharp ND-167U3 modules are specified as the modules of choice for the current design, and the quantity needed is more than about 20; then, they wouldn't be ready for over 6 months. Other manufacturers report even longer wait times; thus, it is important to use the selected modules as an example, and be able to select a different module if it comes time to install the system and the selected modules cannot be readily purchased.

For large arrays, bigger than about 5 kW, it is better to select modules that have a large rated output. Although one could select a module with a low rated output, in general, larger modules are more efficient and have a lower cost per rated watt. Shown below in Figure 24 is a graph depicting efficiency and cost per rated watt for 9 of the largest solar modules found in the SunWize catalog.[50] Only modules from the SunWize catalog have been included, because they offer government prices, which are 30 to 40% less than prices offered to the average consumer. In fact, all components will be selected from this catalog if applicable, due to the fact that the cost is less compared to retail prices.

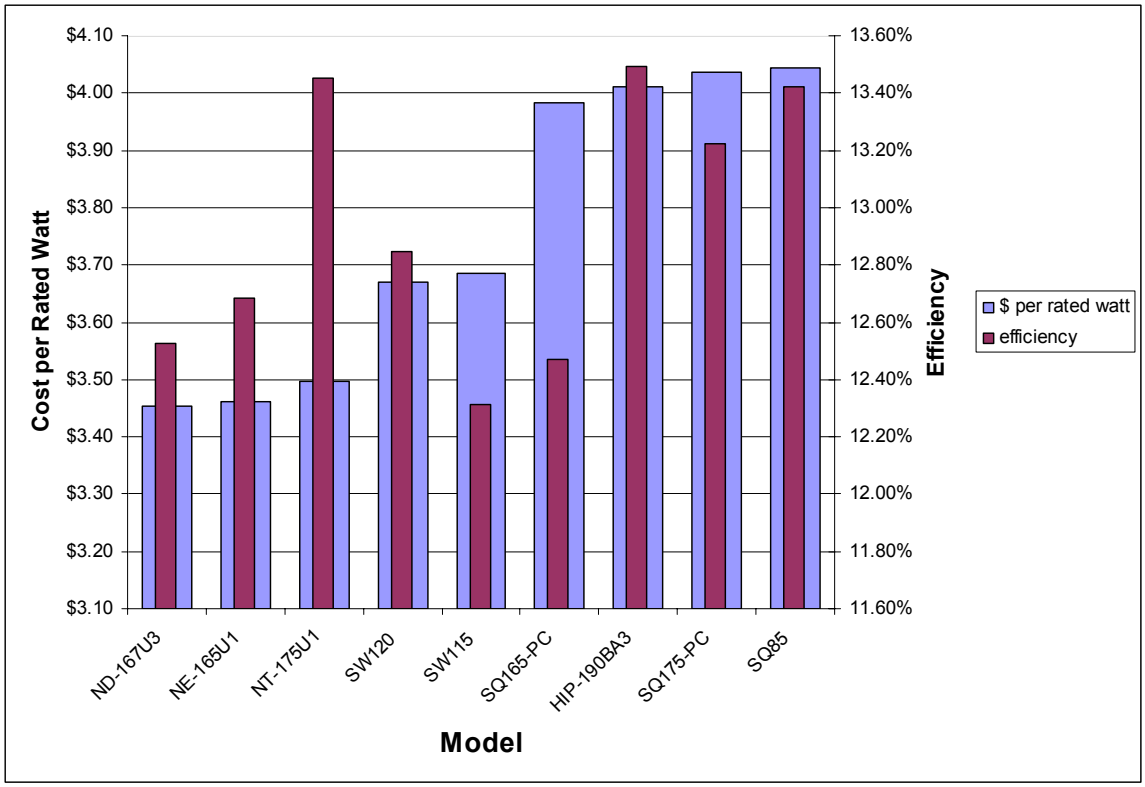

Figure 24: Cost and efficiency comparison of 9 different models of solar modules.

Since space is not an issue for this installation, efficiency has been of secondary importance for module selection, and cost per rated watt is the driving force behind module selection for this installation. The Sharp ND-167U3 175 Watt modules are selected, because they have the lowest cost. If space were an issue, the Sanyo HIP-190BA3 modules could be selected, but the cost would be considerably larger. For example, a 10 kW array composed of the Sharp ND-167U3 modules would cost $34,569, while the same sized array composed of the Sanyo module would cost $40,380, which comes out to be about $6,000 higher than the Sharp array. Although $6,000 is not a huge fraction of the total capital cost, it is still a sum not to be scoffed at, as we are trying to bring Kipahulu the lowest cost energy possible. Thus, the Sharp ND-167U3 module is selected for this installation at a present cost of $576.69 per module.

5.3 Battery Bank

Probably second in importance to the PV array, the battery bank is an essential component to the stand-alone photovoltaic system. Most of the technical aspects have been outlined in Chapter 4, where the corrected amp-hour capacity for the north and south sites is found to be 4,538 and 3,341 amp-hours, respectively.

The battery bank has a set required capacity as defined above, but the voltage must still be set. Like PV cells wired in a module, the voltage of a battery bank is the sum of the individual voltages of batteries wired in a series string, and the capacity of a battery bank is the sum of the capacity of each individual battery string wired in parallel. For example, a battery bank could consist of batteries rated at 2 volts with 100 amp-hour capacities. If there are four strings of six batteries wired in series, then the battery bank will be rated at 12 volts with a capacity of 400 amp hours as shown in Figure 25.

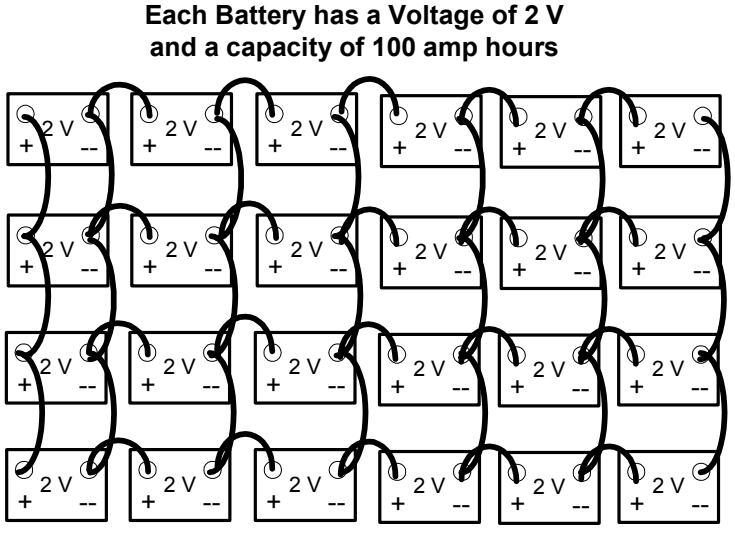

Figure 25: A battery bank depicting parallel and series combinations.

Most battery banks are configured at 12, 24, and 48 VDC; however, a battery bank can be configured at a higher voltage. The larger the system, the higher

the battery bank voltage should be in order to minimize voltage drop, line losses, and conductor/breaker sizes needed for the system. The major voltage limitation is that most charge controllers for stand-alone systems have a battery bank voltage limit of 48 volts. Custom controllers can be purchased; however, the cost is considerable. In order to stay true to simplicity and low cost, it is decided to use a 48 volt battery bank. Since the battery bank voltage and capacity are set, a proper battery must be selected.

Flooded lead-acid batteries, FLA, and valve regulated lead-acid batteries, VRLA, are the most common types of battery types seen in PV applications today. VRLA batteries have the electrolyte immobilized in a gel, gelled electrolyte, or the electrolyte is absorbed in a mat of glass fibers, AGM.[51] In order to minimize gassing, and loss of electrolyte, they have a one-way self-resealing valve that initiates an oxygen recombination cycle and releases pressure, while preventing the outside atmosphere from entering the cell.[52] VRLA batteries are also non-toxic, maintenance free, and can sit a long time without being charged.

Although VRLA batteries have many good qualities, FLA batteries are better suited to large applications where greater currents are needed.[53] The two major drawbacks are:

1. The FLA battery's electrolyte has a potential to freeze, which is inconsequential in a climate such as Kipahulu's, and
2. The water in the electrolyte must be refilled periodically.

Refilling the electrolyte is a maintenance issue; however, after speaking with Jim Fuller of Mt. Rainier National Park, it seems that maintenance isn't a huge issue since they only refill their batteries once every six months.[54] The batteries may need to be serviced slightly more often since Kipahulu is a hotter climate than Washington state; however, this should not be a huge issue if the batteries are charged/discharged properly. Since this is both a large installation and FLA

batteries can take more abuse than VRLA batteries, a FLA battery bank is selected.

Many different FLA batteries are compared to determine the lowest battery bank cost, given the constraints of 48 volts and the corrected capacities specified above. Only two companies: Surrette and C&D Technologies manufacture FLA batteries found in the SunWize catalog. As shown below in Table 3, it is obvious that Surrette models offer a lower cost for equal storage.

Table 3: Required configurations and total costs for battery bank .

Site	Model	Battery Voltage (V)	Required # per String	Battery Capacity (amp hours)	Required # of strings	Cost per Battery	Total Cost
South	Surrette 8-CS-25PS	8	6	1156	3	$850.58	$15,310.44
	Surrette 6-CS-25PS	6	8	1156	3	$631.15	$15,147.60
	Surrette 6-CS-21PS	6	8	963	4	$531.41	$17,005.12
	C&D CPV2500	2	24	2272	2	$709.28	$34,045.44
	C&D CPV2340	2	24	2130	2	$685.53	$32,905.44
	C&D CPV2190	2	24	2272	2	$709.28	$34,045.44
	C&D CPV1660	2	24	1704	2	$557.29	$26,749.92
North	Surrette 8-CS-25PS	8	6	1156	4	$850.58	$20,413.92
	Surrette 6-CS-25PS	6	8	1156	4	$631.15	$20,196.80

	Surrette 6-CS-21PS	**6**	**8**	**963**	**5**	**$531.41**	**$21,256.40**
	C&D CPV2500	**2**	**24**	**2272**	**2**	**$709.28**	**$34,045.44**
	C&D CPV2340	**2**	**24**	**2130**	**3**	**$685.53**	**$49,358.16**
	C&D CPV2190	**2**	**24**	**1988**	**3**	**$663.37**	**$47,762.64**
	C&D CPV1660	**2**	**24**	**1598**	**3**	**$557.29**	**$40,124.88**

There is no physical limit to the number of strings that can be connected in parallel: however, it is advised that no more than four strings be connected in parallel due to the fact that as batteries age, the string currents can become unbalanced; discharging and charging each string disproportionately.[55] In order to further ensure that each string is discharged/charged to an equal DOD, it is also important that the circuit length and wire gauge for each separate string be equal to maintain equal voltage drops.[56]

In order to lessen maintenance time and improve serviceability, it is recommended that each battery be installed with a Water Miser Vent Cap, or equivalent technology. The vent caps have condensing pellets within them that condense and return electrolyte during the charging process. Each vent cap only costs $5.28.

Each battery bank is composed of Surrette 6-CS-25PS FLA batteries. The total capacity and cost for each site is shown in Table 4.

Table 4: Total capacity and cost for each selected battery bank.

Site	Capacity (amp hours)	Cost
North	**4624**	**$20,196.80**
South	**3468**	**$15,147.60**

5.4 Charge Controllers

As explained in Chapter 4, the solar charge controller is a necessary component of any power system where battery storage is incorporated. The charge controller guarantees that the battery SOC will not go too low during discharge and excessive gassing does not occur during the charging phase. Outlined in Chapter 4, warmer batteries experience faster chemical reactions, requiring less voltage and current to reach full charge; conversely, cold batteries experience slower reaction rates, so a more robust charging algorithm must be applied. A charge controller should also incorporate a voltage and temperature sensor in order to compensate for these different reaction rates. Three common types of charge controllers are: series relay, pulse width modulated (PWM), and maximum power point tracking (MPPT), which usually incorporates PWM technology.

The series relay charge controller is by far the simplest and least expensive type of controller on the market. Essentially, a series relay controller turns the load off at a set low voltage, and disconnects the PV array at a prescribed voltage near full state of charge. They are by far the cheapest; however, since the full load is either turned on or off, the battery bank has the potential of charging or discharging more quickly than it is rated for; thus reducing battery life.

Like a series relay controller, a PWM controller either turns the load on or off; however, it uses a transistor to turn the load on and off very quickly. As the battery gets closer to a full state of charge, the charging pulse becomes shorter than the discharge pulse until the battery reaches a set regulation voltage, where the charging pulse is on only long enough to sustain the regulation voltage.[57]

The MPPT controller is by far the most expensive controller type. It tracks the maximum power point of the array to achieve nearly 30% more output from the

array.[58] As discussed above, given a certain cell temperature and irradiance level, a PV module will have a point on the I-V curve where maximum power output can be achieved. This maximum power point corresponds to a specific resistive load as shown in Figure 26. Note that the slope of a current-voltage curve is resistance; thus, the three diagonal lines correspond to loads of constant resistance.

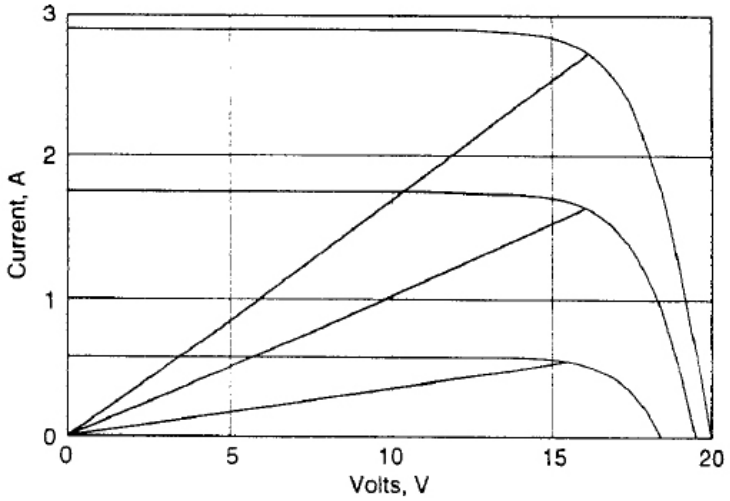

Figure 26: I-V curve at three irradiance levels with resistive loads corresponding to the maximum power point.[59]

Shown in Figure 27 is the I-V curve of a typical module operating at two different irradiance levels.

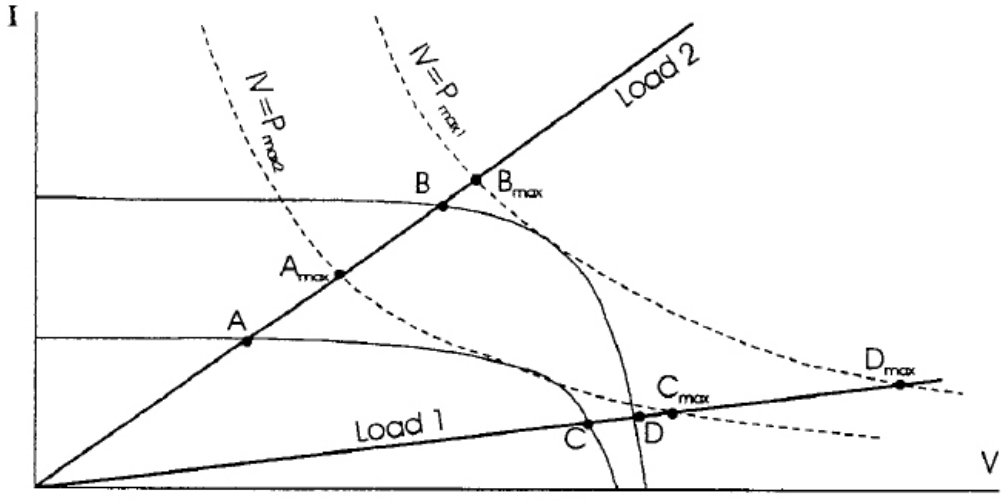

Figure 27: A diagram depicting the maximum power point for two loads.[60]

The two diagonal lines correspond to constant resistive loads that are not at the maximum power point of either irradiance level. The two hyperbolas correspond to lines of constant power. Note that there is one point for each of the I-V curves where these constant power hyperbolas are tangent; corresponding to the maximum power point. Also, note that none of the points A through D intersects at the maximum power point. A MPPT controller adjusts the voltage and current of the array to meet this point of maximum power. For example, if there is a high irradiance, corresponding to the upper I-V curve, and if the MPPT controller is connected to load 2; the MPPT controller will decrease the voltage and boost the current of the PV cell, so that the I-V curve intersects load 2 at B_{max}, instead of at point B. Load voltage and current sensors are used in a feedback loop, and a combination of capacitors and inductors vary the output voltage of the array to match the desired load voltage.[61]

It is decided to use a MPPT controller for this design, because a MPPT controller can extract up to 30% more power from an array than a PWM or relay controller. It uses pulse width modulation in order to effectively and efficiently charge batteries, and it is the controller of choice of most PV designers today. There are only a few companies that manufacture MPPT controllers, and only two models from the SunWize Catalog are applicable to this installation, because they can charge a 48 volt battery bank and can handle relatively large amounts of current.

Both the Blue Sky Energy Solar Boost 6024HL and the Outback Power MX60 are MPPT controllers that can handle 60 amps and charge a 48 volt battery bank. The Outback MX60 is slightly cheaper than the Solar Boost 6024HL, and it is specifically designed to operate with Outback Inverters, which have been selected as the inverters for this system due to flexibility and power consumption issues that will be discussed later. For these reasons, it is decided to use the Outback MX60 as the charge controller for the system; its cost is $431.55.

In order for maximum power point tracking to be effective, or even possible, the array voltage going into the MX60 must be higher than the battery bank voltage, which is 48 volts in this case. The array input current should also be less than 60 amps to allow the MX60 to boost the controller output current, if it is available. The actual array input current should be limited to about 48 amps (125% of short circuit current), due to reasons detailed in section 6.4 and Appendix D. dealing with the 2005 National Electrical Code. When sizing an array, it is best to have the nominal array voltage at least one nominal voltage above the array voltage with the open circuit voltage of the array not exceeding the maximum input voltage of the MX60 of 140 VDC.

As explained above, the Sharp ND-167U3 is selected for this installation, which is a nominal 12 volt module. Normally, the V_{oc} and V_{mp} for panels that have a 12 volt nominal rating are about 21 and 17 volts, respectively. This requires 6 modules wired in series for an array V_{oc} and V_{mp} of 126 and 102 VDC, respectively. The Sharp modules are different than normal 12 volt models, because their V_{oc} and V_{mp} are 29 and 23.5 VDC, respectively. With such a high open-circuit voltage, only 4 modules can be safely wired in series to stay under 140 volts. Wiring four 12-volt modules in series to make a nominal 48 volt array does not meet recommended practice as discussed above; however, since the V_{oc} and V_{mp} of the Sharp ND-167U3 are so high, the designer can use four modules in series to give 116 volts at open circuit and 94 volts at maximum power point.

As the panels warm up, the V_{mp} falls as explained above. If the V_{mp} of the array falls below the battery bank voltage, the MX60 can no longer boost the output current, so it is no longer tracking the power point. Sizing an array with a voltage higher than that of the battery voltage ensures that the MX60 is always able to boost the output current since the maximum power point of the array is always above the battery voltage, and it will enable one to boost the battery voltage

higher when it is called for, such as when equalizing the batteries. This should be taken into account if different modules have to be selected.

For example, the I_{sc} and V_{oc} of the Sharp ND-167U3 modules are 7.91 amps and 29 volts, respectively. As shown in Figure 28, a properly sized subarray made up of these modules will have four modules wired in series with a maximum of five strings in parallel in order to stay below the input current and voltage limits of 140 volts and 48 amps, as discussed above.

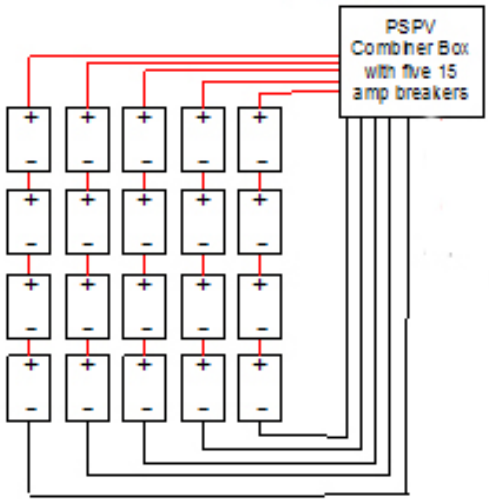

Figure 28: The optimal size of a subarray made up of Sharp ND-167U3 modules feeding an MX60 controller.

5.5 Inverters

If a stand-alone PV system has any AC loads, an inverter is an essential component to switch the 48 VDC from the battery bank to 120 VAC of the building loads; instead, DC electrical output can be simply run through a battery bank straight to the load as shown in Figure 21. In addition to supplying power to AC loads, a good stand-alone inverter must also include a battery charger and transfer switch to charge the battery bank via a back up genset or the grid during periods of low solar irradiation; then, the inverter should automatically disconnect

from the back up genset once the batteries reach a full state of charge. There are three main types of inverters on the market today:

1. The square wave inverter is by far the cheapest, and has relatively high efficiency; however, it also has a large harmonic distortion, which can damage complicated AC loads such as computers and televisions.[62]
2. The modified sine wave inverter is more expensive, has a reasonable efficiency, and produces an output that is not quite a sine wave, but is very close; however, the wave form is often still not smooth enough to operate complicated power electronics.[63]
3. The pure sine wave inverter has the cleanest wave, but is the most expensive. It also has the lowest inverter efficiency; though companies today are making these inverters with efficiencies above 90%.[64]

If the PV system is going to be powering complicated AC loads; then, the pure sine wave inverter is the only choice. There are a number of companies that manufacture pure sine wave inverters for stand-alone applications. It is decided use the Outback FX3048, which is rated to condition 3.3 kW of continuous power. The Outback inverter has been chosen for several reasons:

1. It includes a battery charger and transfer switch.
2. The FX3048 is a sealed inverter with a cooling fan, so the inside is protected from harsh marine environments. Outback also makes a vented unit, which has a higher continuous power rating; but it is recommended against using the vented version in a marine environment.[65]
3. Outback is the only company that makes inverters with a modular design; meaning that the inverters can be stacked together in parallel or series to achieve different output voltages and multiple phases.
4. The FX3048 is offered in the SunWize Catalog at a GSA price.
5. Lastly, all of the charge controllers and inverters in an Outback power conditioning system are tied to a central processor, which in turn is

controlled by the master inverter, which offers other advantages as explained below.

The Outback Power Systems inverters can be stacked in many different configurations depending on specific load requirements.

As shown below in Figure 29, the Outback Inverters can be stacked in four different ways:

1. They can be stacked in parallel, where the individual outputs are additive producing up to 36 kW at 120 VAC.
2. They can be stacked in series, providing either two legs 3 kW 120 VAC power, or a combined 6 kW at 240 VAC.
3. They can be stacked in a combination of series and parallel with the aid of the X-240 balancing transformer, in which up to 9 kW at a time can be sent to one leg at 120 VAC, or the two legs can be combined to provide 12 kW at 240 VAC.
4. The inverters can be configured to provide 120/208 3-phase power, where three inverters, or 3 pairs of parallel stacked inverters, power each leg of the 3-phase power.[66]

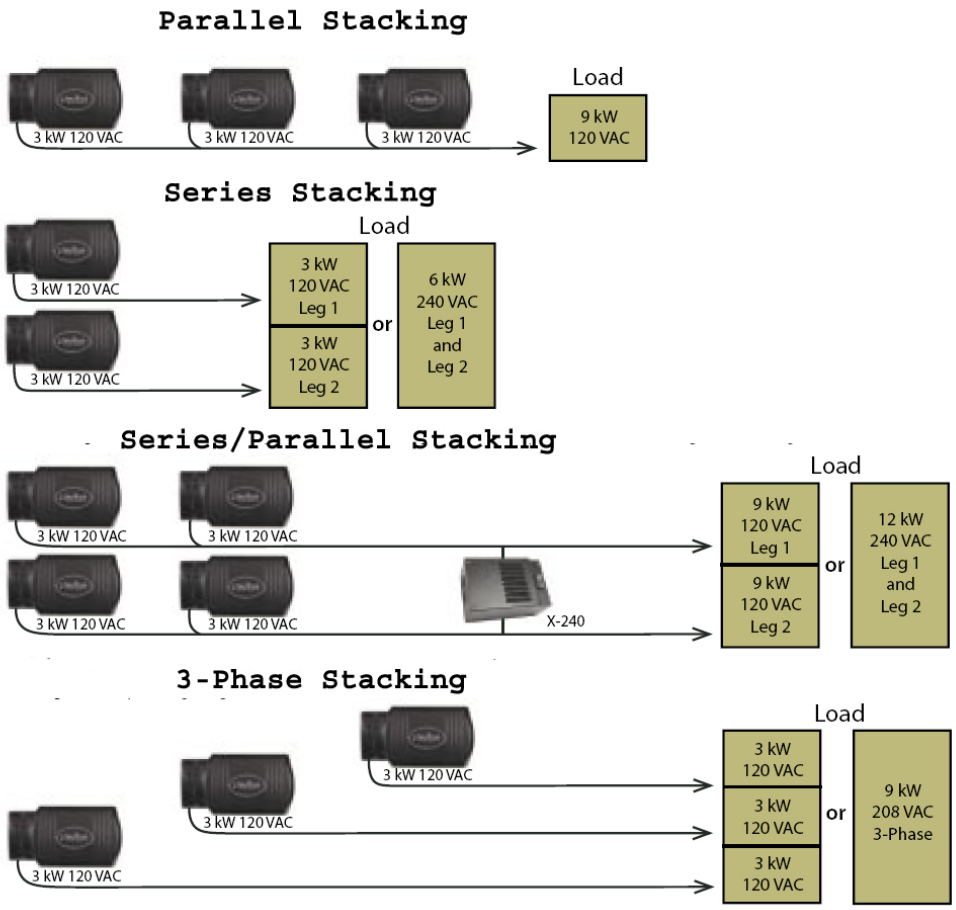

Figure 29: The different stacking configurations of Outback Inverters.[67]

It is decided to stack the inverters in a series/parallel configuration with the use of the X-240 balancing transformer, as shown above. In this configuration, both 120 and 240 VAC loads can be powered, and with the use of the X-240, one or more inverters can be shut off during periods of low consumption. Being able to shut off inverters and controllers during low power consumption ensures that the inverters are operating at their highest efficiency. Note that there are not any present or projected 3-phase loads at Kipahulu. If this should change, then the inverters could be reconfigured for 3-phase operation.

The operation of the X-240 as a balancing transformer is explained by looking at Figure 30. The X-240 is placed after the inverters, and if the load on one leg is greater than the other, the X-240 allows power to pass from one leg to the other.

If the loads were even, or a 240 volt load; then, the X-240 would be idle, but as the load shifts to one side or the other the two inverters share the load. In other words, if there were 2 kW on leg 1 and no load on leg 2, both inverters would supply 1 kW, and 1 kW would transfer from leg 2 to leg 1 through the X-240 transformer.

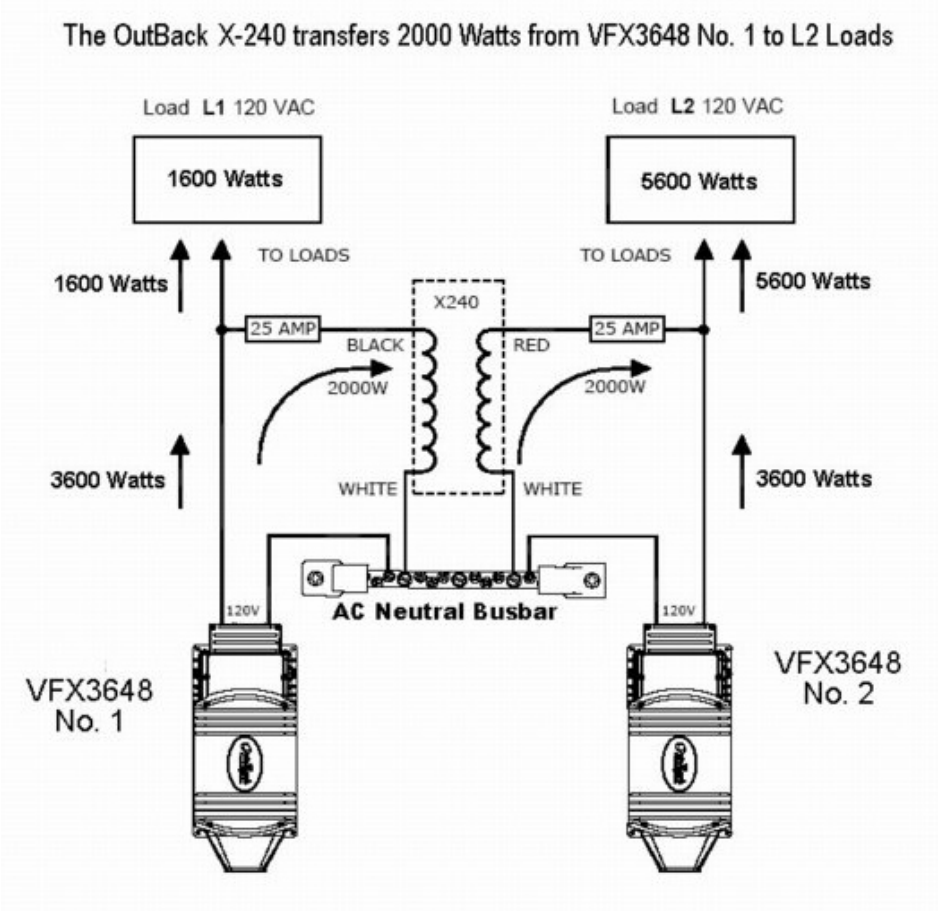

Figure 30: Example of an X-240 load balancing application for 2 series stacked inverters.[68]

The main advantage of the series/parallel stacked configuration is the ability for a master inverter to turn one, or more inverters off, and still supply a balanced 120/240 VAC load. This can be explained by looking at Figure 31 below. This figure is an example of a series/parallel stacked system with an X-240 balancing transformer in between legs. Take notice that the top inverter is the master, which has a green temperature sensing wire running to the battery bank (not pictured), it has a CATV communications cable running into the HUB10, from

which all of the other “slave” inverters and the MX60 charge controllers (not pictured) are connected to the the complete system controller.

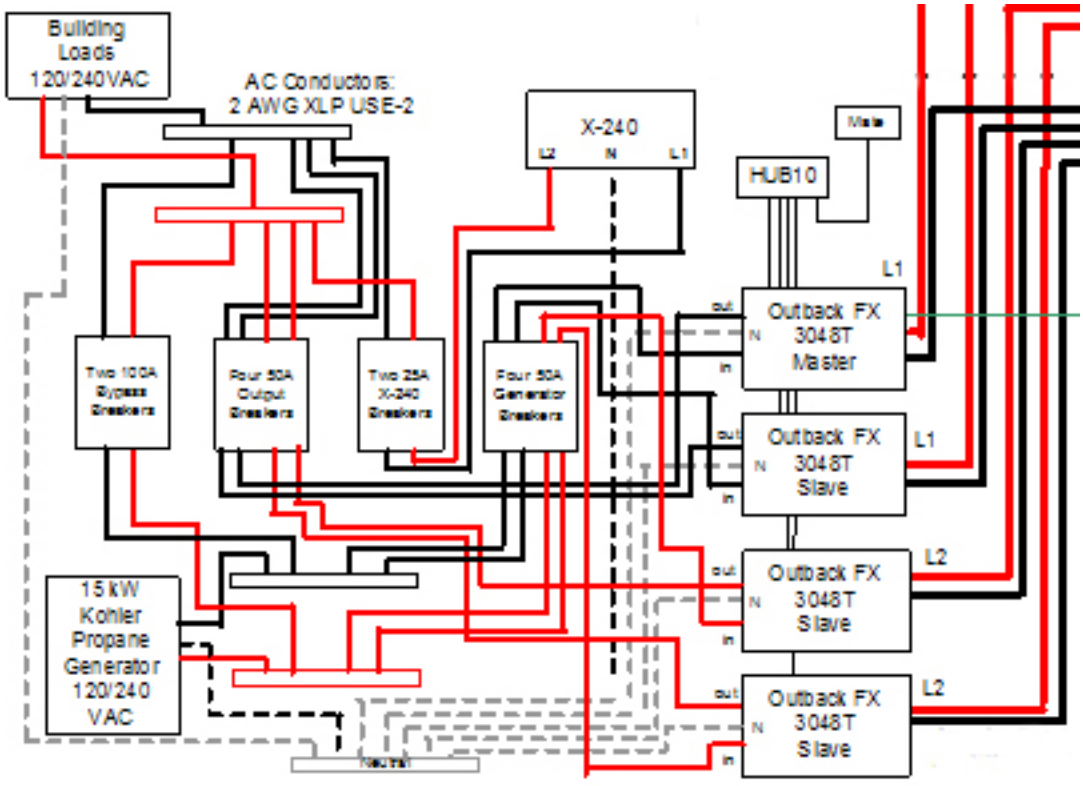

Figure 31: A series/parallel stacked configuration incorporating the X-240 Transformer.

As an example, let’s assume that each inverter can condition 3 kW. If there is 6 kW on each 120 VAC leg of the load; then, each inverter is running at full capacity and the X-240 is idle. If there is 9 kW on one 120 VAC leg of the load and 3 kW on the other; then, each inverter is running at full capacity and the X-240 is transferring 3 kW to the leg with the larger demand. If there is a 6 kW load on one 120 VAC leg and 3 kW on the other; then, the Outback Mate would shut off one inverter that is supplying power to the 3 kW side. If there is a 4 kW load on one leg and a 2 kW load on the other, then the Outback Mate would shut down two inverters (one from each leg), and 1 kW would be sent through the X-240. If the load draw goes down lower than 3 kW, the Outback Mate will shut off all of the “slave” inverters keeping only the master on. The X-240 will allow the

entire 3 kW to be consumed on one of the legs, or send a portion of the power over to the other leg.

The inverters for each site will be designed to supply the peak power demand; thus four Outback Inverters will be used for the north site, and three will be used at the south site. In addition to inverters, each system must have an Outback Mate, a HUB10 to connect all of the components to the Mate, and an X-240 as outlined in Table 5.

Table 5: A breakdown of costs associated with each inverter design.

Component	North Site	South Site
FX 3048 Inverters	$6337.24	$4777.93
Mate	$196.16	$196.16
HUB-10	$249.36	$249.36
X-240	$212.12	$212.12
Total	$6994.88	$5435.57

6. Additional Solar Components

6.1 Introduction

In addition to modules, batteries, inverters, and charge controllers, there are several other components that tie the system together. The system would not be possible without these components, and they can often be the source of considerable cost.

6.2 Array Racks

A back of the envelope calculation is done to determine the size of array required for each site, and it is determined that the north and south sites need 80 and 60 module arrays, respectively. These numbers will be used as examples in this section, but may change later for economic reasons.

When it comes to mounting a solar array, there are many different options. These options include roof mounts, ground mounts, pole mounts, and tracking mounts. In addition to the many methods of mounting the array, there are also many different materials that the racks are fabricated from including, milled aluminum, anodized aluminum, painted steel, galvanized steel, and stainless steel. The materials best suited for a marine environment such as Kipahulu are stainless steel and anodized aluminum. While stainless steel would be adequate to prevent corrosion, anodized aluminum is cheaper, lighter (shipping costs are less), and slightly more appropriate for applications in highly corrosive marine environments. Unirac Company makes an array rack that is both made out of anodized aluminum, and can comfortably hold arrays the size of the ones estimated for Kipahulu. Shown below in Figures 32 through 34 are the three different mounting methods that Unirac offers.[69]

Figure 32: Flush mounted arrays on the roof.[70]

Figure 33: High profile tilted rack.[71]

Figure 34: Low profile tilted rack.[72]

The low profile rack can only accommodate one module along the hypotenuse of the rack, whereas the high profile tilted rack has room for up to four modules along this same dimension. The low profile orientation minimizes the vertical height of the array, and the high profile orientation maximizes the module density in a given area. Since three NPS homes and a maintenance facility are going to

be built at the north site, it has been decided to specify a high profile tilted array at this location to minimize required space.

As expressed in a preliminary report by Sandia Laboratories and in conversations with park employees at Haleakala, the 60 modules that are required for the south site should be mounted on an awning structure to provide both shade and a showcase for the solar panels.[73] In an effort to make this installation aesthetically pleasing, the modules should be laid out in even multiples of 60, as 12 rows of 5 or 10 rows of 6. The modules can be mounted high profile, where the long sides are horizontal and the rails parallel to the rafters, or low profile, where the short ends and rails are perpendicular to the rafters. The pattern that will take up the smallest area is 12 rows of 5 modules in a low profile orientation. A simplified view is shown below in Figure 35, where dimensions are in feet.

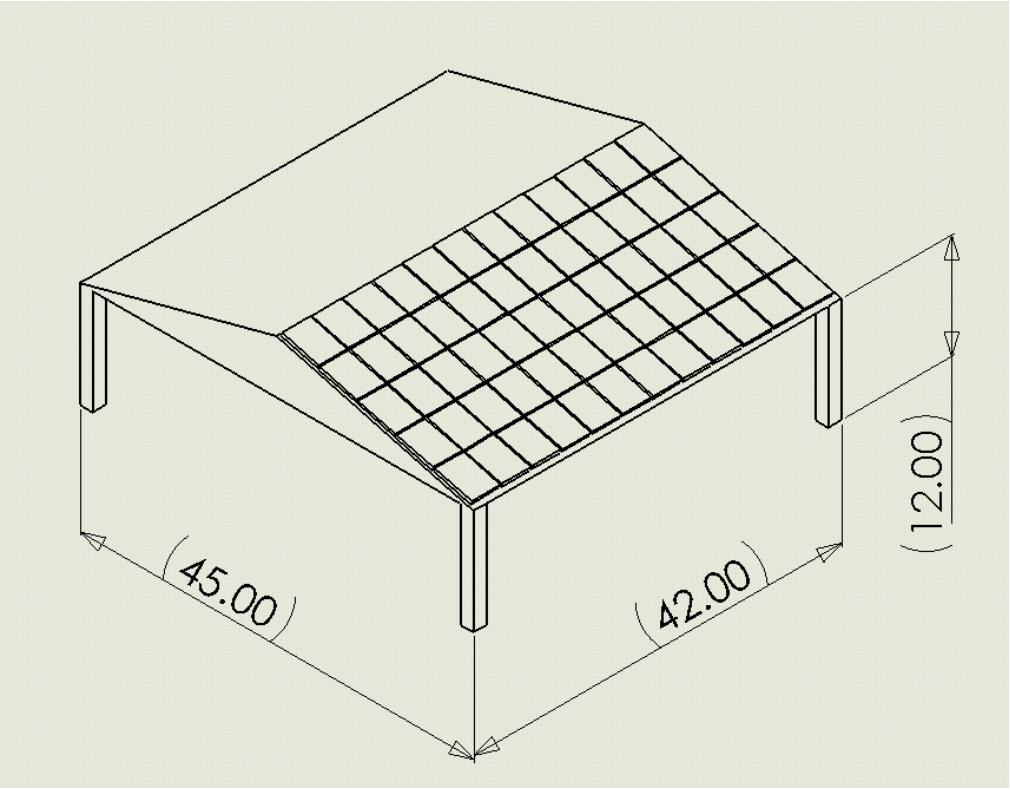

Figure 35: A simplified view of a roof mounted array.

In order to provide a showcase for solar electricity, a shady place to eat lunch and a building to protect the battery bank and power conditioning equipment, it is recommended that a mounting structure be built near the south end of the visitor center approximately in the place of the straw hut, shown below in Figure 36. The approximate dimensions of a structure that could serve the purposes explained above as well as provide adequate area and tilt for the solar modules were submitted to the maintenance department at Haleakala. Their contractors returned a quote of about $75,000 to build such a structure. On the other hand, in order to reduce costs, the array in the north site should be ground mounted on the Unirac tilted array rack. The battery bank and power conditioning equipment should be housed in the new maintenance facility.

Figure 36: A proposed locale of the PV mounting structure for the south site.

For the south site, a small building must be built to house the battery bank, charge controllers, inverters, and circuitry. A building constructed strictly for equipment protection would not be large enough to hold the entire array; thus, the roof should be extended so that it is large enough to hold the array while

providing shade and education for visitors, in addition to protecting the modules from potential vandalism.

Thus, it is decided to mount the north site array on the Unirac Solar Mount High Profile racks, and use the Unirac Solar Mount Flush Mount racks to mount the array for the south site on the specially built shade/equipment-housing structure. Based on array sizes of 80 and 60 modules for the north and south sites, respectively, the capital costs are outlined in Table 6.

Table 6: Cost breakdown of array racks.

Component	North Site	South Site
80 Module High Profile Array Rack	$10,086[74]	N/A
60 Module Flush Mounted Array Rack	N/A	$3,952[75]
Mounting Structure[76]	N/A	$75,000
Shipping Cost[77]	$700	$500
Total	$10,786	$79,452

6.3 Propane Generators

In order to provide reliability during periods of low irradiation, charge batteries effectively, and power large AC loads such as a water pump or table saw that cannot be powered by the battery bank, it is necessary to have a back up engine/generator. Otherwise, in order to meet all electrical power demands throughout the year, the PV array would have to be oversized greatly to supply demands during periods of low irradiation. It is assumed that the loads at Kipahulu will remain constant throughout the year, while the solar irradiation is obviously lower in the winter time, as shown in Chapter 2. A back up generator is thus necessary.

There are many types of engine/generators, ie, “gensets,” operating with different power outputs, fuels, and noise levels. While diesel fuel is probably the cheapest fuel to run a genset, it is also one of the dirtiest fuels both in combustion emissions and liquid fuel spills, which can severely harm a fragile natural environment such as Kipahulu, and has been avoided in other National Park installations in the past few years.[78] It is thus decided to use a genset that runs on gasoline, natural gas, or propane. Gasoline is a little cleaner than diesel; however, the fuel spill potential is still present. Natural gas is a clean fuel, but its price is highly volatile, and transporting natural gas to a remote site like Kipahulu would either require a pipeline be built (assuming natural gas is available on the island), or to ship it as LNG, liquid natural gas; both options would cause delivery costs to be excessive. Propane is a clean burning fuel, has a relatively stable cost compared to natural gas, and is shipped as a liquid; thus, a propane genset will be selected.

There are many companies that make propane gensets; however, every company doesn’t manufacture a unit for every power output. In a stand-alone system without any PV, a genset could carry the load all of the time. Depending on the load requirement, the genset would be running at a percentage of its maximum efficiency as shown in Figure 37, with the maximum electrical efficiency of a genset falling at approximately 90% of its rated output.

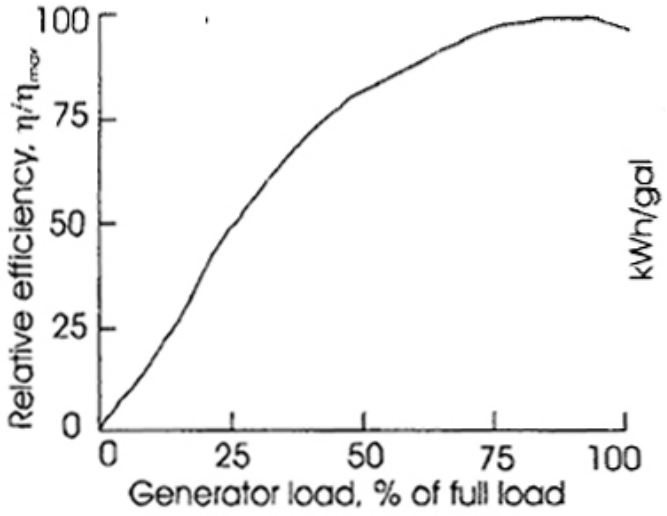

Figure 37: Overall efficiency vs. rated load for a typical genset.[79]

Designing a stand-alone system that is strictly powered by a genset could reduce overall system cost.[80] Fuel and genset operating costs would increase; however, these costs could potentially be offset since a battery bank, inverter, panels and other expensive PV components would no longer be necessary. Since it is the goal of this project to design a renewable energy system, the option for designing a solely genset powered system is only briefly researched, and the genset will be designed primarily with battery charging in mind.

As mentioned in Chapter 4, a battery charging source should be able to supply C/20 or better in order to properly charge the battery bank near full state of charge; although smaller charging rates are still useful when the battery is not at full charge. Since a genset will be used mainly to top off the battery bank, it must at least supply a charge of C/20. From Chapter 5, the battery bank capacity for the north and south sites are 4,624 and 3,468 amp-hours, requiring 231 and 182 amps of charging current to meet the C/20 charging constraint, respectively. From Chapter 1, the peak load requirements for the north and south sites are 13 and 7.2 kW, respectively.

From the above charging and peak load requirements, a Cummins GNAB 11.5 kW propane genset is selected for the south site, and a Kohler 15RYG 15 kW propane genset is selected for the north site. Assuming that the gensets are charging the 48 volt battery bank at maximum efficiency, they will each be running at 90% of their rated output. At 90% of rated output and 48 volts, the Cummins and Kohler generators can supply 215 and 281 amps, respectively. These charging currents meet the above charging requirement of at least C/20 by supplying a charging rate of about C/16 to each battery bank and they are both rated higher than the peak demand for each respective site. The capital cost for each genset is shown below in Table 7.

Table 7: Capital cost breakdown for the selected gensets.

Component	North Site	South Site
Cummins GNAB 11.5	N/A	$7,000
Kohler 15RYG with a battery & a 100 amp transfer switch	$8350	N/A
Start up	$750	?
Delivery to Kipahulu	$1,390	$1,000
Total	$10,490	$8,000

For performing an economic analysis on each system, it is important to know the fuel consumption, maintenance intervals and rebuild intervals. Product literature gives the fuel consumption per hour for each genset. The Kohler 15RYG consumes 85 cubic feet per hour and produces 15 kWh at full load. In other words it produces 6.42 kWh per gallon as shown below in Equation 6.1.

$$EnergyOutPerGallon = \frac{15kWh}{hr} * \frac{hr}{85\,ft^3} \frac{36.39\,ft^3}{gallon} = \frac{6.42kWh}{gallon} \qquad \textbf{Equation 6.1}$$

The fuel efficiency for the Cummins genset is determined in the same way and is determined to be 5.99 kWh per gallon at maximum efficiency.

Operation and management schedules and costs are taken from a field study of a similar installation at Pinnacles National Monument.[81] The gensets used in that installation are two Kohler 20RZ 20 kW units configured for propane. Their maintenance schedule is as follows: oil change every 250 hrs at $125, a valve adjustment every 2,000 hrs at $250, and a complete replacement every 30,000 hrs for $24,000.[82] The maintenance costs are assumed to be equally applied to a smaller generator; thus the maintenance and replacement schedule for the economic analysis is shown in Table 8. Note the costs below are for one genset, not two as in the Pinnacles installation.

Table 8: Maintenance and replacement cost breakdown for the selected gensets.

Maintenance	North Site	South Site
Oil Change every 250 hrs	$62.50	$62.50
Valve Adjustment Every 2,000 hrs	$125.00	$125.00
Replacement Every 30,000 hrs	$9490	$7,000

6.4 Conductors, Over-current Devices, and NEC

The 2005 National Electric Code, or NEC, has been consulted in order to design the system for safety and reliability. The NEC is published about every three years by the National Fire Protection Association. The NEC is a collection of articles that apply electrical safety and efficient utilization considerations to a slew of topics such as: wiring methods and materials, and wiring protection. Article 690 is specifically written about solar PV systems. In order to protect both

technicians and end users, the NEC specifies the size, type and location of fuses, conductors, and breakers to be used. Other considerations such as wire losses, types of wire housing, and wire materials are also taken into consideration.

The requirements and provisions of the NEC are illustrated in Appendix D. All conductors and over-current protection devices have been sized according to the equipment outlined above.

7. Hydro Component Selection

7.1 Introduction

Since resource potential has been determined in Chapter 4, it is now appropriate to select turbines, penstock, intake structures, conducting wire, and other components that are necessary to a micro-hydro system. Shown below in Figure 38 are the basic components of a micro-hydroelectric system. Note that the electrical side of the system has not been included.

Figure 38: The basic components of a micro-hydroelectric system.[83]

7.2 Water Intake

The intake diversion and screen are the first components in the system, as shown above in Figure 38. By definition, an intake is "a structure to divert water into a conduit leading to a power plant."[84] The basic requirements of an intake are to limit the amount of debris and sediment entering the penstock by use of a diversion screen, or thrash rack, and to divert the required amount of flow to a power canal, or penstock, with minimal head loss and impact on the natural environment.[85] There are many different types of intakes, but there are two main types:.

1. A power intake, or forebay, is an intake that feeds water directly to a turbine via a penstock as shown in Figure 39.
2. A conveyance intake, shown in Figure 40, is one that supplies water to other waterways such as canals, flumes, and tunnels. These other waterways are typically followed by a power intake.

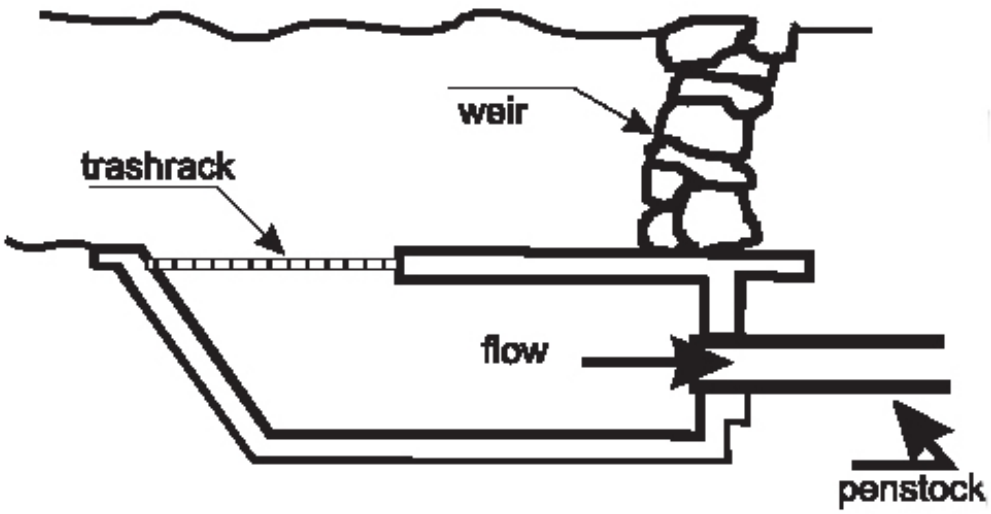

Figure 39: A diagram of a power intake.[86]

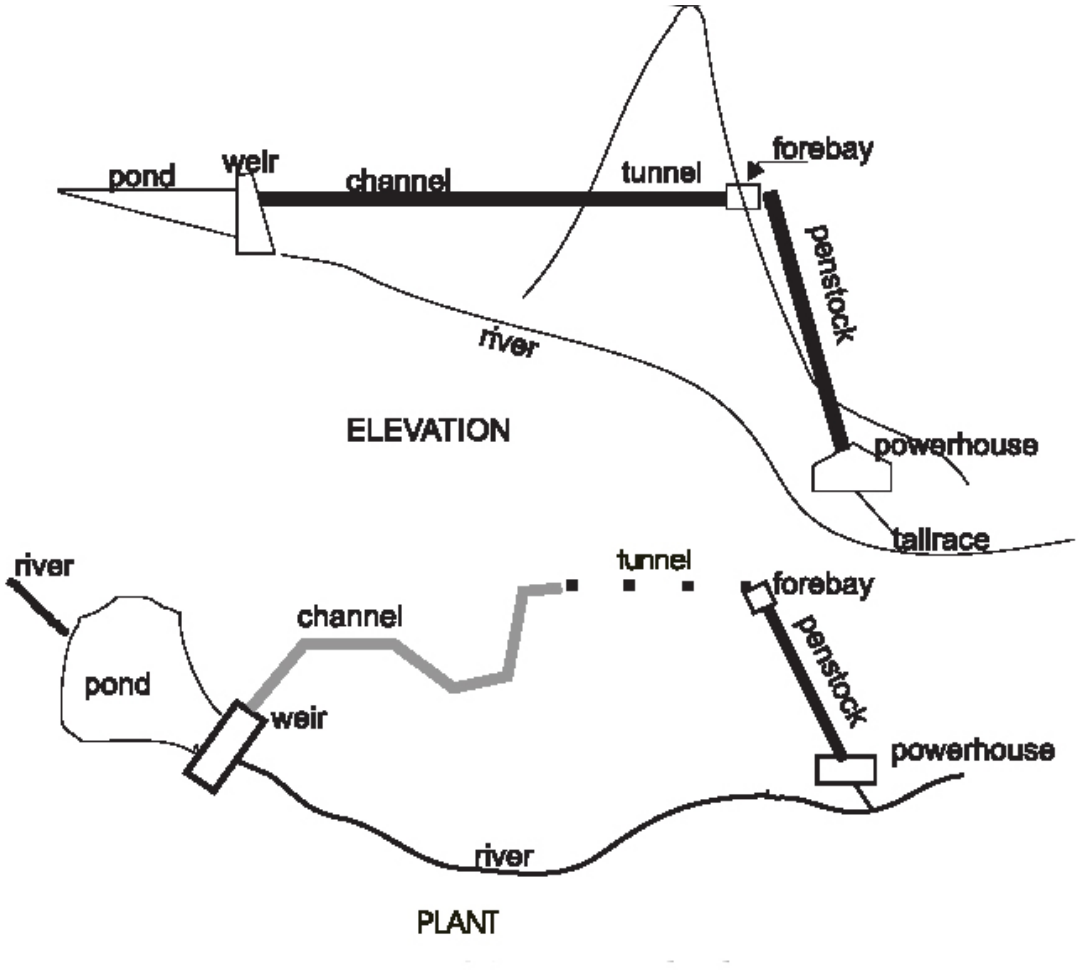

Figure 40: A diagram of a conveyance intake.[87]

Due to the fact that the potential flows at both of the hydro sites for Kipahulu are quite small (200 gpm or less), it is decided that the added cost of designing a open channel canal, or flume will hardly be worth the trouble, and more important, will not be worth the cost. Thus, the water will be fed directly into a penstock via a power intake.

Since the power intake supplies water directly to the penstock, the opening is usually horizontal followed by an inclined penstock as shown in Figure 40, and it can be either located at the end of a conveyance intake, or can take the place of it.[88] In low head hydro systems, the design of the intake is very important due to the fact the head lost through it may be considerable in comparison to the gross

head. However, in a high head scheme, like the situation in Kipahulu, an efficient hydraulic design is not quite as important, because the head lost through the intake will be relatively small compared to the gross head.[89] Although there will be some minimal losses associated with the water passing through the grates of the trash rack itself, the most significant losses found in the power intake occurs due to a loss from the sudden contraction of flow. A spring box power intake manufactured by HI power has been selected for this installation, as shown in Figure 41.

Figure 41: A spring box power intake made by HI Power.[90]

The power intake shown above has a pipe diameter of 4 inches and an intake width of 8 inches. Assuming an input flow rate of 200 gpm, a gross head of 300 ft, and given power intake dimensions, the head loss through this power intake is calculated to be about 0.04 feet. This small head loss is hardly worth worrying about due to the relatively large gross head; thus it is decided to select a power intake system off the shelf similar to the HI Power model shown in Figure 41, which would be situated behind the dam in such a way that it could be completely submerged under the water during periods of low flow as shown in Figure 42.

Figure 42: The power intake submerged under water during periods of low flow.[91]

7.3 Penstock

Shown in Figures 38 through 40, the penstock is the pipe, or tubing that transfers water to the turbine increasing in pressure as the vertical drop increases; thus transferring all of the gross head minus frictional losses to the turbine at the bottom of the hill.[92] Unlike the power intake, frictional loss in the penstock is not negligible unless the pipe is sized large to prevent huge head loss.

The head loss in the penstock can be broken up into three different categories: 1.) head loss through pipes, 2.) head loss through bends, and 3.) head loss through valves along the penstock. The calculations employed to select a penstock with a sufficiently large diameter are displayed in Appendix E.

7.4 Tail Race

As shown above in Figure 7.1, the tail race is a canal that routes water back to the river after it has exited the turbine. One major consideration of the tail race is to make sure that it can sufficiently transport water during periods of high flow. Since the flows in this site are extremely small, and head loss in the tail race will

not impact the overall efficiency of the power plant. Thus, no significant engineering calculations are performed on a tail race. However, it must be long enough to transport the water back to the river.

7.5 Turbine

The function of the turbine is to convert the kinetic energy of the water into rotational energy that drives a generator. There are two major types of turbines: reaction and impulse. Reaction turbines use runners that are completely immersed in the flow, creating power proportional to the pressure drop across the device; where as, the impulse turbine operates in free air and is driven by one or more high pressure jets of water.[93] As there are many different types of both reaction and impulse turbines, the scope of this discussion is not broad enough to cover each one in detail, and the interested reader can find a variety of hydroelectric and fluids engineering books to gain a better grasp on the differences between turbines.

As outlined in Figure 43, impulse turbines, including Turgo and Pelton, should be used in medium to high head schemes with low to medium flow, reaction turbines, including propeller, Kaplan, and Francis, should be used with low to medium head schemes with medium to high flow rates.

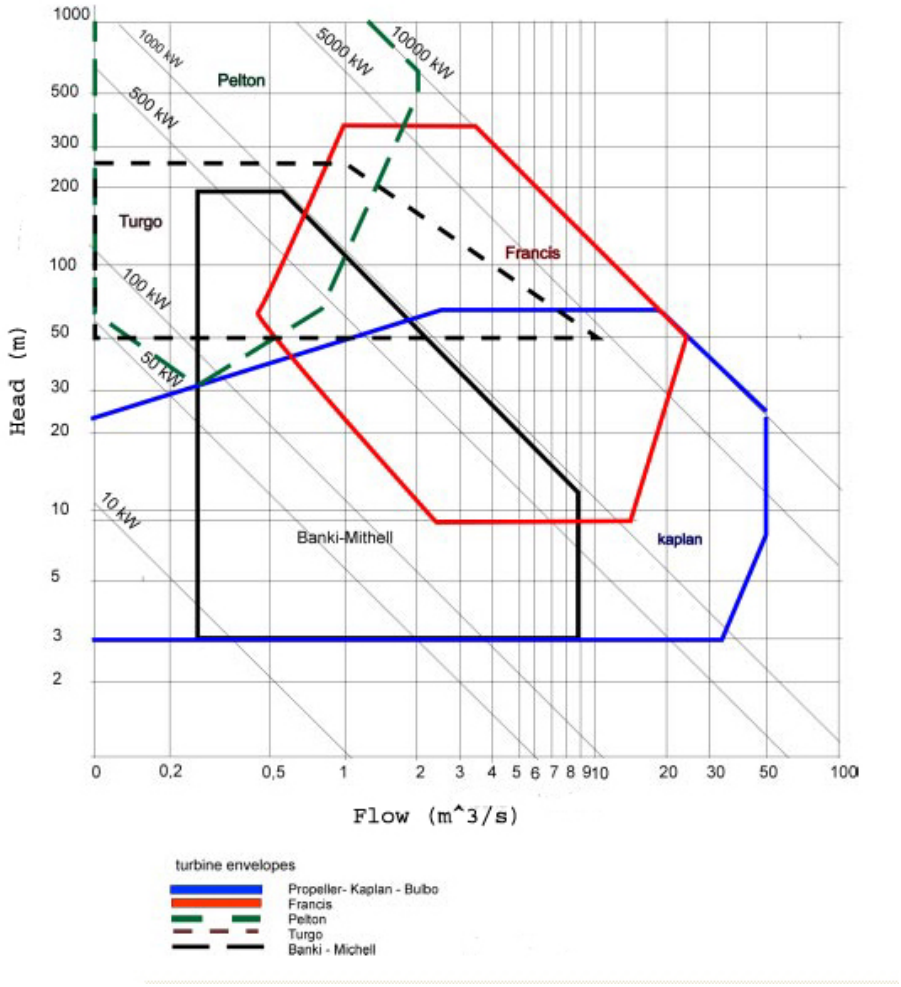

Figure 43: Operational envelopes for different turbines.[94]

As stated in Chapter 4, there is a 346 ft head with 200 gpm at the lower dam. Note that the flow rates given in Figure 43 are cubic meters per second, where 15,850 gpm equals 1 m^3/s. The low flow rates of this application push the turbine choice into the upper left portion of the graph, which is Turgo/Pelton territory. The question is:, Pelton or Turgo?

The Pelton wheel is an impulse turbine where one or more high pressure nozzles with needle valves impinge flow onto a runner with a series of buckets, or cups, attached to the wheel. Most of the larger, more advanced Pelton turbines also have deflection plates to help stop flow on certain jets during periods of low load

draw, as shown in Figure 44; however, smaller Pelton wheels that do not have deflection plates must have an external shunt load to draw on the turbine when the battery bank is fully charged.

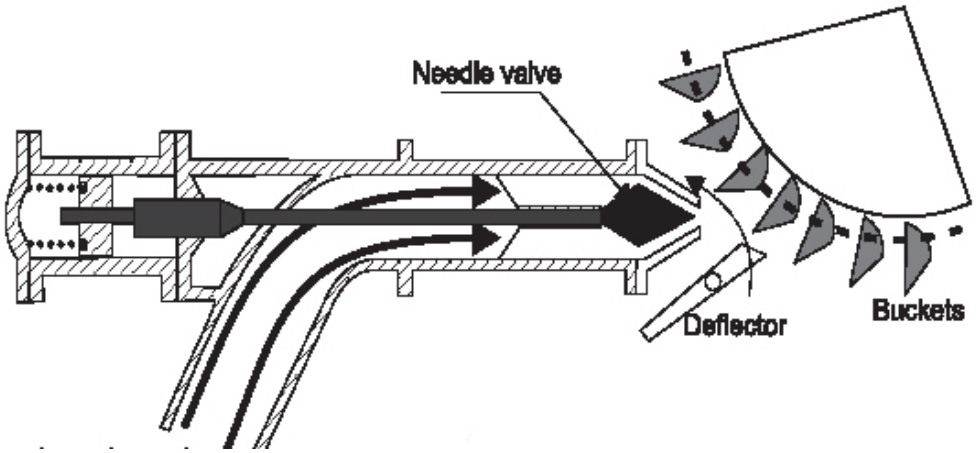

Figure 44: The Pelton wheel, needle valve, and deflection plates.[95]

It should also be noted in Figure 44 the nozzle is actually directly in line with the runner, which is not the case for a Turgo turbine, which is normally optimized for higher flows than the Pelton Wheel.[96] It can achieve these higher flow rates do to the fact that instead of aiming the jets parallel to the rotation of the runner, the nozzles are aligned at about 20º above horizontal and leave through runner blades on the under side of the runner as shown in Figure 45.

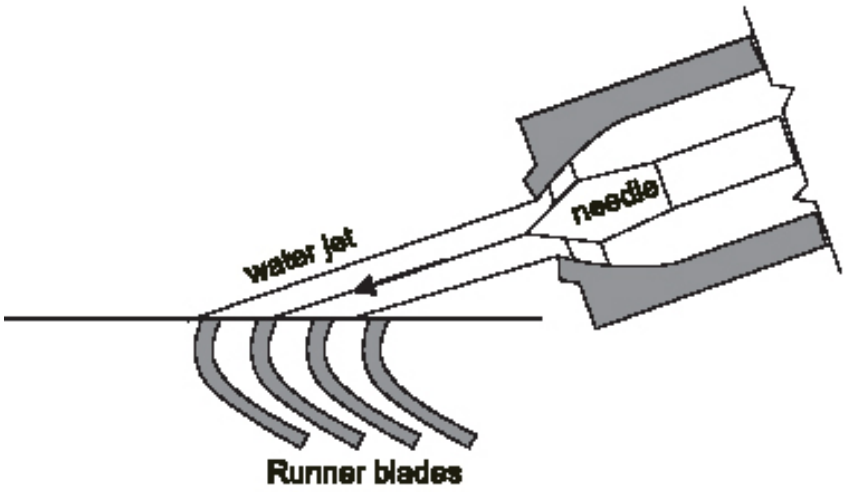

Figure 45: A Turgo runner with 20º impinging flow moving through its runner blades.[97]

Maximum flow through a Pelton turbine is restricted due to the fact that flow leaving each bucket can interfere with adjacent buckets; conversely, flow hitting a Turgo runner moves through it, giving rise to higher rotational speed and subsequently higher efficiencies.[98] One company that manufactures turbines with both Turgo and Pelton runners, recommends Pelton runners for flows up to 200 gpm and Turgo runners for flows between 200 gpm and 600 gpm.[99] Since there are very few companies that make low flow impulse turbines, and the above company is the only one that has a Turgo option, based on this information it is decided to select a Pelton turbine for this application.

7.6 Shunt Loads

As noted above, most low flow Pelton turbines do not have diversion plates to regulate load control. These small turbines are designed to be permanently connected to a battery bank. If the battery is disconnected and there is no load on the turbine, the runner will start to over-speed causing voltage spikes and increased wear on the mechanical equipment; since the increased rotational velocity is both proportional to voltage rise and mechanical fatigue in moving parts.[100] This is unacceptable, because the voltage spikes could harm the electrical equipment, and the mechanical fatigue will reduce the functional life time of the equipment, thereby increasing O&M costs.

In order to prevent a turbine from “over-speeding,” a shunt, or diversion load, must be connected to the battery bank that is roughly the same power requirement as the turbine output. This load will be connected to a shunt controller that is either pulse width modulated, turning the load on and off at varying frequencies depending on battery SOC, or charger/relay type, which turns on the load at a certain regulation voltage, when the batteries are near full SOC and shutting the load off once the batteries fall below a set voltage.[101] There are many charge controllers that can serve as diversion controllers;

however, certain controllers like the Outback MX60 should not be used due to possible voltage spikes that are greater than its maximum input of 150 VDC, as explained above in Chapter 6.

The easiest and most available shunt loads are heaters. As air heaters would be virtually useless in a climate such as Maui, water heaters could have some utility, for bathing, washing clothes, etc. Although DC-rated water heaters are somewhat limited in availability, Alternative Power & Machine Company manufactures and sells such heaters rated between 12 and 84 VDC, able to consume 0.2 to 17 kW of power. An example water diversion load is shown below in Figure 46.

Figure 46: A water heating diversion load.[102]

In addition to DC shunt loads, numerous AC shunt loads can be used; however, the power must be inverted first.

7.7 System Design

PVC or polyethylene plastic pipes are attractive materials for medium sized heads due to their low surface roughness coefficient and their relatively low cost, ranging between $0.50 and $5.31/ft for small diameter pipe.[103] As explained in Chapter 4, in order to utilize the entire 1200 feet of head at the north site, the penstock material would have to be constructed of steel, or some material with a

higher pressure rating than PVC. In order to achieve a gross head of only 500 feet, the pipeline must be run about 1.25 miles. Two inch, three inch, and four inch diameter steel pipe costs approximately $3.06/ft, $5.00/ft, and $6.59/ft, respectively.[104] This would make the cost for penstock alone anywhere between $20,000 and $40,000, which doesn't even cover the cost of the turbine, power house, and conductor cable to transport the power three miles. For these reasons and because only a meager 10 gpm can be extracted from the upper dam with any sort of reliability (producing only 500 watts), it is decided to power both sites with water extracted from the lower dam, which can provide 200 gpm with high reliability.

The 200 gpm can either be sent through one larger turbine, or split with 100 gpm feeding two smaller turbines. It seems reasonable to send the entire flow through one turbine due to the fact that a single larger turbine is cheaper than two smaller turbines. However, since the turbines must be permanently connected to a battery bank it is decided to employ two smaller turbines that are each connected to respective battery banks at the north and south sites due to difficulties with transferring power between battery banks and coordinating shunt loads. As shown in Figure 48, one penstock running from the lower dam will feed the two turbines. This flow is recombined into Palikea Stream via a tail race, and each site is wired separately. The required length of penstock is determined by GPS measurements to be approximately 1100 feet with a gross head of approximately 220 feet. If 100 gpm of flow is used per turbine; then an allowable penstock diameter can be determined by equations found in Appendix E.

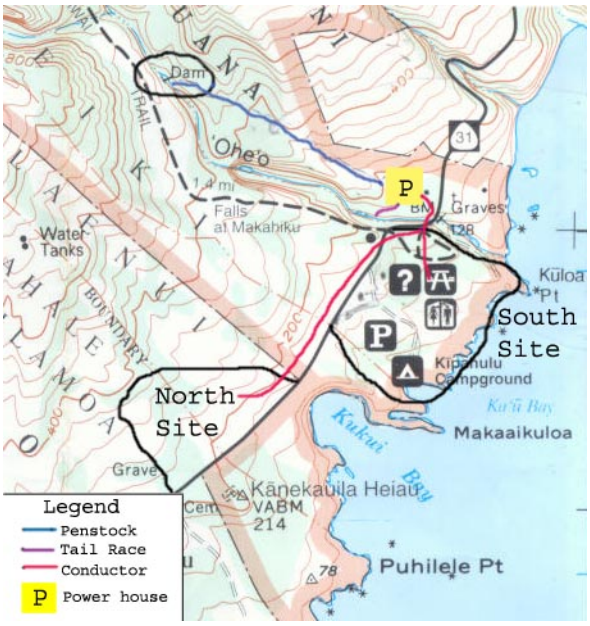

Figure 47: Lower dam will feed turbines supplying power to both the north and south sites.

One Pelton turbine on the market today designed to operate at low flow rates and high heads is the HI-Power Hydroelectric HV 1200 Turbine. At a net head of 115 feet and a flow rate of 100 gpm, the turbine is rated to 1.2 kW with an output voltage that can range between 120 and 440 volts of "wild" AC. With this high transmission voltage, the electricity can be sent long distances before being stepped down to battery voltage. It comes complete with a rectifier, transformer, and required fuses shown in Figure 49.

Figure 48: The HI-Power Hydroelectric HV 1200 turbine with accessories.[105]

It is found that 6'' PVC piping is large enough to accommodate a flow rate of 200 gpm resulting in a head loss of only 4% from a gross head 220 feet. This result is a low estimate since it is assumed that there are no bends in the pipe. In order to determine the actual number and degree of bends, the penstock run would need to be surveyed in more detail. It is difficult to predict the contribution to head loss that bends will have; however, It should be noted that if the bends are kept smaller than 22.5 degrees, a flow rate of 200 gpm in a 6'' diameter pipe will result in a head loss of less than a quarter of an inch per bend. It would take thousands of bends to cause any significant head loss; thus 6'' diameter pipe is proved to be sufficient to maintain adequate pressure at the turbine inlet.

Both the Morningstar TS-45 and the Xantrex C-40 can operate as a reliable diversion controller at a battery bank voltage of 48 VDC and have maximum input currents of 45 amps and 40 amps, respectively. The TS-45 and C-40 are both PWM controllers, which will lengthen the life of the battery bank as opposed to an "on/off" controller.[106] At 1200 watts and 48 volts, the controller will have to deal with 25 amps. Both controllers will do the job; however it is decided to use the Xantrex C-40, since it is both cheaper and more closely sized to the turbine than the TS-45.

The shunt load should be slightly larger than the hydroelectric output to ensure that the batteries will not become over charged. A 1.4 kW water heater has been selected for each site from APM Hydro at a cost of $406.[107]

The only component left to select is the required size of conducting wire. The conducting cable must at least be large enough to meet amperage standards made by the NEC as outlined in Appendix D; however, since the transmission voltage can be set as high as 440 VAC, and conductor lengths will be 0.25 miles and longer, voltage drop is the main concern. USE-2, underground service entrance, cable or the like should be selected, since it can be used in wet or dry

environments, and has a continuous operating temperature of 90 ºC. From GPS measurements, the conductor must run 0.25 miles to the south site, and another 0.5 miles to the north site. Setting the turbine output voltage to 440 VAC on both turbines and selecting 8 AWG USE-2 conducting cable, will keep voltage drops to under 2% for both circuits, which comes out to conductor capital cost for the north and south sites of $6,217 and $2,072, respectively. Including an installation cost of 10% of the capital, the capital cost for each hydroelectric site is broken down in Table 9.

Table 9: A capital cost break down of each hydroelectric system.

Component	North Site	South Site
HV 1200 Turbine with power conditioning	$3,000	$3,000
Water Intake	$400	$400
Turbine Housing	$125	$125
Xantrex C-40 Charge Controller	$105	$105
Digital Readout Meter	$65	$65
Battery Temperature Sensor	$19	$19
6 inch diameter PVC pipe at $5.31 per ft	$3053	$3053
Shunt Load	$406	$406
Conducting Cable	$6,217	$2,072
Installation (includes the cost of building a small power house)	$1,332	$918
Total	$14,617	$10,163

Replacement costs include bearings on the alternators, the Pelton wheels, and the charge controllers; these will need to be replaced every couple years as

shown in Table 10. The replacement costs are used in performing a life cycle cost analysis on the system, outlined in Chapter 8.

Table 10: A replacement cost breakdown for the hydro components.

Component	Cost	Years Until Replacement
Bearings	$37	5
Pelton Wheel	$275	5
Xantrex C-40	$105	10

8. Economic Analysis and System Configurations

8.1 Introduction

After defining electricity consumption and demand, assessing energy resource potential, and selecting appropriate equipment to harness this energy, it is necessary to perform an economic analysis in order to determine the optimum system configuration for Kipahulu. The four system configurations that are analyzed are as follows:

1. Solar PV with backup propane-fired gensets.
2. Solar PV with micro-hydro and backup propane-fired gensets
3. Propane-fired gensets only
4. Grid Extension.

Each configuration is sized to meet the total projected electrical demand and consumption laid out in Chapter 1. The optimal system arrangement is determined within each configuration. For example, in the case of configuration 1, the size of the solar array will be inversely proportional to generator run time; thus, there will be an optimal arrangement where increased generator operating and maintenance expenses will offset the capital cost of a larger array. The same is true for configuration 2; since the hydro resource potential is assumed constant as outlined in Chapters 3 and 7. For system configuration 3, the genset only system, the propane generator must be sized large enough to meet peak electrical demand and small enough so it runs as close as possible to full loading for maximum efficiency. Unlike the other system configurations, there is not really an optimal arrangement for configuration 4, grid extension. Maui Electric has quoted an installed capital cost for the grid extension and the cost of grid electricity will be assumed constant corresponding to 2005 rates. The optimum

system arrangement is determined within each configuration, and the optimum arrangements from each of the configurations are compared amongst each other in regards to total capital cost, life cycle cost, annualized life cycle cost, reliability and cost of electricity.

8.2 Economic Model

The initial costs of these options will be different as will the costs of operation, maintenance, and repair or replacement. A Life Cycle Cost (LCC) analysis can help compare the power supply options.

The upfront capital cost of a purchase often does not give a true picture of the future implications of that acquisition. For example, the capital cost of two vehicles will be different as will the operational costs (fuel mileage), replacement, maintenance and repair costs. The more expensive car upfront may prove to be more cost effective over the lifetime of the vehicle due to savings in fuel, repair, and maintenance. Likewise, in order to compare different energy system configurations and determine the most cost effective design, a life cycle cost analysis is performed.[108] When comparing system configurations, it is convenient to refer to all costs in present value dollars. The costs may be upfront, happen yearly or every couple of years over the lifetime of the system, which is usually defined to be 20 years for a PV system.[109] Since the original request for this study is to design a PV system for Kipahulu, each system configuration is analyzed over a 20 year lifetime. The life cycle cost of each system analyzed is composed of five distinct parts:

1. The capital cost of the system can include modules, array racks, inverters, charge controllers, gensets, penstock, turbines, batteries, conductors, over-current devices, any miscellaneous balance of system components, any necessary installation and shipping costs, and the initial cost of a grid extension, if applicable. The capital cost is in present value.

2. The operating cost of the system includes all operational costs associated with the system over its life time. The only operating cost for system categories 1 through 3, in this analysis, is the cost of fuel for running the propane generators. The cost of buying grid electricity is treated as an operating cost for category 4. Operating costs need to be converted into present value.
3. The maintenance cost of the system can include watering the batteries, cleaning modules, turbine maintenance, replacing fuses, and any required generator maintenance like oil changes and valve adjustments. Maintenance costs need to be converted into present value.
4. The replacement cost of a system can include batteries, charge controllers, inverters, turbine rotors, and generators (if run often enough) that need to be replaced throughout the life time of the system. Replacement costs need to be converted into present value.
5. The salvage value of a system is its net present value at the end of the system life. The salvage value is commonly defined as 20% of the installed capital cost of any equipment that can be moved off site.[110]

The present value of a cost is dependant on two variables: the inflation rate, i, and the discount rate, d. The inflation rate is a gauge of how the value of money diminishes over time. For example, if the annual inflation rate is 2%, then an item that costs $1,000 today will cost $1,020 dollars next year. The discount rate is a measure of the return that can be earned on a present day investment.[111] For example, if a $1,000 investment is made today at a discount rate of 8%, the investment will be worth $1080 dollars next year. The net present value, NPV, of any future cost is defined as the required capital investment at the present day in order to purchase the item later, assuming a return rate of d and an inflation rate of i.[112] Instead of using the nominal discount and inflation rates, in renewable energy feasibility studies it is common practice to use the real, or net discount rate defined by Equation 8.1.

$$d_{net} = \frac{1 + d_{nom}}{1 + i} - 1$$ **Equation 8.1**[113]

where,

- d_{net} is the net discount rate
- d_{nom} is the standard nominal discount rate in the U.S. today, assumed to be 8%
- i is the inflation rate

The NPV for any future expenditure or gain is determined from Equation 8.2.

$$NPV = \frac{F}{(1 + d_{net})^n}$$ **Equation 8.2**[114]

where,

- NPV is the net present value of the future sum
- F is the future sum of money
- d_{net} is the net discount rate defined in Equation 8.1
- n is the year given year in the future

If there is a recurring cost such as fuel or operating cost that happens yearly, the cumulative present worth of an annual cost is given by Equation 8.3.

$$Pa = \left[1 - \frac{1}{(1 + d_{net})^n}\right] \frac{A}{d_{net}}$$ **Equation 8.3**[115]

where,

- Pa is the cumulative present worth of an annual cost
- d_{net} is the net discount rate
- n is the period of years over which the sum is paid
- A is an annual sum of money

The life cycle cost, LCC, of an item is then given by Equation 8.4.

$$LCC = C + M_{pw} + O_{pw} + R_{pw} - S_{pw}$$ **Equation 8.4**[116]

where,

- LCC is the life cycle cost
- C is the capital cost

- M_{pw} is the present worth of the maintenance costs
- O_{pw} is the present worth of the operating costs
- R_{pw} is the present worth of the replacement costs
- S_{pw} is the present worth of the salvage value

One common way to compare two or more configurations is to compare the cost of electricity, COE, which is defined below in Equation 8.5.

$$COE = \frac{Costs_{Annual}}{Energy_{Annual}} \qquad \textbf{Equation 8.5}$$

where,

- COE is the cost of electricity in $/kWh
- $Costs_{Annual}$ are the annualized costs broken up over the entire lifetime of the project in $, which can be found by Equation 8.5.
- $Energy_{Annual}$ is the annual energy production in kWh

$$Costs_{Annual} = ACC + ARC + AOC - ASC \qquad \textbf{Equation 8.5}^{117}$$

where,

- ACC is the annualized capital cost
- ARC is the annualized replacement cost
- AOC is the annualized maintenance and operating cost
- ASC is the annualized salvage cost

Since the total capital cost of a project will be paid off over the lifetime of the system, it would be inaccurate to include the entire capital cost in calculating the cost of electricity. The correct measure to take is to multiply the total capital cost by the capital recovery factor, CRF, shown in Equation 8.6.

$$CRF = \frac{d_{net}\left(1 + d_{net}\right)^{n}}{\left(1 + d_{net}\right)^{n} - 1} \qquad \textbf{Equation 8.6}^{118}$$

where,

- CRF is the capital recovery factor

- d_{net} is the net discount rate
- n is the system life of the project

The annualized capital cost is then given by Equation 8.7.

$$ACC = CRF * CC$$ **Equation 8.7**[119]

where,

- ACC is the annualized capital cost
- CRF is the capital recovery factor
- CC is the total capital cost

Since operating and maintenance costs are already given in annual amounts, the annual operating cost will not need to be modified.

In order to annualize replacement and salvage costs, it is necessary to first put this cost into present value using Equation 8.2; then apply a CRF that is specific to the year in which the cost occurs, as shown in Equation 8.8.

$$ARC = \frac{RC}{(1+d_{net})^{n}} \frac{d_{net}}{(1-(1+d_{net})^{-n}}$$ **Equation 8.8**[120]

where,

- ARC is the annualized replacement cost
- RC is the actual replacement cost
- d_{net} is the net discount rate
- n is the year in which this replacement occurs

Note that an annualized salvage cost can be determined by Equation 8.8, by substituting the salvage cost for the replacement cost, and setting n equal to the system life, since that is the year when salvage will occur.

The operating and maintenance costs will be composed of yearly generator fuel consumption, yearly generator oil changes, and annual PV maintenance. The replacement costs will be composed of generator valve replacements and

generator rebuild outlined in Table 8, and PV component replacements outlined in Table 11.

Table 11: Time to first replacement for PV components.

Component	First Replacement (years)
Batteries	5
Inverters	10
Charge Controller	10

Note that batteries will need to be replaced every 5 years, or 3 times throughout the life of the system, and inverters and charge controllers will need to be replaced every 10 years, or once throughout the system lifetime of 20 years.[121]

The replacement times and costs for the hydro components are displayed in Table 10. Hydro salvage credits are not included, because often the salvage value is just enough to cover the cost of decommissioning the system.[122]

8.3 System Model

The PV/hydro hybrid system model can be explained with the aid of Figure 49.

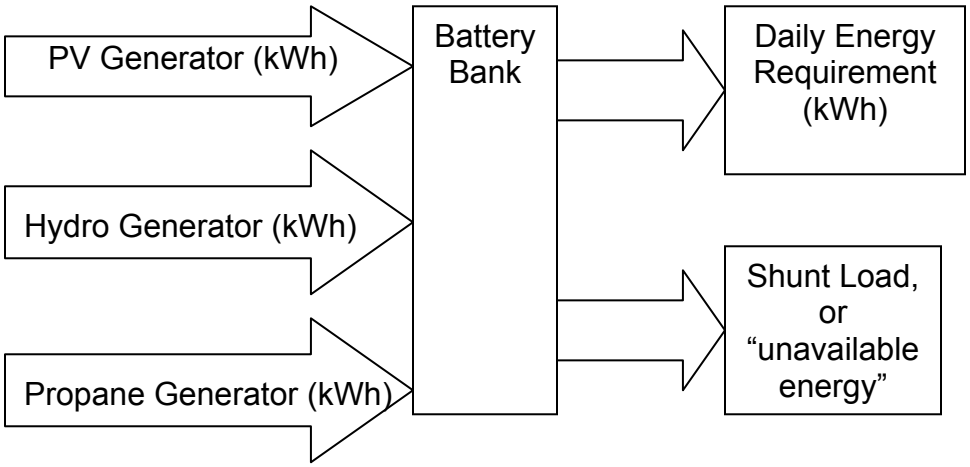

Figure 49: An energy flow diagram for a PV hybrid system.

Shown in Figure 49, the system is modeled as a battery bank supplying a daily energy requirement with three different power generators supplying energy into the battery bank. The daily energy requirement does not change throughout the year, and after accounting for inverter inefficiencies, battery charging/discharging inefficiencies, and wire losses, the daily energy requirement has been converted into amp -hours and found by Equations 4.3 and 4.4 to be 1,638 and 1,205 amp hours per day for the north and south sites, respectively.

8.3.1 PV Generator

The PV generator contribution is determined as the sum of the hourly contributions throughout one day. As explained in Chapter 3, hourly solar irradiance and temperature data are supplied by the NRSDB. Each hour, the panels are temperature derated and their maximum power point efficiency is calculated by Equation 8.8 if the sun is out, and set to zero if there is no irradiance. Also note if the cell temperature is less than the standard test

temperature; then, η_{MPP} is set equal to the power point efficiency at standard test conditions.

$$\eta_{MPP} = \left(\frac{P_{\max}\left[1 + C*\left(T_{cell} - T_{SOC}\right)\right]}{G_{SOC} A_{\mathrm{mod}ule}} \right) \quad \textbf{Equation 8.8}$$

where,

- η_{MPP} is the temperature adjusted max power point efficiency
- P_{max} is the maximum power output at standard test conditions in watts
- C is a temperature correction factor for the maximum power at an elevated temperature
- T_{cell} is the module operating temperature calculated from Equation 5.5
- T_{SOC} is the module operating temperature at standard test conditions, or 25 ºC
- G_{SOC} is the solar irradiance at standard operating conditions, or 1,000 W/m^2
- A_{module} is the module area in m^2.

It should be noted that by using Equation 8.8, it is assumed that the modules are operating at their maximum power point, or a MPPT charge controller is connected in the circuit. If a MPPT charge controller is not used; then, Equation 8.8 would have to be modified. The hourly energy produced is then calculated by Equation 8.9.

$$E_{hourly} = \eta_{MPP} N_{\mathrm{mod}ules} A_{\mathrm{mod}ule} G \quad \textbf{Equation 8.9}$$

where,

- E_{hourly} is the hourly energy produced in watt-hours
- η_{MPP} is the temperature adjusted maximum power point efficiency given in Equation 8.8
- $N_{modules}$ is the number of modules in the array
- A_{module} is the module area in m^2.
- G is the hourly solar irradiance from a typical meteorological year, as explained in Chapter 2, in watt-hours/m^2.

The hourly energy production is then summed over each day to arrive at the total PV energy contribution throughout the year.

8.3.2 Hydro Generator

For the system model, the hydro generator can either be on or off. Meaning that there is either hydro installed at the site and it is producing a constant 1200 W for each respective site all of the time, or there is no hydro installed. The hydro contribution has been considered to be constant, even though the lower dam can only supply 200 gpm 91% of the time for the driest month of the year, as shown in Figure 16. This assumption is thought to be reasonable because of the findings shown in Figure 13 of Chapter 3, which shows that if the hydro resource is low; then the solar will probably take up the slack. With a constant power output of 1200 watts, each turbine supplies 28.8 kWh of energy per day to each respective battery bank. This sum is added to the daily PV contribution to give the total daily PV/hydro contribution.

8.3.3 Propane Generator

First the PV/hydro contribution, or the PV contribution if there is no hydro, is converted to amp-hours and compared to the corrected daily amp-hour consumption. If the daily renewable energy contribution is larger than the daily consumption; then, the batteries are set to full charge and the excess energy is discarded, or sent to the shunt load. Any time the charge controllers have to either shunt the PV array or send energy to the water heater, this energy is thought of as discarded. Although, technically the water heater is producing useful energy, it is assumed that this energy has not been produced for total production purposes.

If the daily renewable energy contribution is smaller than the daily consumption; then the battery state of charge is calculated. If the battery state of charge is below 70%; then, the generator will turn on, and charge the batteries full. If the battery SOC is not below 70%; then, the model moves to the next day, adding the previous days charge deficiency to the daily consumption and a new battery SOC is calculated. Once the battery falls below 70%, the batteries are fully charged by the propane generator and the process repeats itself. The daily SOC of the batteries for the month of January is shown in Figure 50 for the north side with a hydro turbine and a 40 module array.

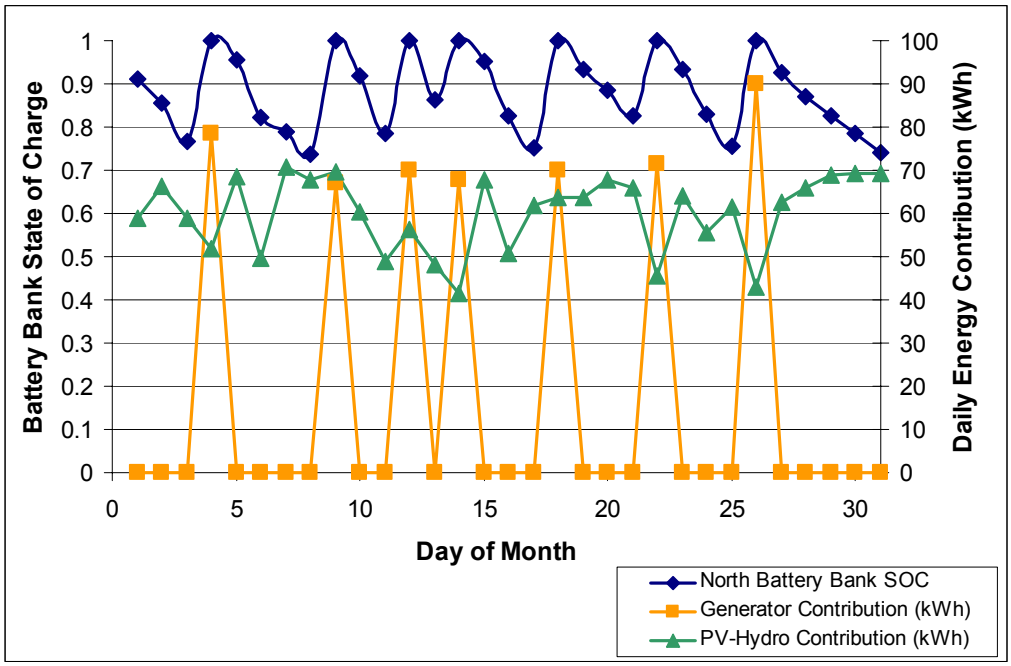

Figure 50: A System model for the month of January.

Notice that the generator turns on sporadically, anywhere from once every three or four days to every other day. Also notice that during days when the PV/hydro contribution is low, the generator is more likely to turn on within a day or two. As an example, look at the sixth day of February. The renewable contribution to the battery bank was relatively low at about 50 kWh compared to the approximately 79 kWh consumed at the north site for that day. This low contribution was not low enough to warrant the need for the propane genset to turn on; however, it

was low enough to cause the genset to turn on two days later; even though the renewable contribution to the battery bank was relatively high for those two days.

The generator run time is determined by dividing the total generator energy contribution by its charging power in kW as shown in Equation 8.10.

$$RunTime = \frac{\mathrm{Pr}\,oduction}{Ch\,\mathrm{arg}\,ingPower} \qquad \textbf{Equation 8.10}$$

where,

- RunTime is the generator run time in hours
- Production is the daily generator contribution in kWh
- Charging Power is 90% of the power rating of the generator in kW as outlined in Chapter 6.

This generator run time is then summed over the year, and is used to determine annual replacement intervals for oil changes, valve adjustments and replacements from the hourly replacement intervals given in Table 8.

Shown by Equation 8.11, the daily fuel consumption is calculated by dividing the yearly generator energy contribution in kWh by the generator fuel conversion efficiency found by Equation 6.1.

$$FuelConsumption = \frac{\mathrm{Pr}\,oduction}{FuelConversionEfficiency} \qquad \textbf{Equation 8.11}$$

where,

- FuelConsumption is the daily fuel consumption in gallons
- Production is the daily generator contribution in kWh
- FuelConversionEfficiency is the generator fuel conversion efficiency at 90% of its rated load in kWh/gallon.

The daily fuel consumption is then summed over the year and multiplied by the cost of propane to determine the annual fuel cost. The Utilities Gas Company in Kahului can deliver the fuel to the site and has quoted a cost of propane of $3.75

per gallon, which includes tax and shipment to Kipahulu.[123] This cost of propane is much larger than initially assumed, which plays a significant role in the economic analysis. For reference, the Kohler 15 RYG genset is found to have a fuel conversion efficiency of 6.42 kWh per gallon from Equation 6.1. If the cost of propane is $3.75 per gallon, the generator would be producing energy at $0.58 per kWh without any capital, replacement, or maintenance costs factored in. If delivered fuel costs are assumed to be $1.38 per gallon, as they were 10 years ago for a similar study at Dangling Rope Marina on Lake Powell,[124] the generator would be nominally producing energy at $0.21 per kWh. This is traditionally a more common cost of electricity for a propane-fired generator disregarding capital and replacement costs.

8.3.4 Determining the Optimal Configuration

In order to determine the optimal configuration, a MatLab code has been written to iterate through different configurations, and return the system arrangement that produces the lowest CoE. Due to the fact that the goal of this project is to design a renewable energy system, both the north and the south sites are initially assigned array sizes of 28 and 12 modules, respectively in the model. Since each system has a PV array, both battery and inverter banks sizes are assumed to be constant for each system regardless of the array size. If one was modeling a propane-fired genset only system, the battery and inverter banks would be left out, and the generator efficiency would have to be derated, because it would not always be operating at peak efficiency. For each PV/hybrid system, the generator will be assumed to be charging the batteries at its highest efficiency, or 90% of its rated output.

The model calculates all of the costs associated with each system; then it augments the PV array and calculates all of the costs for the enlarged system. For this particular model, the code increases the array by a string of 4 modules

after each iteration. In order to ensure that the array voltage is always above the battery voltage, the modules have to be strung in groups of four, as discussed in Chapter 5. If a different module is chosen; then the code determines the optimal string size that is both below the maximum voltage input of the MX60 and comfortably above the battery bank voltage and augments the array by this new string size.

When the array is augmented, charge controllers, conductors, breakers, and array rack sizes are adjusted accordingly, battery and inverter bank sizes remain constant, and generator replacement and operating costs diminish according to decreased generator run time. The CoE is calculated for each system, and the configuration with the lowest CoE is the chosen one.

8.4 Results

The north site is modeled with and without the inclusion of hydro. Similarly, the south site is modeled with and without the hydro; in addition to being mounted on the roof, or ground mounted. Shown below in Figures 51 and 52 are the results for the north and south sites both with and without hydro.

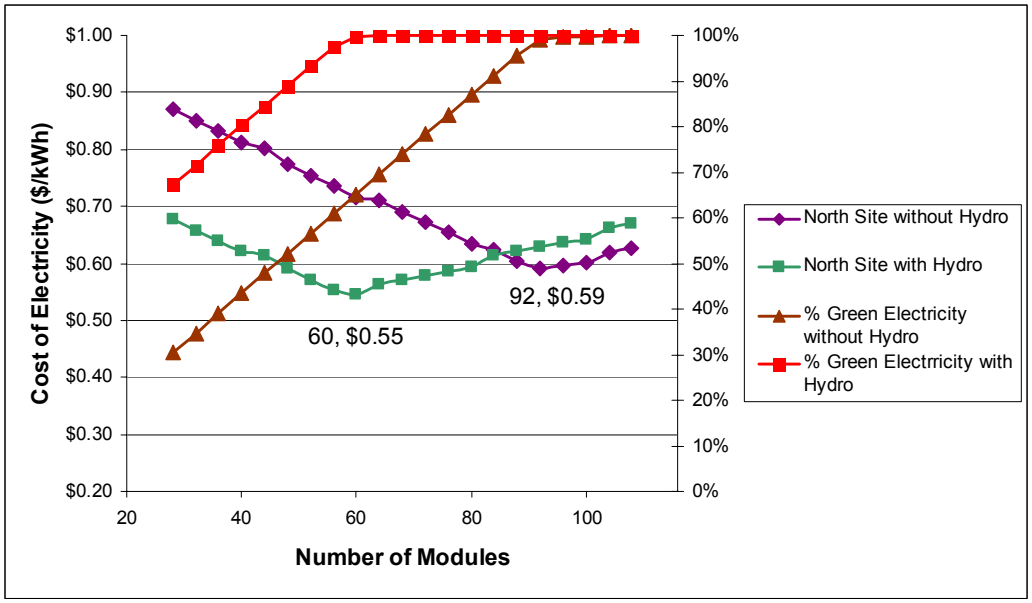

Figure 51: Cost of electricity vs. array size for the north site both with and without hydro.

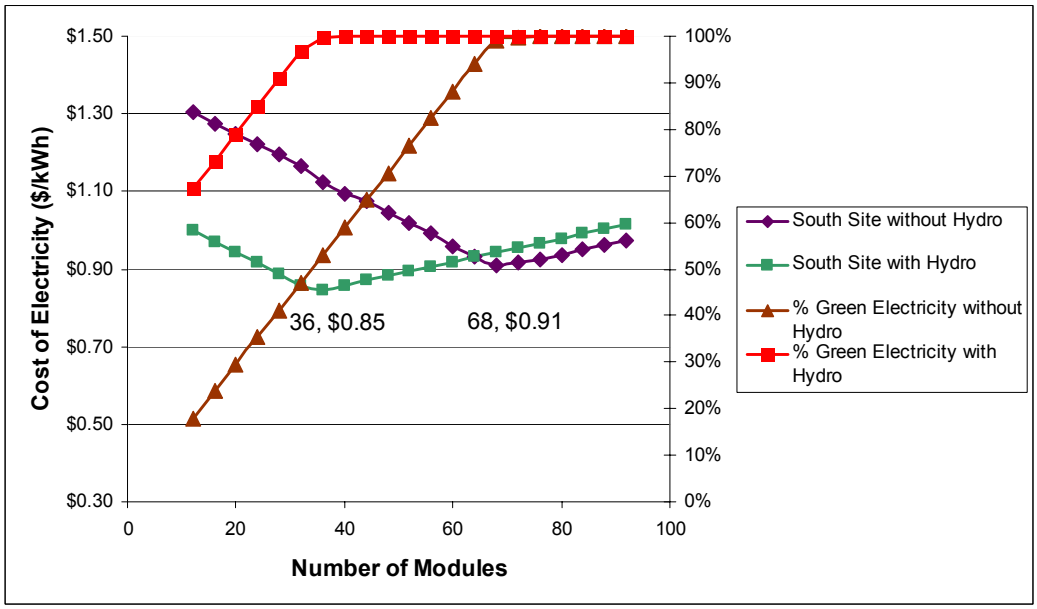

Figure 52: Cost of electricity vs. array size for the south site both with and without hydro.

The optimal array sizes for the north site with and without hydro are 60 and 92 modules, respectively, producing electricity at $0.55/kWh and $0.59/kWh. Because of the large cost associated with building the structure to both mount the modules and house the electrical equipment at the south site, the optimum configurations have a considerably higher cost of electricity than the north site

with array sizes of 36 and 68 modules producing electricity for $0.85/kWh and $0.91/kWh with and without hydro, respectively. It is obvious that the addition of hydro into either site is beneficial to the overall economics, taking 4 and 6 cents off the COE per north and south site, respectively.

It is also important to note the large cost of propane plays a major role in the optimum configuration. As shown above, the optimum configuration occurs nearly at the same point where the system is producing nearly 100% green electricity – that is, the propane gensets are seldom used. The effect of the cost of propane on the optimum north site configuration is shown below in Figure 8.5.

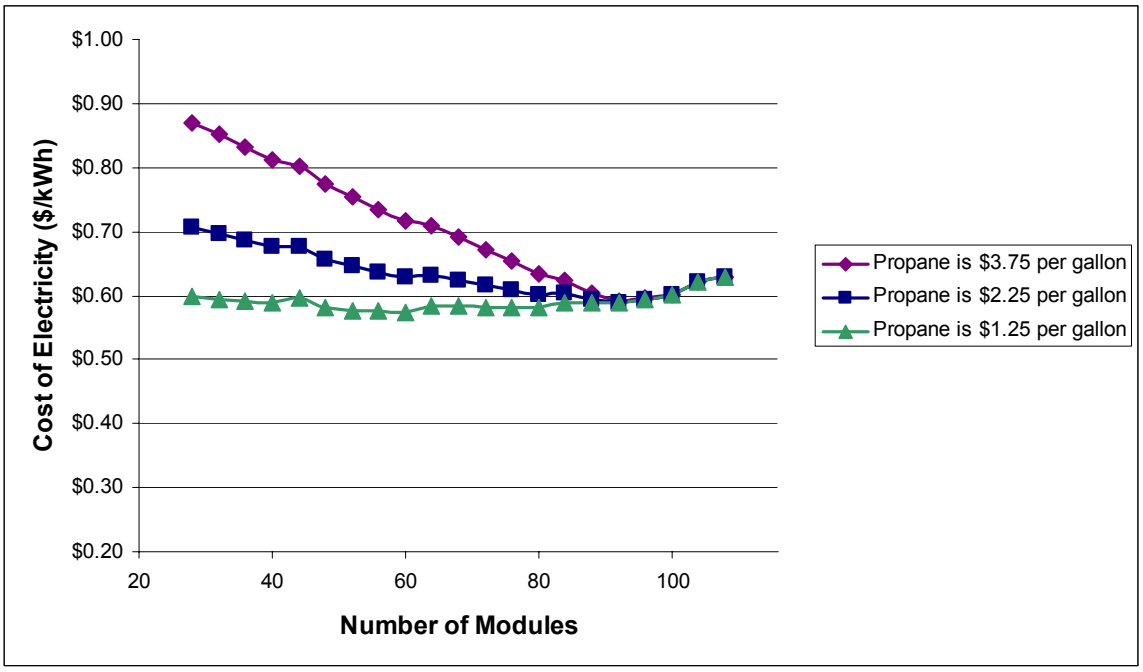

Figure 8.5: Cost of electricity vs. array size for the North site for 3 different propane costs.

Shown in Figure 8.5, changing the cost of propane from $3.75 per gallon to $2.75 per gallon flattens out the curve, meaning that an increased array size has less of an effect on decreasing the CoE; however, $2.25 per gallon is still large enough to force the array large enough to provide nearly 100% of the energy from the green sources (PV/hydro). Decreasing the cost of propane to $1.25 per gallon flattens out the curve even more than the previous case, and the cost is low

enough to make it more economical to have a small array allowing the generator to run more often. Another point worth noting is the small spikes in each curve at 40, 60, 80, and 100 modules. These small spikes correspond to the addition of another charge controller into the system and all of the necessary breakers, conductors, and junction boxes that go with it. The spikes are more pronounced at a lower cost of propane for the reason that the curve is flatter. Since propane has been quoted at $3.75 per gallon, this number is used for all further analysis.

Figures 53 through 56 are pie graphs showing the life cycle cost breakdown for each of the optimum configurations for the north and south sites.

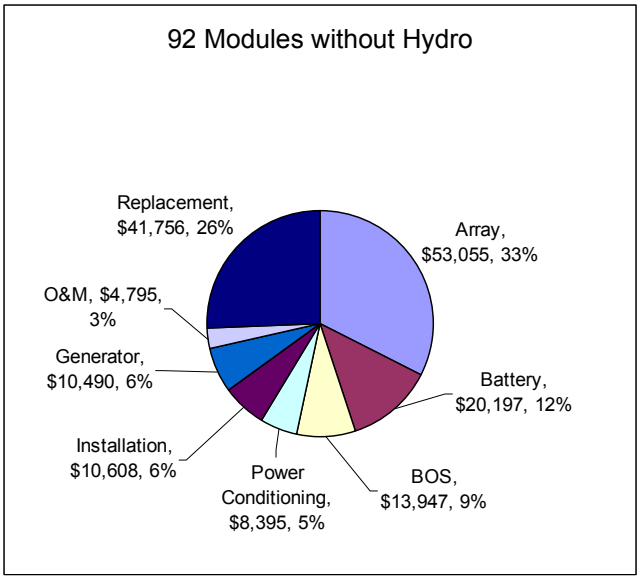

Figure 53: LCC breakdown for the north site without hydro.

The cost breakdowns shown in Figures 53 and 54 are not surprising. The O&M cost is quite small for both configurations, noting from above that the generator run time is very low for each optimum configuration. The capital cost of the array is the largest cost for the system without hydro, while replacement costs make up the majority of the cost for the system with hydro.

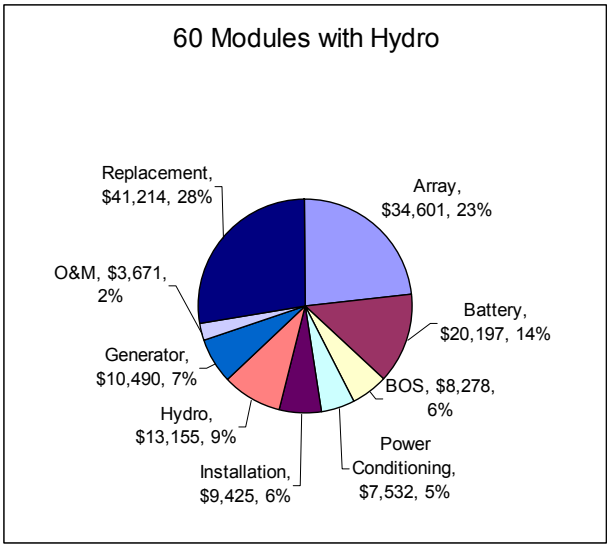

Figure 54: LCC breakdown for the north site with hydro.

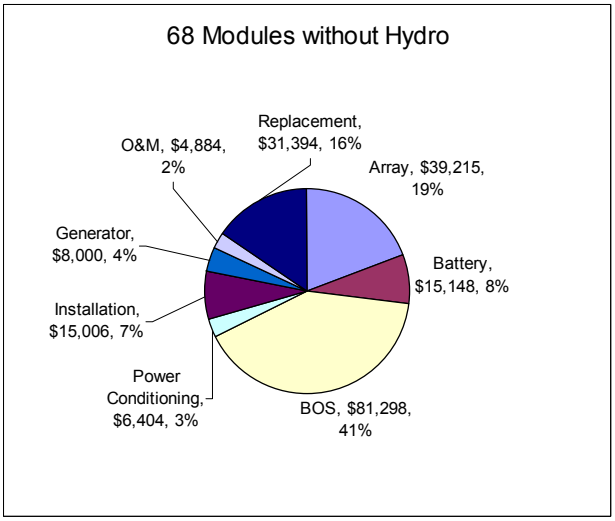

Figure 55: LCC breakdown for the south site without hydro.

Likewise for the south site, the O&M costs shown in Figures 55 and 56 make up a small percentage of the LCC. An obvious difference between the two sites is the fact that the balance of system, BOS, for the south site is by far the largest contributor to the overall LCC. The need for the $75,000 structure to both mount modules and house electrical equipment is the major contributor to this cost.

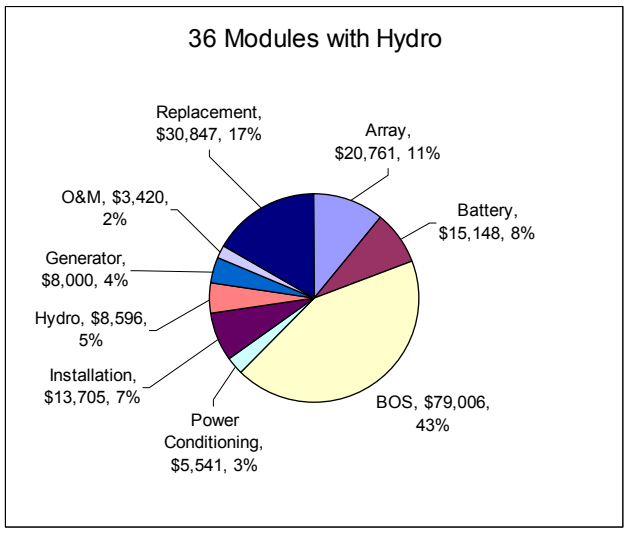

Figure 56: LCC breakdown for the south site with hydro.

Shown below in Figure 57 is a cost comparison assuming that the south site is mounted on high profile array racks, similar to that of the north site.

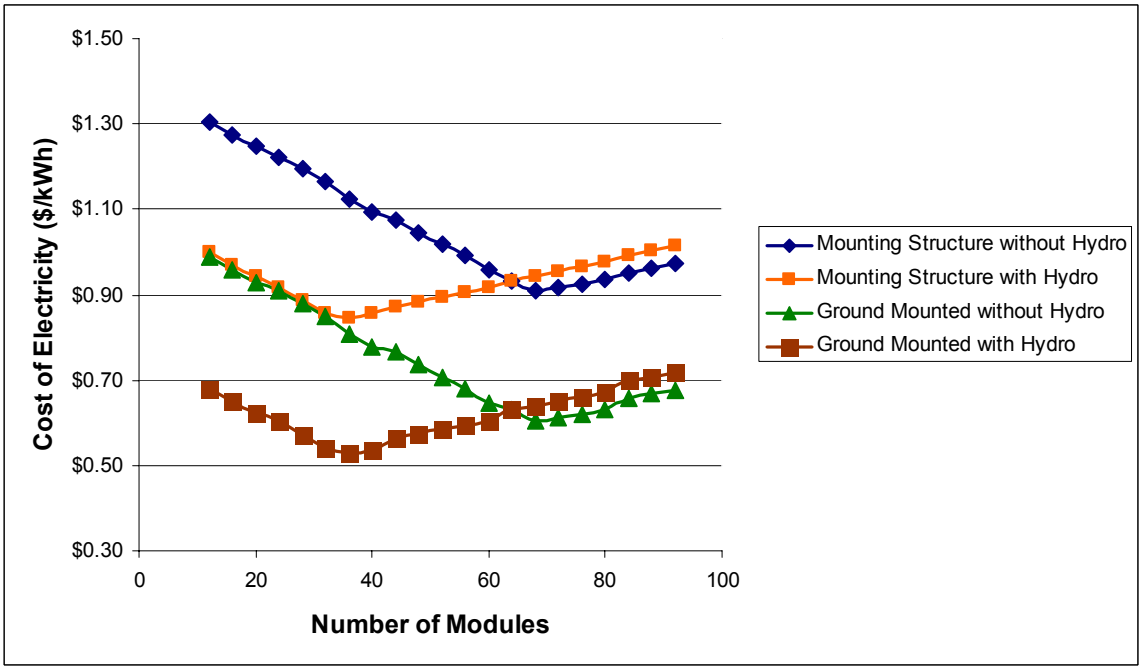

Figure 57: Comparison of the CoE for the south site with and without hydro.

If the modules are mounted on the ground, the CoE of is estimated to be about 30 cents less at the optimum configuration with propane costs held at $3.75/gal. Another point to note is that the quote from Haleakala Maintenance Department

of $75,000 to build the mounting structure is just an estimate; it could be higher or lower. As shown in Figure 57, a change in the cost of the mounting structure will shift the curve up or down; however, the optimum array size remains constant.

In summary, the optimum configurations for each site with and without hydro use the backup genset very little. The addition of hydro into each system reduces the CoE by 4 to 6 cents per kWh; however, it may not be worth the added complexity or capital cost that will be required for this system. It is still recommended to build a mounting structure for the south site array. Although it is expensive, it is necessary to at least build a structure to house the electrical equipment.

The complete Electrical Diagrams for each of the optimum configurations are displayed in Appendix F. The parts lists are shown in Appendix G.

8.5 Generator Only System

Although it is not the goal of this study to design a system that is solely composed of a generator (ie, genset), a generator only system has been modeled for benchline comparison. In order to model a system that is running on a generator only, one can not assume that it is running at peak efficiency charging batteries. The generator will meet whatever load is present; thus, if an 11 kW generator is only powering a 5 kW load; it will be running at a lower efficiency.

The average percentage of rated output a generator produces must be estimated; however, this is not an easy estimation. The CoE for power produced by a generator at a constant fuel cost is highly sensitive to the percentage of rated output at which the generator is running. Not only will the generator have to run longer at a lower charging output, it will also be running at lower fuel

conversion efficiency. Longer run time and higher fuel consumption are both costly over the system life, increasing maintenance, replacement, and fuel costs. Fuel is assumed to cost $3.75 per gallon, and the maintenance and replacement schedules are the same used in the above model taken from Table 8. The Kohler 15RYG genset is modeled in Figure 58, and the COE pertains to this generator providing the north site with its yearly energy demand.

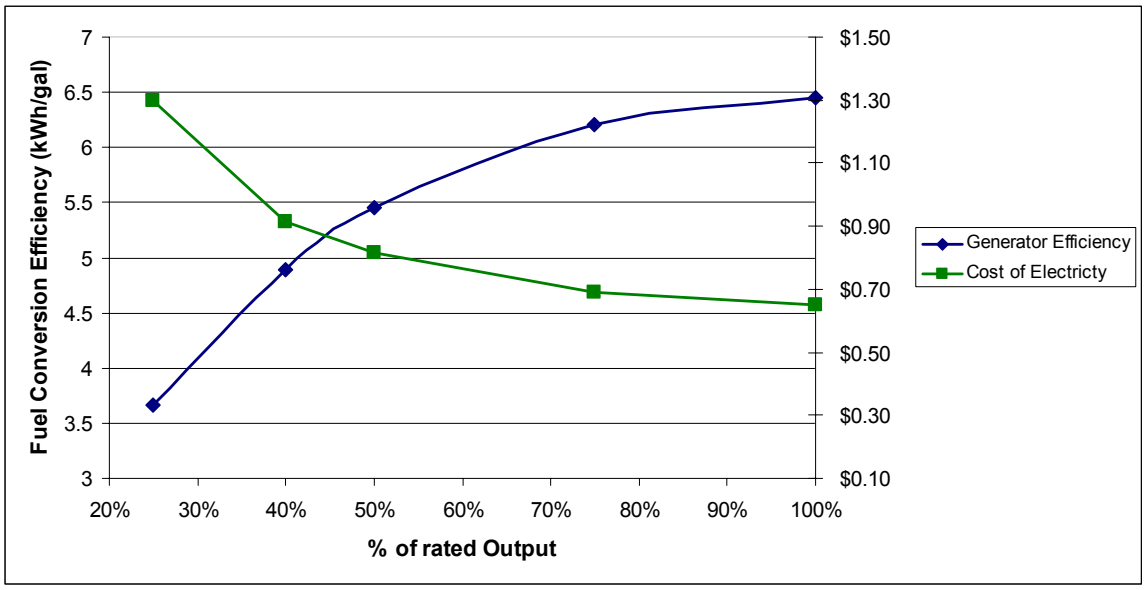

Figure 58: The effect of generator load on fuel conversion efficiency and CoE for the Kohler 15RYG genset.

In a similar installation at Pinnacles National Monument, the gensets are replaced every 7 years. They use the same replacement interval of 30,000 hours, which corresponds to an average generator loading of about 40%.[125] This generator loading is used for this model. Even running at 100% of its rated capacity, the 15 kW Kohler generator cannot produce electricity at less than $0.68/kWh, which is a higher cost of electricity than both renewable configurations with and without hydro. This genset system does not include any battery bank, or inverters. It is composed solely of the engine/generator, which causes the capital cost of this configuration to be by far the cheapest. Capital savings upfront are nowhere near large enough to offset the huge O&M cost shown in Figure 59. High fuel cost and inefficient electrical loading are the major

contributors to this huge annualized cost. Assuming a 40% load, the operating cost of a propane genset at the north site would be nearly $50.00 per day on fuel alone as shown below.

$$\frac{64.5kWh}{day} * \frac{gallon}{4.9kWh} * \frac{\$3.75}{gallon} = \frac{\$49.36}{day}$$

This would add up to over $18,000 per year in propane cost, which is the vast majority of the O&M cost with the remainder composed of routine oil changes and valve adjustments. Take note that the capital and replacement costs have been annualized for comparison.

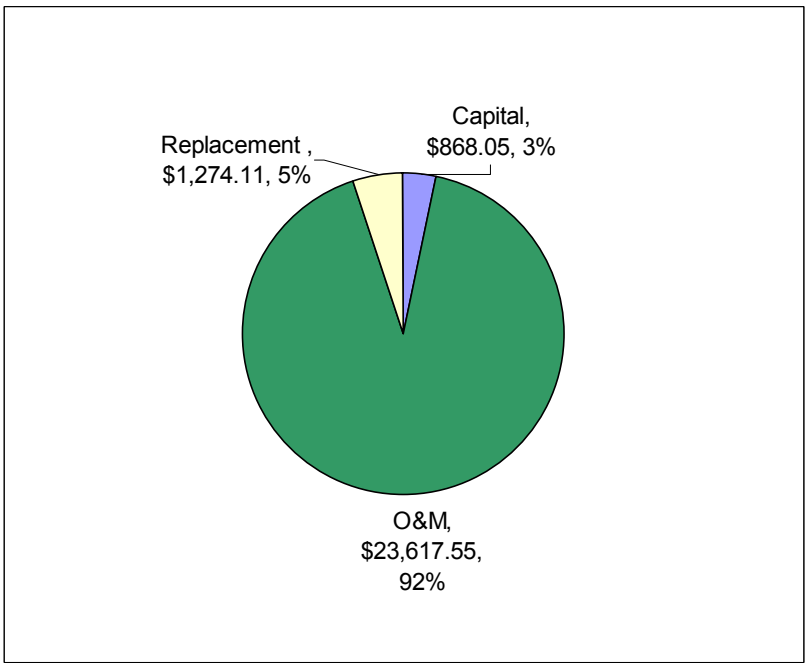

Figure 59: The annualized life cycle cost breakdown of a generator only system powering the north site.

The life cycle cost of a generator only system is compared to the life cycle cost of electricity produced from a PV/hydro system installed at the north site. Shown in Figure 60, the generator only system comes out as the best option if propane prices fall far below what they are today to $1.38 per gallon. However, at present $3.75/gallon cost, the generator only approach is the most expensive.

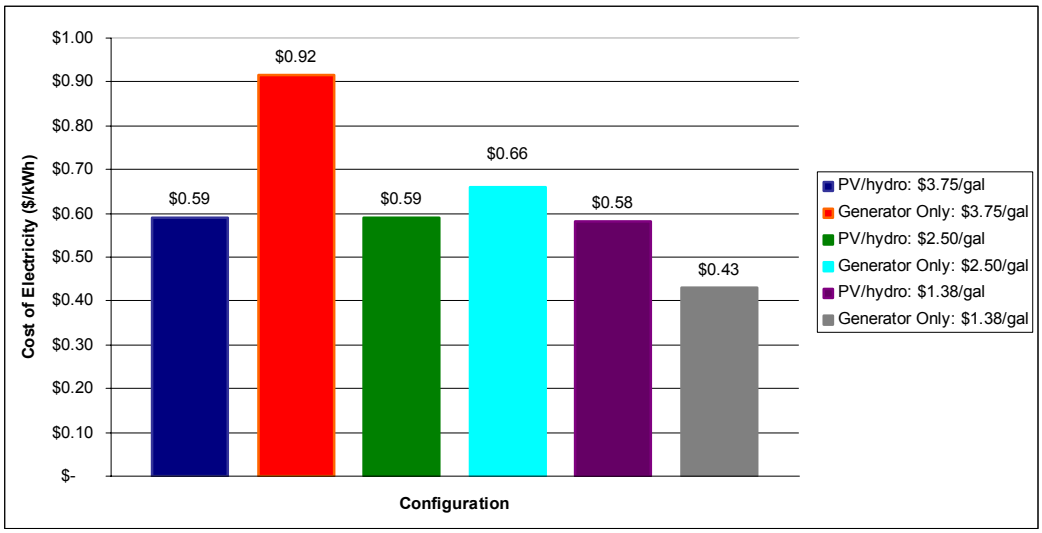

Figure 60: The effect of propane cost on the CoE for both a PV/hydro system and a generator only system powering the north site.

Shown above, the generator only columns correspond to the CoE for the generator operating at a loading of 40% at three different costs of propane. It is clear that the generator only system is not even cost competitive when propane costs $2.50 a gallon. If propane costs $1.38 per gallon the generator only system is the most economical option. Since propane will probably never cost $1.38 per gallon again due to a world wide rise in fuel prices, the generator only system should not be considered. Even if the generator runs at 100% of its rated load, the system is still not cost competitive at such high fuel costs. The model displayed in Figure 60 does not include the additional costs associated with a battery and inverter bank, which would be necessary if the generator were assumed to run at 100% loading. In addition, it should be noted that there is no green power contribution from propane, since it is derived from oil refining or separation from natural gas.

8.6 Grid Connection

Mark Prince, from the Maui Electric Company's Engineering Department has provided a quote for a grid extension. The grid is approximately four miles north

of the Kipahulu Visitor Center on Hwy 31. Maui Electric has offered to extend a 3-phase delta configuration to the two sites at Kipahulu for approximately $711,000 installed capital cost.[126] This is an approximate cost, estimated to be valid +/- 10%. This is a huge capital investment, and it does not include the life cycle cost of buying expensive Maui electricity, which according to Frank Baublits, the chief of maintenance at Haleakala National Park, costs about $0.27 per kWh including tax and surcharges.[127] Grid electricity on Maui is generated from a central power plant fired on imported fuel oil. The annualized cost breakdown from this investment is shown in Figure 61. Take note that the operating and management cost is composed of the cost associated with buying electricity from Maui Electric at the set price of $0.27/kWh. In addition, the capital investment of extending the grid has been annualized.

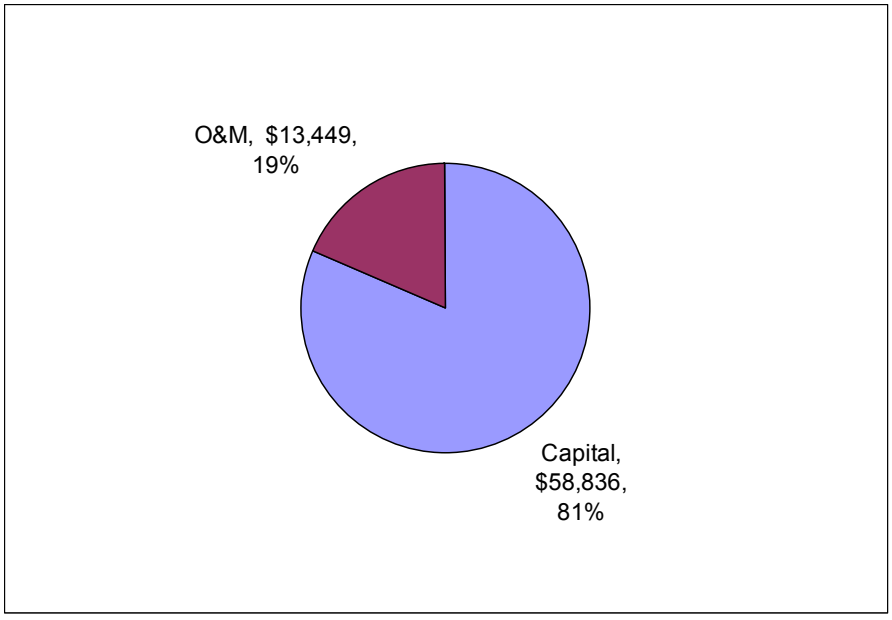

Figure 61: The annualized life cycle cost breakdown of a generator only system powering both the north and south sites.

9. Conclusions

As outlined in section 8.1, four different system configurations have been analyzed: 1.) solar PV with a backup genset, 2.) solar PV with micro-hydro and a backup genset, 3.) genset only, and 4.) grid extension. Each system configuration is sized to meet the electrical demand and consumption as defined in Chapter 1.

A life cycle cost analysis is performed on each investment and are compared to one another as shown below in Table 12. The PV only configuration is a 92 panel ground mounted PV system for the north site and a 68 panel roof mounted PV system for the south site, each equipped with a backup generator and no hydropower. The PV/hydro configuration consists of a 60 panel ground mounted PV system for the north site and a 36 panel roof mounted PV system for the south site, each equipped with a backup generator and HI Power HV 1200 hydro turbines. The genset only system consists of a 15 kW Kohler 15RYG propane fired genset and an 11.5 kW Cummins GNAB11.5 propane fired genset powering the north and south sites, respectively. Initial capital cost, total life cycle cost, annualized life cycle cost, and cost of electricity are shown for comparison.

Table 12: A comparison of the four respective system configurations.

Configuration	Capital Cost	Life Cycle Cost	Annualized Life Cycle Cost	Cost of Electricity ($/kWh)
PV without hydro	**$284,482**	**$368,870**	**$36,342**	**$0.73**
PV with hydro	**$259,348**	**$336,660**	**$33,831**	**$0.68**
Genset Only	**$18,490**	**$576,769**	**$49,096**	**$0.99**
Grid	**$711,000**	**$844,384**	**$69,873**	**$1.71**

From looking at the results displayed in Table 12, the two renewable options have significantly lower life cycle costs than both the genset only system and the grid extension. The renewable options also have a lower capital cost than a grid

extension, assuming that the park service would incur the entire cost of extending the grid. It is no surprise that the genset only system has by far the lowest capital cost. However, the capital cost is far overshadowed by the high fuel, maintenance, and replacement costs that would result from installing this configuration.

It is now a question of which renewable system to install: PV with hydro or PV without hydro. The system with the inclusion of hydro has the lowest capital and life cycle cost by about $30,000 in each category. This being said, it is only about a 10% improvement, and it may not be worth the additional system complexity. There will be greater maintenance and installation issues to overcome with the hydro system; however, the hydro resource is an excellent complement to the solar, with low solar irradiation usually being compensated by high stream flow availability and vice versa. If there were no backup genset, the PV/hydro combination would certainly be a better choice than augmenting the solar array, due to this complimentary relationship.

In closing, solar PV systems with and without hydro have lower life cycle costs than both a genset only system and grid extension. The PV system without hydro is slightly more expensive, but it may prove to be less hassle in both maintenance and installation. Adding hydro to the system will slightly decrease both capital and life cycle costs, and will most certainly increase the availability of renewable energy; thus decreasing backup genset run time. The National Park Service is encouraged to select the system with which they feel most comfortable. It is our recommendation that if there is sufficient help for system maintenance the solar PV with hydro would be the better choice; however, the PV only system is definitely a lower risk investment.

The full electrical diagrams and parts lists for the north and south sites are found in Appendices F and G, respectively. Appendices A – D give background details.

End Notes

[1] Maui
[2] Post
[3] National Geographic Society
[4] National Solar Radiation Data Base.
[5] Post
[6] Solar Insolation Maps
[7] Goldman
[8] Beckman, p. 14
[9] Beckman, p. 91-92
[10] Beckman, p. 96
[11] Fritz, p. 2.4
[12] Harris
[13] Penche, p. 66
[14] Daily Stream Flow For Nation: Site 16501000
[15] Daily Stream Flow For Nation: Site 16501200
[16] Messenger p. 51
[17] Lead Acid Battery Terminology Glossary
[18] Lasnier, p.101
[19] Lasnier, p.110
[20] Messenger, p. 54
[21] Messenger, p. 53
[22] Lasnier, p.130
[23] Lasnier, p.117
[24] Lasnier, p.131
[25] Lasnier, p.118
[26] Stevens, p. 1
[27] Stevens, p. 1
[28] Stevens, p. 4
[29] Wiles
[30] Messenger, p. 68
[31] Messenger, p. 67
[32] Messenger, p. 67
[33] Messenger, p. 194
[34] Messenger, p. 53
[35] Lasnier, p. 113
[36] Linden, p. 24.53
[37] Messenger, p. 197
[38] Messenger, p. 197
[39] Messenger, p. 197
[40] NESEA Solar Electricity
[41] Beckman, p. 771
[42] Beckman, p. 771
[43] Beckman, p. 771
[44] Beckman, p. 771
[45] Beckman, p. 772
[46] Beckman, p. 774
[47] King, p. 6
[48] Messenger, p. 48
[49] Messenger, p. 48

[50] SunWize Technologies pgs. 2-9
[51] SunWize Technologies, p. 23
[52] Lead Acid Battery Terminology Glossary
[53] SunWize Technologies, p. 23
[54] Fuller
[55] Love
[56] Parallel Operation of Dynasty VRLA Batteries
[57] Shultze, p. 1
[58] SunWize Technologies, p. 21
[59] Beckman, p. 782
[60] Messenger, p. 64
[61] Messenger, p. 73
[62] Messenger, p. 75
[63] Messenger, p. 77
[64] SunWize Technologies, p. 30-37
[65] Singh
[66] Outback Catalog, p. 11
[67] Outback Catalog, p. 11
[68] Outback Power Systems User Forum
[69] Solar Mount
[70] Solar Mount
[71] Solar Mount
[72] Solar Mount
[73] Post
[74] Hool
[75] Solar Mount Estimator
[76] Baublits
[77] Trujillo
[78] Rosenthal, p. 1
[79] Messenger, p. 85
[80] Rosenthal, p. 7
[81] Durand, p. 1
[82] Durand, p. 4
[83] New, p. 1
[84] ASCE
[85] Penche, p. 112
[86] Penche, p. 103
[87] Penche, p. 16
[88] Penche, p. 116
[89] Penche, p. 117
[90] Hydro Induction Power Products
[91] Hydro Induction Power Products
[92] New, p. 2
[93] Twidell, p. 182
[94] Penche, p. 175
[95] Penche, p. 157
[96] New, p. 5
[97] Penche, p. 158
[98] Penche, p. 158
[99] Hydro Induction Power Products
[100] Schultz, p. 1
[101] Schultz, p. 1

[102] Diversion Loads
[103] HISCO Products
[104] McMaster-Carr
[105] Hydro Induction Power Products
[106] Schultze, p. 1
[107] Diversion Loads
[108] Life Cycle Costing
[109] Messenger, p. 139
[110] Life Cycle Costing
[111] Messenger, p. 136
[112] Messenger, p. 136
[113] Previsic, p. 12
[114] Life Cycle Costing
[115] Life Cycle Costing
[116] Life Cycle Costing
[117] Life Cycle Costing
[118] Newnan, p. 61
[119] Newnan, p. 61
[120] Polagye
[121] Hybrid Power Systems
[122] Life Cycle Costing
[123] Utilities Gas Company
[124] Dangling Rope Marina
[125] Thomas, p. 3
[126] Prince
[127] Baublits

References

ASCE. Committee on Intakes. Guidelines for the Design of Intakes for Hydroelectric Plants, 1995.

Baublits, Frank. "Mounting Structure Cost." Email to Haleakala Maintenance Department. November 21, 2005.

Crowe, Clayton T, John A. Roberson, and Donald F. Elger. Engineering Fluid Mechanics. 7th ed. New York: John Wiley & Sons, 2001.

Daily Stream Flow For Nation. December 2005. USGS Water Resources. Accessed on June 22, 2005 from <nwis.waterdata.usgs.gov/nwis/discharge?introduction>.

Diversion Loads. December 2005. APM Hydro. Accessed on November 16, 2005 from <http://www.apmhydro.com>.

Fritz, Jack J. Small and Mini Hydropower Systems. New York: McGraw-Hill, 1984.

Fuller, Jim. Mount Rainer National Park. Personal Interview. August 14, 2005.

Goldman, Herman. Maui Electric. Personal Interview. June 20, 2005.

Harris, Don. Harris Hydroelectric. Personal Interview. September 3, 2005.

HISCO Products. November 2005. Hawaii Irrigation Supply Company. Accessed on December 1, 2005 from <http://www.hiscosales.com/products.shtm>.

Hool, Timothy J. Unirac Sales. Personal Interview. October 25, 2005.

Hydro Induction Power Products. June 2004. Hydro Induction Power. Accessed on June 30, 2005 from <www.hipowerhydro.com/Products.htm>.

Hybrid Power Systems. 2002. Sandia National Laboratories. Accessed on December 4, 2005 from <http://www.sandia.gov/pv/docs/HybridSizing.html>.

King, D.L., W.E Boylson, and J.A Kratochvil. "Photovoltaic Array Performance Model." Photovoltaic Systems Research and Development. May 1996. Sandia National Laboratories.

Lasnier, France, Tony Gan Ang. Photovoltaic Engineering Handbook. New York: Adam Hilger, 1990.

Lead Acid Battery Terminology Glossary. September 2005. C&D Technologies Tech Support. Accessed on August 5, 2005 from <http://www.cdstandbypower.com/contact/tech_support/pdf/7745.pdf>.

Life Cycle Costing. January 2002. Sandia National Laboratories. Accessed on December 1, 2005 from <http://www.sandia.gov/pv/docs/LCcost.htm>.

Linden, David. Handbook of Batteries. New York: McGraw-Hill, 1995.

Liquid Flow Meters. 2001. Omega Engineering. Accessed on December 4, 2005 from <http://www.omega.com/techref/images/fi1.gif>.

Love, David. SunWize Technologies. Personal Interview. August 12, 2005.

Maui. 2005. Google Maps. Accessed on December 4, 2005 from <http://maps.google.com/>.

Messenger, Roger, Jerry Ventre. Photovoltaic Systems Engineering. Boca Raton: CRC Press, 2000.

National Geographic Society. "Haleakala National Park Topographic Map." Evergreen, CO: National Geographic Maps, 2000.

NESEA Solar Electricity. January 2001. Northeast Sustainable Energy Association. Accessed on November 18, 2005 from <http://www.nesea.org/energy/info/PV_standalone.gif>.

National Fire Protection Association. The National Electrical Code Handbook. Boston: National Fire Protection Association, 2005.

National Solar Radiation Data Base. Available data Sets. Accessed on June 21 from http://rredc.nrel.gov/solar/old_data/nsrdb/

New, Dan. "Intro to Hydropower Part 1: Systems Overview." Home Power. October 2004. Accessed on August 20, 2005 from < http://www.homepower.com/files/HP103_14.pdf>.

Outback Catalog. August 2005. Outback Power Systems. Accessed on September 21, 2005 from <http://www.outbackpower.com/pdfs_spec/OutBackCatalog.pdf>.

Outback Power Systems User Forum. August 2005. Outback Power Systems. Accessed on November 11, 2005 from <http://www.outbackpower.com/forum/>.

Parallel Operation of Dynasty VRLA Batteries. September 2005. C&D Technologies Tech Support. Accessed on August 5, 2005 from <http://www.cdstandbypower.com/contact/tech_support/pdf/7745.pdf>.

Penche, Celso. "A Layman's Guide on how to develop a small hydro site." Literature on microhydro. April 2002. microhydropower.net. Accessed on July 6, 2005 from <http://europa.eu.int/comm/energy/library/hydro/layman2.pdf>.

Previsic, Mirko, Omar Siddiqui, and Roger Bedard. "Economic Assessment Methodology for Offshore Wave Power Plants." EPRI Wave Energy Conversion Project. November 2004. Electric Power Research Institute. Accessed February 3, 2006 from <http://www.epri.com/oceanenergy/waveenergy.html#reports>.

Prince, Mark. "Grid Extension." Email to Maui Electric Company. October 17, 2005.

Post, Harold. "Power Systems Assessment at Haleakala National Park." Email to Frank Baublits at Haleakala National Park. 16 Oct. 2002.

Rosenthal, Andrew L., Steven J. Durand, Michael G. Thomas, and Harold N. Post. "Economics and Performance of PV Hybrid Power Systems: Three Case Studies." Photovoltaic Systems Research and Development. June 1998. Sandia National Laboratories. Accessed on November 22, 2005 from <http://www.sandia.gov/pv/docs/Systems_and_Applications.htm>.

Schultze, Bob. "Wrench Realities." Home Power. August 1999. Accessed on August 18, 2005 from <http://www.homepower.com/files/shuntregulationhp72.pdf>.

Singh, Nevin. Outback Power Systems. Personal Interview. September 5, 2005.

Solar Insolation Maps. March 2003. State of Hawaii Strategic Industries Division. Accessed on June 15, 2005 from <http://www.state.hi.us/dbedt/ert/solar-maps.html>.

Solar Mount. January 2005. Unirac. Accessed on October 21, 2005 from <http://www.unirac.com/solarmount.htm>.

Solar Mount Estimator. 2005. Unirac. Accessed on October 21, 2005 from <http://www.unirac.com/solarmount/sm_config.htm>.

Stevens, John, Garth P. Corey. "A Study of Lead-Acid battery Efficiency Near Top-of-Charge and Impact on PV System Design." Photovoltaic Systems Research and Development. May 1996. Sandia National Laboratories. Accessed on November 22, 2005 from <http://www.sandia.gov/pv/docs/BattIntro.htm>.

SunWize Technologies, 2005-06 Solar Electric Product Catalog. Kingston, NY: SunWize Technologies, 2005.

Thomas, Michael, Harold Post, Andrew Rosenthal, and Steven Durand. "Economic Analysis of PV Hybrid Power System: Pinnacles National Monument." Photovoltaic Systems Research and Development. September 1997. Sandia National Laboratories. Accessed on November 5, 2005 from <http://www.sandia.gov/pv/docs/Systems_and_Applications.htm>.

Trujillo, Trina. "Shipping Quote." Email to Unirac Sales. November 7, 2005.

Twidell, John, Tony Weir. Renewable Energy Resources. London: E & FN Spon, 1986.

Utilities Gas Company. Phone Conversation. November 16, 2005.

Wiles, John. "Photovoltaic Power Systems and the 2005 National Electrical Codes Suggested Practices." Photovoltaic Systems Research and Development. February 2005. Sandia National Laboratories. Accessed on November 9, 2005 from <http://www.sandia.gov/pv/docs/John_Wiles_Code_Corner.htm>.

Appendices

Appendix A: Existing and Estimated Electrical Consumption and Demand

Facility	Load/ Appliance	Recommended appliance	#	Power (W)	Sleep Power (W)	Time/ day (hrs)	(sleep mode) Time / day (hrs)	Peak (W)	Energy (kWh/day)
Visitor Center/ Ranger Station	Lights	American Light 800 Lumens	4	15	0	10	0	60	0.6
	Laptop Computers	IBM ThinkPad R51 Series	4	65	9.3	8	2	260	2.1544
	Printers	HP Designjet 110plus nr	1	90	15	1	9	90	0.225
	Fans		2	60		10		120	1.2
	refrigerator	Sun Frost RF-16	1	30		24		30	0.72
	TV/ VCR	energy star	1	150		8		150	1.2
	Microwave		1	600		0.5		600	0.3
	security cameras								
	Plug Loads		1	300		10		300	3
total								**1610**	**9.3994**

Facility	Load/ Appliance	Recommended appliance	#	Power (W)	Sleep Power (W)	Time/ day (hrs)	(sleep mode) Time / day (hrs)	Peak (W)	Energy (kWh/day)
Entry Station	Lights	American Light 800 Lumens	3	15	0	10	0	45	0.45
	Laptop Computers	IBM ThinkPad R51 Series	1	65	9.3	9	1	65	0.5943
	Air Conditioner	12KS51/12KLS51 - Wall Mounted Air Conditioner 11,800 Btu/h	1	1200	0	10	0	1200	12
	Plug Loads		1	100		10		100	1
total								**1410**	**14.0443**

Facility	Load/ Appliance	Recommended appliance	#	Power (W)	Sleep Power (W)	Time/ day (hrs)	(sleep mode) Time / day (hrs)	Peak (W)	Energy (kWh/day)
Lindbergh House	Lights	American Light 800 Lumens	10	15	0	10	0	150	1.5
	Laptop Computers	IBM ThinkPad R51 Series	3	65	9.3	8	2	195	1.5786
	Printers	HP Designjet 110plus nr	1	90	15	1	8	90	0.21
	Copier		1	1100		0.5		1100	0.55
	Air Conditioner	12KS51/12KLS51 - Wall Mounted Air Conditioner 11,800 Btu/h	1	1200		10		1200	12
	Fans		2	60		10		120	1.2
	refrigerator	Sun Frost RF-16	1	30		24		30	0.72
	Microwave		1	600		0.5		600	0.3
	Plug Loads		1	300		10		300	3
total								**3785**	**21.0586**

Facility	Load/ Appliance	Recommended appliance	#	Power (W)	Sleep Power (W)	Time/ day (hrs)	(sleep mode) Time / day (hrs)	Peak (W)	Energy (kWh/day)
Maintenance facility	Lights	American Light 800 Lumens	12	15	0	10	0	180	1.8
	Fans		4	60	0	10	0	240	2.4
	Microwave		1	600	0	0.5	0	600	0.3
	refrigerator	Sun Frost RF-16	1	30	0	24	0	30	0.72
	AC well pump	high efficiency	1	1500	0	6	0	1500	9
	table saw	Bosch 10" worksite table saw Model 4000	1	1800	0	3	0	1800	5.4
	Laptop Computers	IBM ThinkPad R51 Series	1	65	9.3	3	8	65	0.195
	air compressor	DeWalt Heavy-Duty 2.7 Max HP 4 Gallon Electric Hand Carry Air Compressor with Panel	1	1800	0	3	0	1800	5.4
total								**6215**	**25.215**

Facility	Load/ Appliance	Recommended appliance	#	Power (W)	Sleep Power (W)	Time/ day (hrs)	(sleep mode) Time / day (hrs)	Peak (W)	Energy (kWh/day)
1 NPS House	Lights	AM Conservation group AM 27 1750 lumens	11	27	0	10	0	297	2.97
	Fans		5	60	0	18	0	300	5.4
	Microwave		1	600	0	0.5	0	600	0.3
	refrigerator	Sun Frost RF-16	1	30	0	24	0	30	0.72
	TV/ VCR	energy star	1	150	0	6	0	150	0.9
	washer	GE® Extra-Large Front Loading Washer with Stainless Steel Basket	1	600	0	0.5	0	600	0.3
	dryer	LP gas motor	1	200	0	0.5	0	200	0.1
	plug loads	misc	1	100		24		100	2.4
total								**2277**	**13.09**

Appendix B: Solar Equations

Solar Angles

The important angles are defined as:

- Φ, latitude Angle

  It is the observer's angular location on the globe north or south of the equator.

- δ, declination angle

  It is the tilt of the earth's axis of rotation varying from -23.45º during the winter solstice and 23.45º during the summer solstice. The declination angle is given in degrees by Equation B1:

$$\delta = 23.45 * \sin(360 * \frac{284 + n}{365}).$$ **Equation: B1**[1]

  where,

  - δ is the declination angle
  - n is the day of the year. For example, n = 365 on December, 31 and n = 1 on January, 1.

- ω, hour angle

  It is the angular displacement of the sun with respect to the local meridian. The sun rotates 15º per hour; thus the hour angle is negative in the morning, positive in the afternoon, and equal to zero at solar noon. In order to calculate the hour angle, solar time in hours must be determined by correcting standard time given by Equation B2.

$$SolarTime = S\tan dardTime + \frac{4 * (L_{st} - L_{loc}) + E}{60}$$ **Equation: B2**[2]

  where,

[1] Beckman, p. 13
[2] Beckman, p. 11

- SolarTime is the local solar time in hours
- StandardTime is the local standard time in hours
- L_{st} is the standard meridian for the local time zone
- L_{loc} is the meridian of the site's location
- E is the equation of time; taking into account deviations in the earth's rate of rotation. Its value is given by Equation B3, and B is given by Equation B4, where n is the day of the year as defined in Equation B2.

$$E = 229.2 * (0.000075 + 0.001868\cos B - 0.032077\sin B - 0.014615\cos 2B - 0.04089\sin 2B)$$ **Equation: B3**[3]

$$B = (n-1)\frac{360}{365}$$ **Equation: B4**[4]

The hour angle, ω, can then be determined by Equation B5.

$$\omega = (SolarTime - 12) * 15^\circ$$ **Equation: B5**[5]

- β, tilt angle

It is the angle between the collector and the horizontal plane of the surface in question.

- θ, incidence angle

It is the angle between the beam radiation of the sun and the normal to the tilted surface that this radiation is incident. The incident angle can be calculated by Equation B6.

[3] Beckman, p. 11
[4] Beckman, p. 12
[5] Beckman, p. 12

$$\theta = \cos^{-1}[\sin(\delta)\sin(\phi)\cos(\beta) - \sin(\delta)\cos(\phi)\sin(\beta)\cos(\gamma) + \cos(\delta)\cos(\phi)\cos(\beta)\cos(\omega) + \cos(\delta)\sin(\phi)\sin(\beta)\cos(\gamma)\cos(\omega) + \cos(\delta)\sin(\beta)\sin(\gamma)\sin(\omega)]$$.

Equation: B6[6]

- γ, surface azimuth angle

The surface azimuth angle is the angle between the projection of the collector on a horizontal surface and the local meridian. It is equal to zero due south, positive to the west, and negative to the east. For optimum design purposes, the collectors will be oriented due south; thus γ will be set to zero.

- θ_z, zenith angle

The zenith angle is the angle between a line perpendicular to the horizontal surface and the position of the sun, and is given by Equation B7.

$$\theta_z = \cos^{-1}[\cos(\phi)\cos(\delta)\cos(\omega) + \sin(\phi)\sin(\delta)]$$ **Equation: B7**[7]

Solar Irradiation Incident on a Collector

The angular path of the sun is determined by the above equations, and the total solar radiation incident on a surface can be calculated, which is composed of three basic components, direct beam, diffuse, and reflected radiation. Direct beam radiation is the radiation received by the sun that has not been scattered by clouds or the atmosphere. Diffuse radiation is beam radiation that has been scattered by the atmosphere. Reflected radiation is total solar radiation (the sum of diffuse and beam radiation) that has been reflected back onto the tilted surface. Note that there will be no reflected component on a horizontal surface. Assuming an isotropic sky, meaning that diffuse and reflected radiation are

[6] Beckman, p. 15
[7] Beckman, p. 15

received uniformly from all directions, the total incident radiation on a tilted collector, G_c, can be determined by Equation B8.

$$G_c = G_b R_b + G_d\left(\frac{1+\cos\beta}{2}\right) + G_T\rho\left(\frac{1-\cos\beta}{2}\right)$$ **Equation: B8[8]**

where,

- G_c is the total radiation incident on a tilted collector
- G_d is diffuse radiation
- G_b is direct beam radiation
- G_T is the sum of beam and diffuse radiation
- R_b is the ratio of the beam radiation on a tilted surface to the beam radiation on a horizontal surface; given by Equation B9.

$$R_b = \frac{\cos\theta}{\cos\theta_z}$$ **Equation: B9[9]**

- β is the tilt angle of the collector
- ρ is the albedo, or reflectance, of the ground; ranging between about 0.7 for snow and 0.2 for common ground.

Equation B8 is not quite complete due to the fact that diffuse radiation is not completely isotropic. Instead, it is composed of three parts:

1. The isotropic part is diffuse radiation received uniformly by the entire sky.
2. Circumsolar diffuse results from forward scattering of radiation around the sun.
3. Horizon brightening refers to diffuse radiation concentrated near the horizon.[10]

Each of these diffuse components, along with a ground reflected component and direct beam component are depicted below in Figure B1. Note that the

[8] Beckman, p. 95
[9] Beckman, p. 25
[10] Beckman, p. 91-92

circumsolar diffuse radiation is coming from the same direction as the beam radiation.

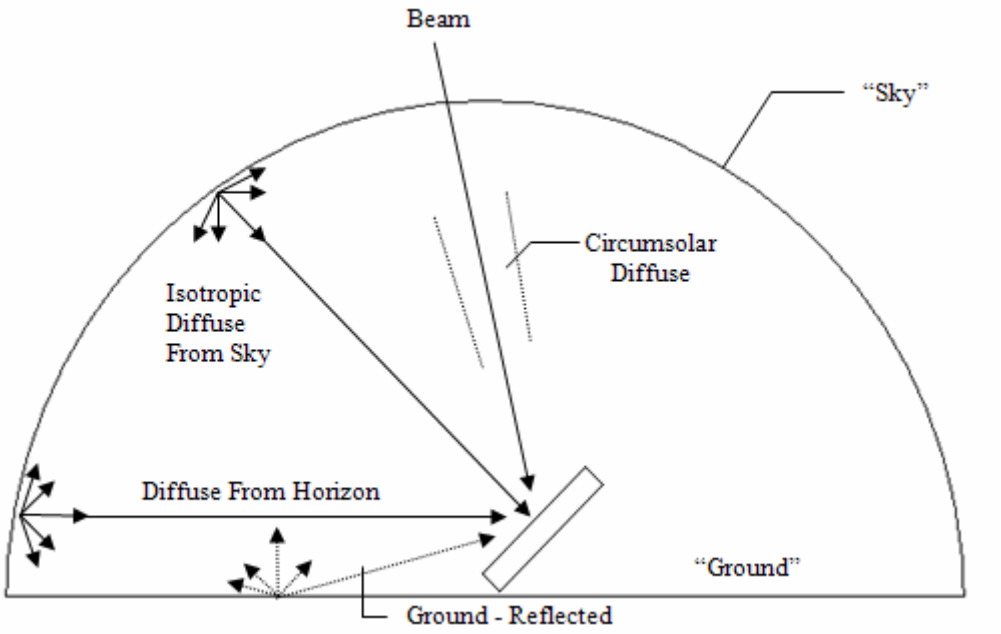

Figure B 1: Beam, diffuse, and reflected solar radiation on a tilted surface.[11]

Since circumsolar radiation is coming from the same direction as beam, it will be a function of R_b and A_i, where R_b is the geometric factor found by Equation B9 and A_i is the anisotropy index. Given by Equation B10, the anisotropy index is a function of the transmittance of the atmosphere and determines the fraction of horizontal diffuse radiation that can be modeled as forward scattered.

$$A_i = \frac{G_b}{G_o}$$ **Equation: B10**[12]

where,

- G_b is direct beam radiation
- G_o is horizontal extraterrestrial radiation.

The total diffuse radiation, $G_{d,T}$, is now a combination of isotropic and circumsolar components given by Equation B11.

[11] Beckman, p. 96
[12] Beckman, p. 97

$$G_{d,T} = G_d\left[(1-A_i)\left(\frac{1+\cos\beta}{2}\right)+A_i R_b\right]$$ **Equation: B11**[13]

In order to account for horizon brightening, Klucher, Temps, and Coulson came up with a correction factor, F, to apply to the isotropic diffuse. F is given by Equation B12, where f is the fraction of total radiation that is beam, shown in Equation B13.

$$F = 1+ f\sin^3\left(\frac{\beta}{2}\right)$$ **Equation: B12**[14]

$$f = \sqrt{\frac{G_b}{G_T}}$$ **Equation: B13**[15]

With the additional diffuse components added to Equation B8, the total solar radiation incident on a tilted collector is given by Equation B14.

$$G_c = (G_b + G_d A_i)R_b + G_d(1-A_i)\left(\frac{1+\cos\beta}{2}\right)\left[1+ f\sin^3\left(\frac{\beta}{2}\right)\right] + G_T\rho\left(\frac{1-\cos\beta}{2}\right)$$ **Equation: B14**[16]

The above equation is referred to as the HDKR model, named after the scientists that derived it. Although the isotropic model, Equation B8, is the simplest, the HDKR model, Equation B14, produces results that are closer in agreement to measured values; thus, Equation B14 will be used to predict solar radiation incident on a tilted collector.

[13] Beckman, p. 97
[14] Beckman, p. 97
[15] Beckman, p. 97
[16] Beckman, p. 98

Appendix C: Chemistry of the Lead-acid Battery

The basic lead acid battery consists of a lead anode and a lead oxide cathode submersed in a sulfuric acid bath. The discharging reactions at the anode and cathode are shown in Equations C1 and C2, respectively, with the net reaction shown in Equation C3. Shown in Figure C1, the charging reactions are the discharge reactions in reverse.

Anode: $Pb + SO_4^{2-} \xrightarrow{discharge} PbSO_4 + 2e^-$ **Equation C1**[17]

Cathode: $PbO_2 + SO_4^{2-} + 4H^+ + 2e^- \xrightarrow{discharge} PbSO_4 + 2H_2O$ **Equation C2**[18]

Overall: $PbO_2 + Pb + 2H_2SO_4 \xrightarrow{discharge} 2PbSO_4 + 2H_2O$ **Equation C3**[19]

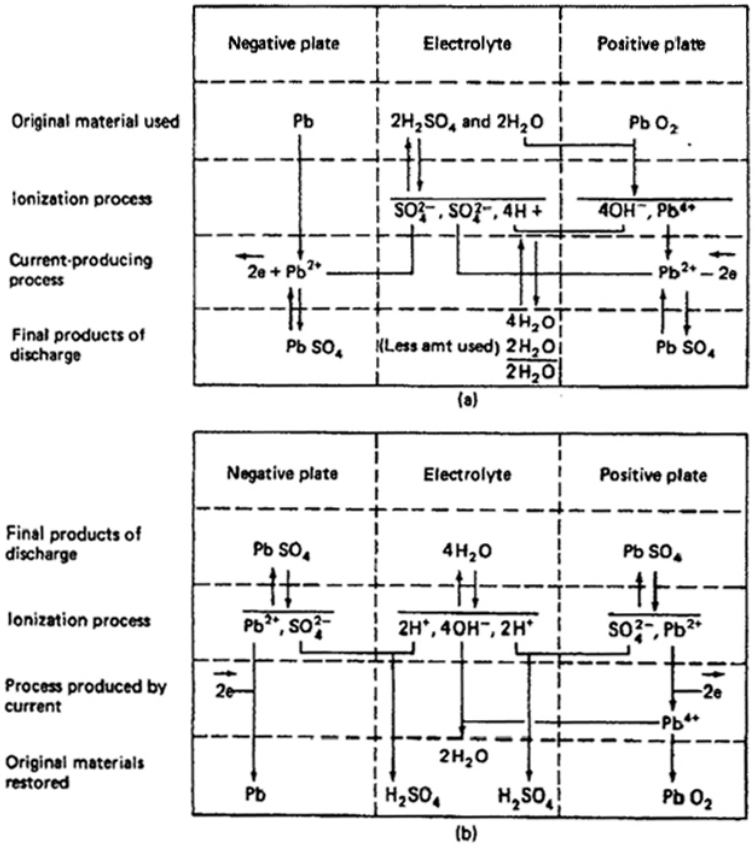

Figure C1: The charging and discharging reactions of the lead-acid cell.[20]

[17] Lasnier, p. 109
[18] Lasnier, p. 109
[19] Lasnier, p. 109

As shown above in Figure C1 and Equations C1 through C3, sulfate ions from the electrolyte combine with lead at the anode to produce lead sulfate plus two electrons. Sulfate ions from the electrolyte are also consumed at the cathode as they replace the oxygen ions in the lead oxide producing lead sulfate and water. As sulfate ions are removed from the electrolyte, two electrons must enter the cathode terminal and leave the anode terminal, by way of an external circuit, in order maintain charge neutrality.[21] Due to the fact that the cathodic reaction produces water, measuring the specific gravity of the electrolyte with a hydrometer is the conventional method used to determine the state of charge of a battery. As the acidic solution becomes weaker and more lead sulfate builds up on each respective plate, the voltage potential decreases eventually to the point that the battery can no longer deliver a current.[22]

If a voltage applied to the battery terminals is greater than the voltage between the two plates, the above reactions work in reverse. Two electrons leave the cathode terminal and subsequently enter the anode terminal to free up a sulfate ion to solution and combine with a lead ion producing elemental Pb. When the electrons exit the cathode, they are replaced by an oxygen ion, which combines with a lead ion to form PbO_2 and releases a sulfate ion back into the electrolyte.[23] In addition to combining with lead ions to form elemental lead, some electrons also combine with hydrogen ions to produce gaseous hydrogen: a process known as gasing. When the anode has been entirely transformed back to Pb, electrons can no longer liberate sulfate ions; thus the electrons proceed into the electrolyte, combine with hydrogen ions and produce large amounts of H_2 gas, which can lead to a flammability hazard as well as cause severe corrosion on the cathode.[24]

---

[20] Linden, p. 111
[21] Messenger, p. 52
[22] Lasnier, p.110
[23] Messenger, p. 53
[24] Messenger, p. 53

Appendix D: The National Electrical Code

Cables and Over-current Device Sizing

Calculations for conductor sizes and over-current device ratings are based on the requirements of both the NEC and on UL Standard 1703, which provides installation instructions for PV products. Wire ampacity data and temperature derating factors are found in Tables 310.16 and 310.17 in the 2005 NEC.[25] An example wiring diagram is shown below in Figure D1 to help illustrate the requirements of the NEC. There are two sub-arrays each rated at 3.3 kW, which have been set up to supply the proper input current and voltage to the Outback MX60 as detailed above. There is a 48 volt battery bank rated at 3,976 amp-hours. There are two Outback inverters rated at 3.3 kW each, and there is an 8 kW backup genset. Both systems utilize an Outback Mate hooked up to all of the charge controllers, master and slave inverters, and a remote battery temperature sensor. Each system also employs an X-240 autotransformer for 120/240 VAC load balancing. All conductors, breakers, and fuses are selected to meet the NEC and are identified in the drawings.

[25] National Fire Protection Association, p. 297-298

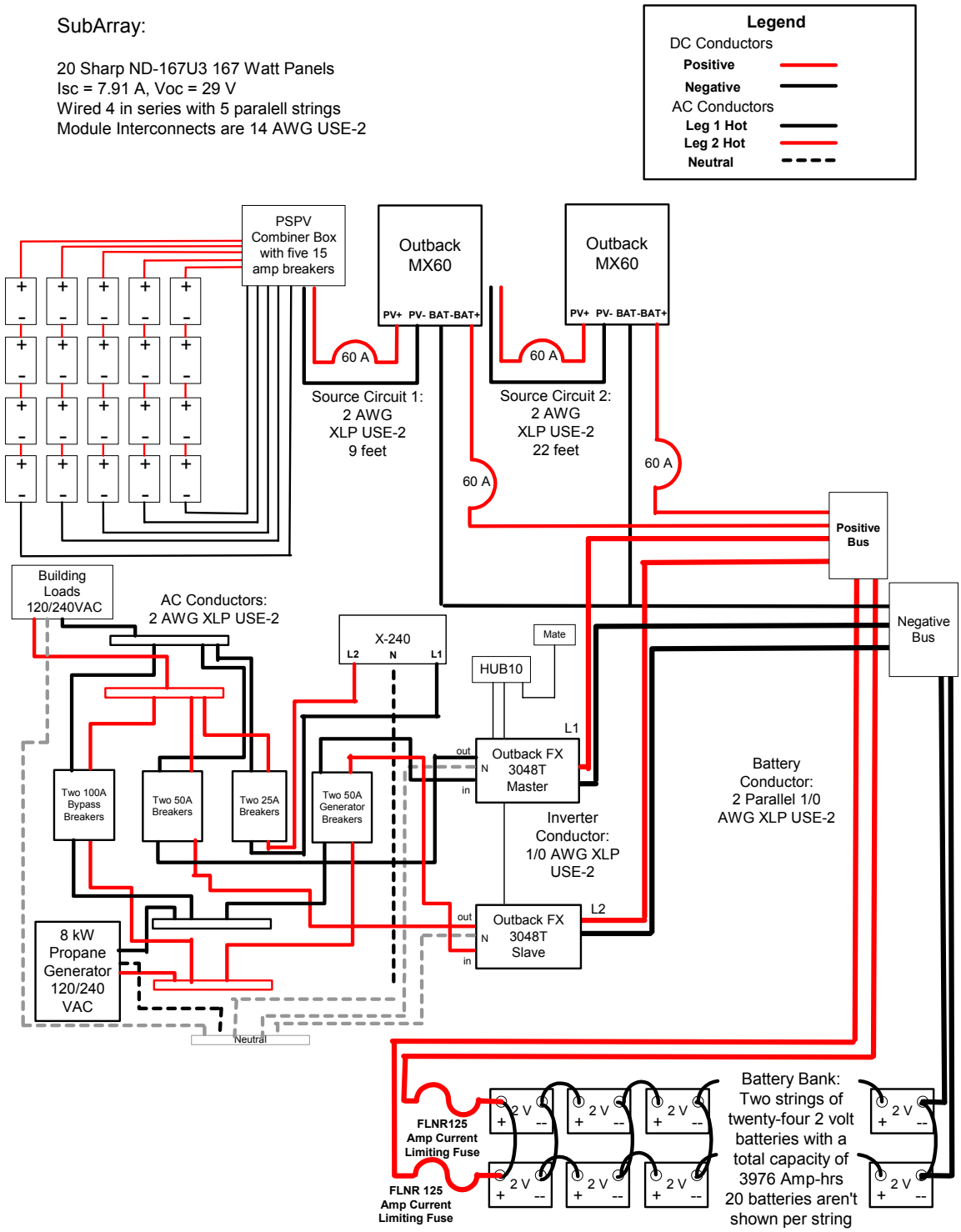

Figure D 1: Example wiring diagram to Illustrate NEC requirements.

Positive, negative, and ground fault conductors on the DC side, in addition to hot and neutral conductors on the AC side are color coded in the above diagram. It is also important to note that AC and DC breakers are different components and in no circumstance should a DC breaker be installed on the AC side and vice versa.

There are six basic steps to sizing a conductor:

1. Article 690-8a states that the maximum current should be the sum of parallel module rated short circuit currents multiplied by 125%.[26] This is sometimes referred to as the continuous current. This 125% correction factor is required because the short-circuit current of a module is referenced at a peak irradiance of 1,000 W/m^2; however, the intensity of the sun at solar noon can often exceed 1,000 W/m^2.[27] Each module string circuit conductor is rated at 125% of the individual module I_{sc}. Each sub-array source circuit conductor should be rated at 125% of the sum of the individual short circuit currents in the sub-array. The battery input circuit should be rated the same as the source circuit rating, since there are two conductors. If there was only one conductor, then each battery input conductor must be rated at 125% of the short-circuit current from both subarrays. The inverter input circuit should be rated to handle the continuous inverter input current, when the inverter is producing rated power at the lowest possible input voltage.[28] For example, in Figure 6.19, each inverter is rated to 3.3 kW, the lowest operating voltage of the battery bank is about 44 volts, and the inverter efficiency is about 90%. The input current is then:

$$I = \frac{3{,}000W}{(44volts) * (0.9)} = 76A\,.$$

[26] National Fire Protection Association, p. 1024
[27] Wiles, p. 32-33
[28] National Fire Protection Association, p. 1024

The inverter output conductor should have a rating equal to the continuous current output rating; however, it is recommended that this conductor be oversized to allow for the surge capability of the inverter.

2. Article 690-8b states that the conductor and over-current device must be rated at 125% of the current determined in step 1, which is to prevent over-current devices from operating at more than 80% of their rating; however, circuits containing over-current devices that are listed for continuous operation at 100% of their rating are permitted to be employed at the full rating.[29] All of the breakers selected have 100% duty ratings, so the second 125% correction factor is only applied to the conductors.

3. Cables should have an ampacity at 30ºC of 125% of the current determined in step 1 in order to guarantee proper operation of attached over-current devices.[30]

4. A cable size and insulation temperature rating must be selected from the NEC Ampacity Tables 310-16 and 310-17. The size of the cable is determined from the 75 ºC insulation level; then the cable is derated for temperature, conduit fill, and other provisions. The derated ampacity must be larger than the ampacity determined in step 1. If the ampacity isn't larger; then a larger cable or higher insulation temperature must be selected.[31]

5. The derated ampacity of the cable in step 4 must be greater than or equal to the over-current device rating determined in step 2. If this is not the case; then a larger gauge conductor must be selected.

[29] National Fire Protection Association, p. 1024
[30] National Fire Protection Association, p. 1029
[31] Wiles, p. I-2

Stated in article 110-3b, cables must be compatible with the temperature ratings of terminals on over-current protection devices. Most over-current devices have terminals rated to 60 or 75 ºC. If a cable with 90 ºC insulation has been selected, the 30ºC ampacity of a of the same size cable with 60 ºC or 75 ºC insulation must have a derated ampacity larger than that determined in step 1.[32]

The charging circuit in Figure 6.7 is used as an example. The charging circuit is the circuit connecting the charge controllers to the battery bank. At this point all 20 module strings have been combined together. The individual module short circuit current is 7.91 amps. The conductor size and protection are determined as follows.

1. The continuous current is found in accordance with article 690-8a.

$$Isc = (5strings) * \frac{7.91amps}{string} * 125\% = 49.4amps$$

2. The breaker is sized to operate at 80% of rated capacity in accordance with 690-8b. Thus, this current is 1.25 x 49.4, or 61.79 amps. However, the breakers selected have a 100% duty rating, so a 60 amp breaker will suffice.

3. This is the same calculation as step 2, where the cable ampacity without temperature deratings must be 125% of 49.4, or 61.79 amps.

4. From Table 310-16, a 4 AWG USE-2 copper wire with 90 ºC insulation is rated to 95 amps. Now a temperature derating must be applied. The wire is in conduit, and it is assumed the wire will be operating at the maximum expected cell temperature of 64 ºC, obtained from Equation 6.5. The temperature derating factor for copper conductors in conduit with 90ºC insulation at 64 ºC is 0.58.[33] Shown below, the derated ampacity of the

[32] Wiles, p. I-2
[33] National Fire Protection Association, p. 297

conductor is 55.1 amps, which is greater than the ampacity determined in step 1.

$$I = (95 amps) * (0.58) = 55.1 amps .$$

Also note that the cable ampacity without temperature deratings is 95 amps.

5. Standard ratings for over-current devices are shown in article 240-6 of the NEC. It is possible to protect a cable with a derated ampacity of 55.1 amps with a 60 amp over-current device.
6. Presently there are no over-current devices that have terminals listed for 90ºC insulation, and most are listed for 75 or 60ºC insulation. The selected over-current device has terminals that are rated at 75ºC insulation, so the cable derated ampacity must be checked again at 75ºC. The derated ampacity of a 4 AWG conductor with 75ºC insulation is (85 amps) x 0.58, or 49.3 amps, which is smaller than the required ampacity found in step 1; thus the next larger conductor must be selected. In Tables 310.16 and 310.17 of the NEC, a 3 AWG conductor is the next largest; however, no companies appear to make a 3 AWG conductor with the required insulation, so a 2 AWG conductor is selected. A 2 AWG conductor with 75ºC insulation has a derated ampacity at 64ºC of 66.7 amps, which meets the above criteria.

All of the conductors in for this installation have been sized according to the methods outlined above.

In addition to conductor and over-current protection sizing, there are many other issues that the NEC addresses. Some of the additional requirements and codes are outlined below; however, the serious system designer should become familiar with the entire NEC, not limited to the information found in this report.

Batteries

A short circuit condition in a battery bank can be a severe situation, with a single 6 volt 220 amp-hour battery being able to produce short-circuit currents as high as 8,000 amps, which can generate temperatures and magnetic forces that can destroy underrated over-current devices.[34] The interrupt capability of an over-current device is specified as the amperes interrupt rating, or AIR, and reach 20,000 amps in some dc rated fuses. A current limiting fuse must be used in a battery circuit that has breakers that have a low AIR rating.[35] As shown above in Figure 6.19, two 125 amp RK5 current limiting fuses protect each string of the battery bank.

DC Grounding

For systems over 50 volts, which is the open-circuit voltage multiplied by a temperature coefficient found in Table 690.7 of the NEC, the DC side of the system must be grounded, which is usually the negative conductor. In addition, all systems regardless of voltage must have equipment grounding conductors to ground exposed metal parts of non-current carrying conductors.[36] In order to reduce fire hazards, roof mounted PV systems must include ground fault protection devices, as outlined in Article 690.5 of the NEC.[37]

Generators

The NEC requires that the conductors between the generator and the first installed field device be rated at 115% of the nameplate rating.

Voltage Drop Considerations

[34] Wiles, p. 40
[35] Wiles, p. 42
[36] National Fire Protection Association, p. 1031
[37] National Fire Protection Association, p. 1021

All of the other conductors and over-current devices are sized similarly to the methods above. However, the NEC also requires that the total voltage drop in feeder and branch circuits must be less than 3%. The PV source circuits could be located as far as 100 feet way from the charge controllers. In order to keep voltage drop within this limit, these conductors should be oversized. Nominal ohmic resistances per 1,000 feet are found for each wire size in Chapter 9 of the NEC, which should be used to calculate voltage drop. Note that voltage drop must be calculated for the entire length of the wire (both positive and negative conductors); thus if a source circuit is 22 feet away from the charge controller, the circuit length is 44 feet. Percent voltage drop can be calculated from Equation D1.

$$\%VD = 100 * \frac{I}{V_s} R \frac{2d}{1{,}000}$$ **Equation D1**[38]

where,

- %VD is the percentage voltage drop
- V_s is the source voltage in volts
- I is the load current in amps
- R is the wire resistance in ohms per 1,000 feet
- d is the one way circuit distance in feet.

Note that Equation D1 assumes that the load voltage is essentially equal to the source voltage.

[38] Messenger, p. 91

Appendix E: Hydro Calculations

Water Intake

The intake loss can be estimated by Equation E.1.

$$h_c = K_c\left(\frac{V_2^2}{2g}\right)$$ **Equation E.1**[39]

where,

- h_c is the head loss in feet
- V_2 is the velocity in the penstock (feet/s)
- g is the acceleration of gravity: 32.2 feet/s^2
- K_c is a coefficient which varies by the level of contraction shown below in Equation E.2. Note that d is the penstock diameter and D is the width of the intake channel as shown in Figure E1.

$$K_c = 0.42\left(1-\frac{d^2}{D^2}\right)$$ **Equation E.2**[40]

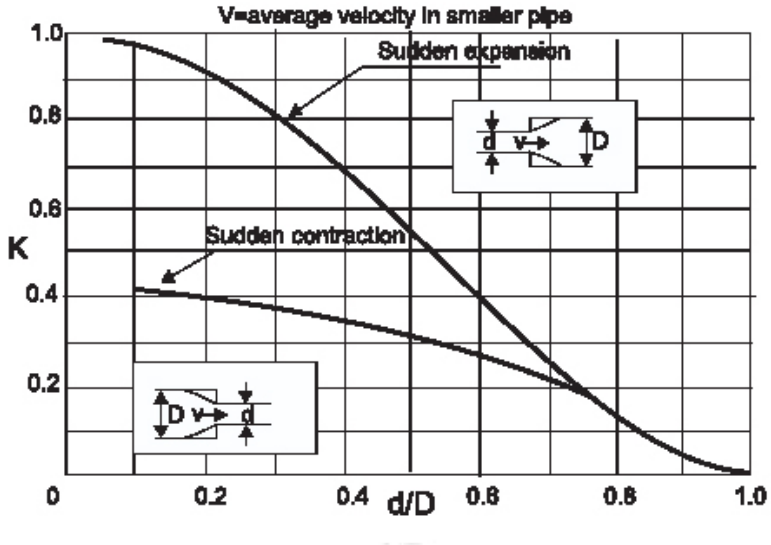

Figure E 1: A diagram depicting the variables in Equations E.1 and E.2.

[39] Penche, p. 38
[40] Penche, p. 38

As an example to illustrate the insignificance of this head loss, the flow rate is set to 100 gpm and the dimensions of a spring box intake made by HI Power, shown in Figure E2, are assumed.

Figure E 2: A spring box power intake made by HI Power.[41]

The power intake shown in Figure E2 has a pipe diameter of 4 inches and an intake width of 8 inches. In order to calculate the head loss, the mean velocity in the penstock must be calculated, which can be found by Equation E.3.

$$V = \frac{Q}{A}$$ **Equation E.3**[42]

where,

- V is the average velocity in the tube
- Q is the flow rate
- A is the cross sectional area

Employing Equations E.1 to E.3 with a flow rate of 100 gpm and d/D given above, V_2, K_c, and h_c are 2.5 ft/s, 0.315, 0.03 ft. With a gross head of over 300 feet a head loss of 0.03 feet is hardly worth worrying about; thus it is decided to select a power intake system off the shelf similar to the HI Power model shown in Figure E2.

[41] Hydro Induction Power Products
[42] Crowe, p. 104

Penstock

Head Loss in Pipes

Developed by Henry Darcy and Julius Weisbach, the frictional loss of steady state, incompressible flow traveling through a pipe is given by Equation E.4.

$$h_f = f \frac{L}{d} \frac{V^2}{2g}$$ **Equation E.4**[43]

where,

- h_f is the frictional head loss
- L is the length of the pipe
- d is the pipe diameter
- V is the average velocity in the pipe
- g is the acceleration of gravity
- f is a dimensionless number which is based on the Reynolds number of the flow if the flow is laminar, and on the Reynolds number and relative roughness height if the flow is turbulent.

Shown in Figure E3, turbulent flow is characterized by violent mixing throughout; in contrast, laminar flow has a smooth velocity profile devoid of mixing.

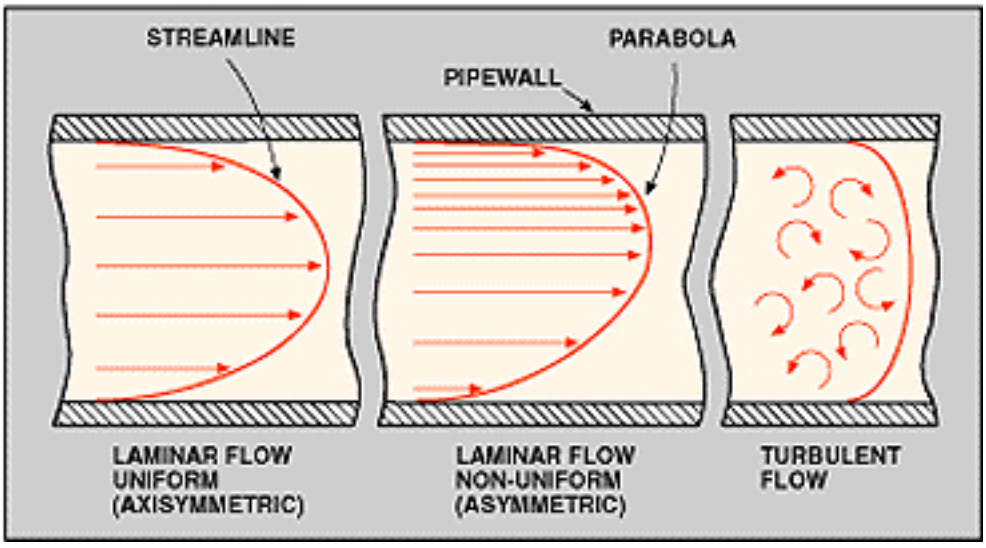

Figure E 3: Velocity profiles for three different flow regimes.[44]

[43] Crowe, p. 415
[44] Liquid Flow Meters

The Reynolds number, Re, is a dimensionless number relating to both laminar and turbulent flows given by Equation E.5.

$$\mathrm{Re} = \frac{\rho V d}{\mu}$$ **Equation E.5[45]**

where,

- ρ is the density of water (1.94 slugs/ft^3)
- V is the average velocity (ft/s)
- μ is the dynamic viscosity of water (2.36*10^{-5} lbs-s/ft^2 at 60 ºF.
- d is the pipe diameter in feet

Osborn Reynolds performed many experiments in the late 1880's finding that for Re values below 2,000 the flow exhibits laminar behavior, for Re values above 4,000 the flow is turbulent, and for Re values in between 2,000 and 4,000, the flow is in transition.[46]

If the flow is found to be laminar, the friction factor can be determined by Equation E.6, and if the flow regime is turbulent, f is calculated by the Colebrook-White equation shown as equation E.7.

$$f = \frac{64}{\mathrm{Re}}$$ **Equation E.6[47]**

$$\frac{1}{\sqrt{f}} = -2\log\left(\frac{e/d}{3.7} + \frac{2.51}{\mathrm{Re}\sqrt{f}}\right)$$ **Equation E.7[48]**

where,

- Re is the Reynolds number
- e is a roughness coefficient shown, which represents an average roughness height of abnormalities on the pipe wall; ranging from about 6*10^{-5} in for polyethylene to almost 0.35 in for riveted steel[49]
- d is the diameter of the pipe

[45] Crowe, p. 97
[46] Crowe, p. 97
[47] Crowe, p. 415
[48] Penche, p. 28
[49] Crowe, p. 418

Note that all units must be consistent. Also note that while the friction factor for laminar flow is fairly easily found by Equation E.6, if the flow is turbulent, Equation E.7 must be employed.

Head Loss in Bends

As a fluid flows through a bend there is a separation of flow, causing an increase in pressure on the outer wall and a decrease in pressure on the inner wall. Eddies develop in the flow in response to this pressure gradient, producing a head loss, which can be calculated by Equation E.8.

$$h_b = K_b \frac{V^2}{2g}$$ **Equation E.8**[50]

where,

- h_b is the head loss in the bend
- V is the average velocity in the pipe
- g is the acceleration of gravity
- K_b is a loss coefficient based on the radius of curvature of the pipe, r, and the pipe diameter, d, as shown in Figure E4.

[50] Crowe, p. 426

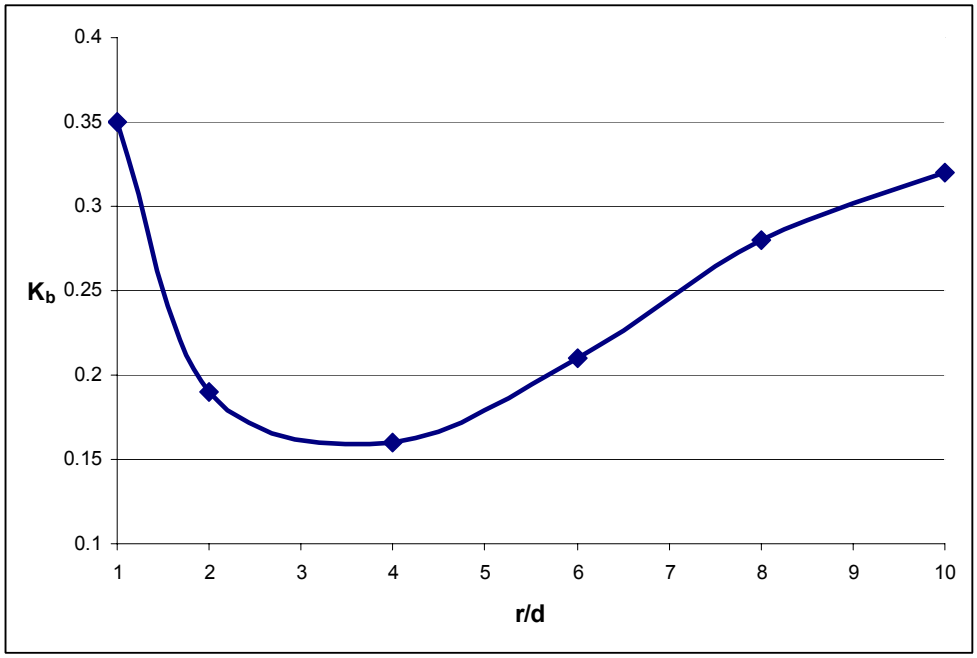

Figure E 4: Kb as a function of r/d for a 90 degree bend.[51]

As shown in Figure E4, K_b decreases until approximately r/d equals 4; then begins increasing again due to the fact that the elbow becomes significantly longer. It has been found that for seamless pipes, the loss in bends less than 90º is approximately proportional to the bend angle.[52] For this analysis it will be assumed that for any necessary bends that have to be made in the penstock to overcome obstacles, the elbows will have 4 to 1 ratio of radius of curvature to diameter with 22.5º pipe elbows as shown in Figure E5.

Figure E 5: 22.5º female pipe elbow.[53]

[51] Crowe, p. 429
[52] Penche, p. 39
[53] Plastic Pipe Fittings and Pipe

Head Loss in Valves

Valves are necessary in a micro-hydroelectric scheme to disconnect the turbine for periodic maintenance. Depending on the type of valve, there is a loss coefficient, K_v, associated with it shown in Figure E6. The corresponding head loss is obtained by multiplying K_v by the dynamic head as in Equations E.1 and E.8.

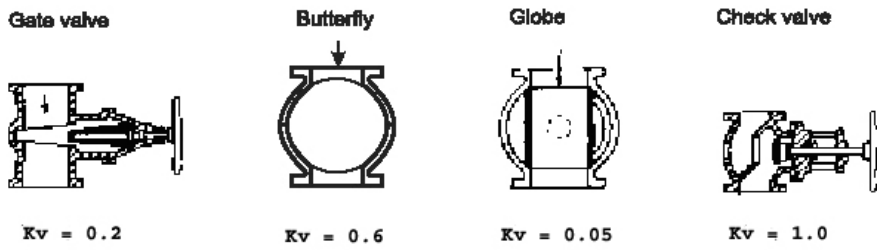

Figure E 6: Different values of Kv for 4 valve types.[54]

[54] Penche, p. 40

Appendix F: Electrical Diagrams

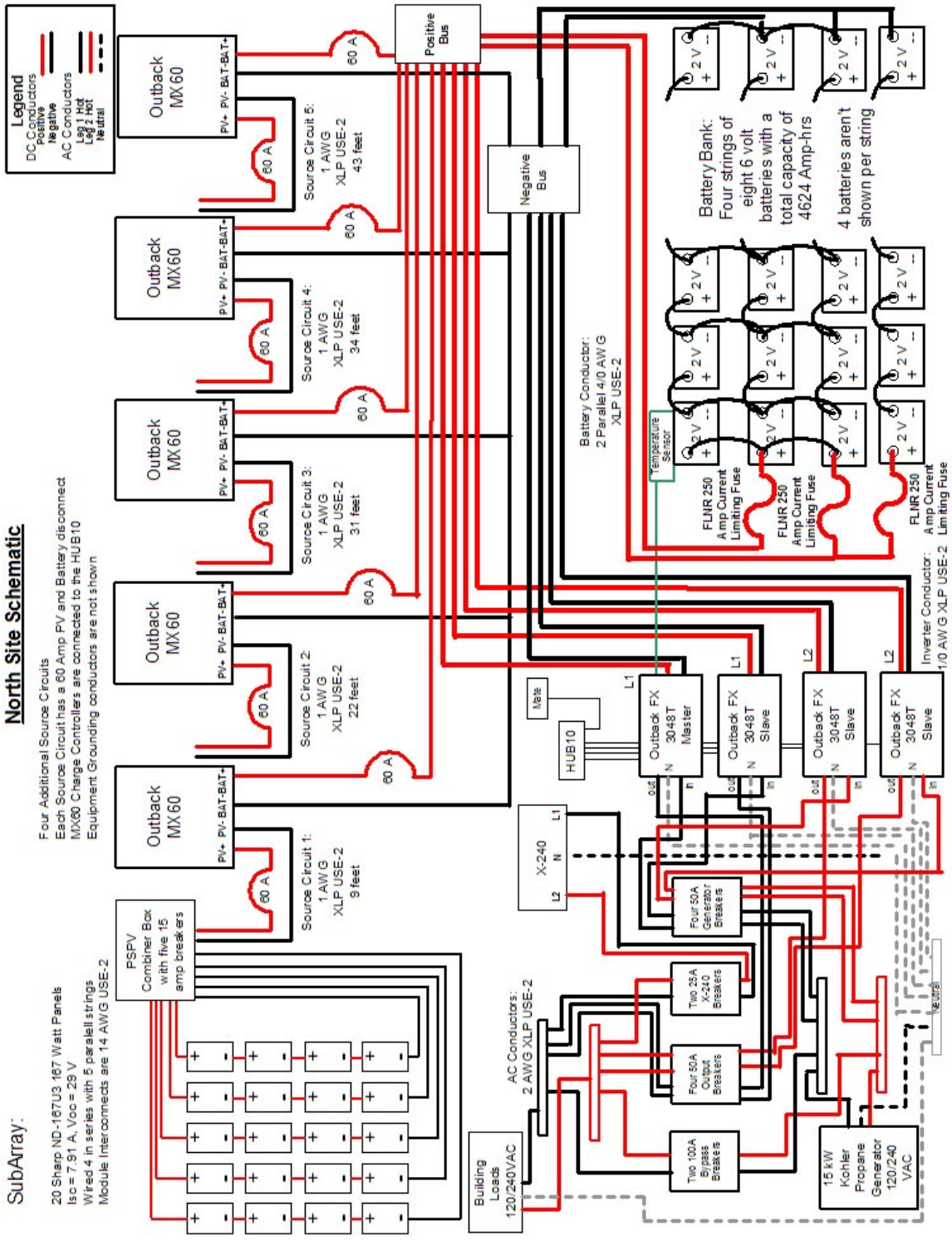

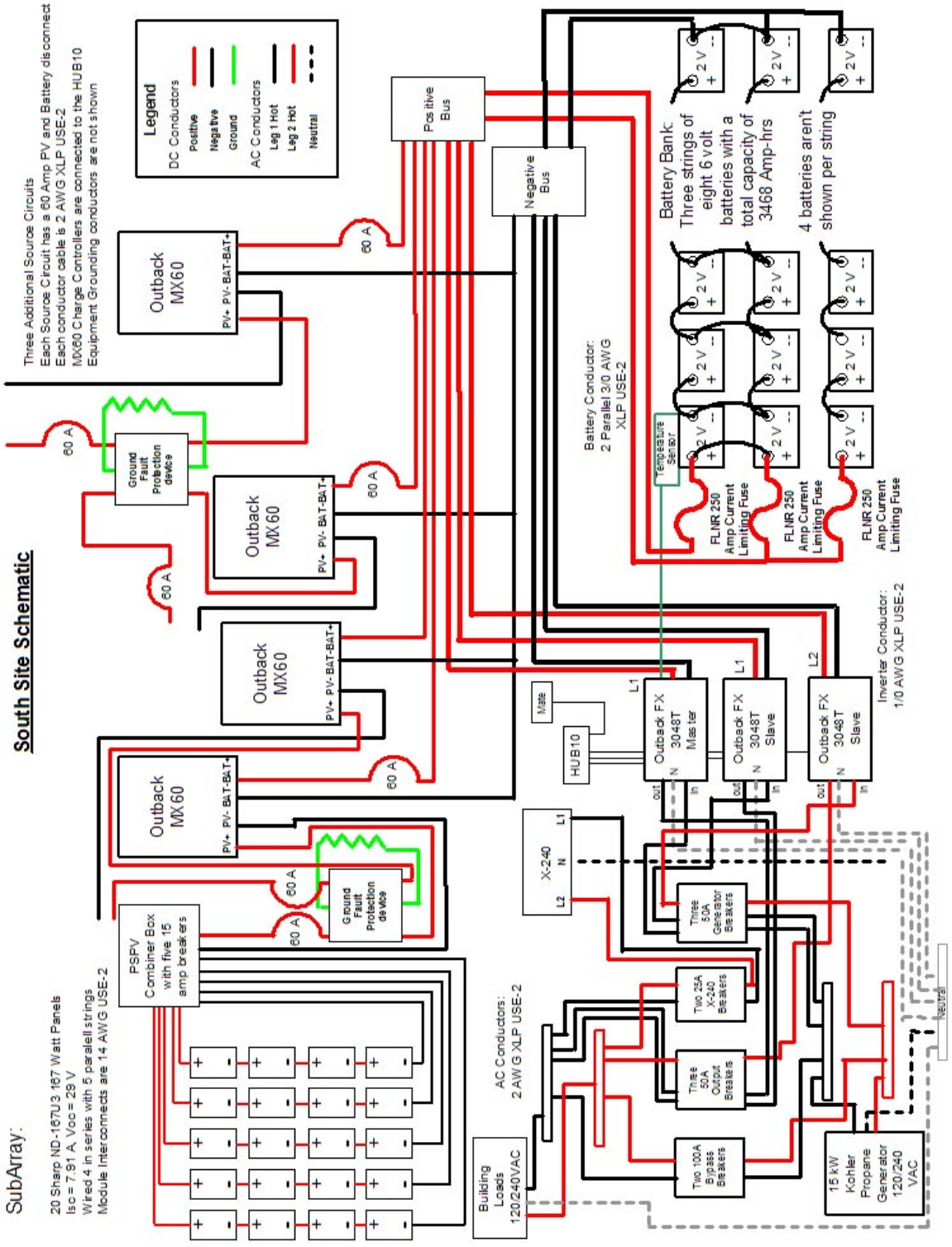
South Site Schematic
SubArray:
20 Sharp ND-167U3 167 Watt Panels
Isc = 7.91 A, Voc = 29 V
Wired 4 in series with 5 parallell strings
Module Interconnects are 14 AWG USE-2
PSPV Combiner Box with five 15 amp breakers
Ground Fault Protection device
Outback MX60
PV+ PV- BAT-BAT+
60 A
Three Additional Source Circuits
Each Source Circuit has a 60 Amp PV and Battery disconnect
Each conductor cable is 2 AWG XLP USE-2
MX60 Charge Controllers are connected to the HUB10
Equipment Grounding conductors are not shown
Legend
DC Conductors
Positive
Negative
Ground
AC Conductors
Leg 1 Hot
Leg 2 hot
Neutral
Positive Bus
Negative Bus
Battery Conductor:
2 Parallel 3/0 AWG
XLP USE-2
Battery Bank:
Three strings of eight 6 volt batteries with a total capacity of 3468 Amp-hrs
4 batteries aren't shown per string
2 V
Temperature Sensor
FLNR 250 Amp Current Limiting Fuse
Inverter Conductor:
1/0 AWG XLP USE-2
Mate
HUB10
Outback FX 3048T Master
Outback FX 3048T Slave
L1
L2
N
out
in
X-240
Three 50A Generator Breakers
Two 25A X-240 Breakers
Three 50A Output Breakers
Two 100A Bypass Breakers
AC Conductors:
2 AWG XLP USE-2
Building Loads 120/240VAC
15 kW Kohler Propane Generator 120/240 VAC
Neutral

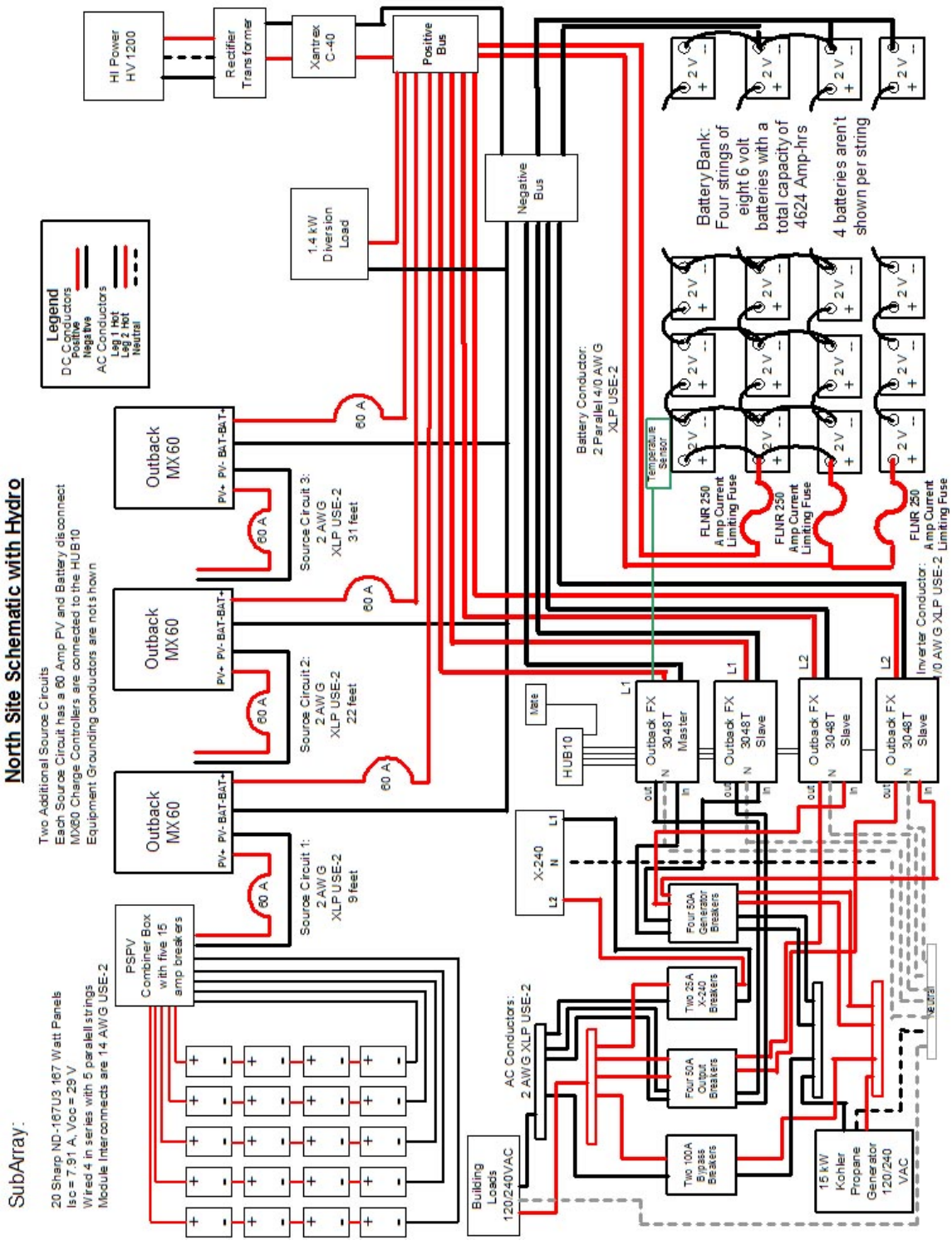
North Site Schematic with Hydro
SubArray:
20 Sharp ND-167U3 167 Watt Panels
Isc = 7.91 A, Voc = 29 V
Wired 4 in series with 5 parallell strings
Module Interconnects are 14 AWG USE-2
PSPV Combiner Box with five 15 amp breakers
Two Additional Source Circuits
Each Source Circuit has a 60 Amp PV and Battery disconnect
MX60 Charge Controllers are connected to the HUB10
Equipment Grounding conductors are not shown
Source Circuit 1: 2 AWG XLP USE-2 9 feet
Source Circuit 2: 2 AWG XLP USE-2 22 feet
Source Circuit 3: 2 AWG XLP USE-2 31 feet
Outback MX60
PV+ PV- BAT- BAT+
60 A
Legend
DC Conductors
Positive
Negative
AC Conductors
Leg 1 Hot
Leg 2 Hot
Neutral
HI Power HV 1200
Rectifier Transformer
Xantrex C-40
Positive Bus
Negative Bus
1.4 kW Diversion Load
Battery Conductor: 2 Parallel 4/0 AWG XLP USE-2
Temperature Sensor
Battery Bank: Four strings of eight 6 volt batteries with a total capacity of 4624 Amp-hrs
4 batteries aren't shown per string
2 V
FLNR 250 Amp Current Limiting Fuse
Inverter Conductor: 4/0 AWG XLP USE-2
Mate
HUB10
Outback FX 3048T Master
Outback FX 3048T Slave
L1
L2
X-240
Four 50A Generator Breakers
Two 25A X-240 Breakers
Four 50A Output Breakers
Two 100A Bypass Breakers
AC Conductors: 2 AWG XLP USE-2
Building Loads 120/240VAC
15 kW Kohler Propane Generator 120/240 VAC
Neutral

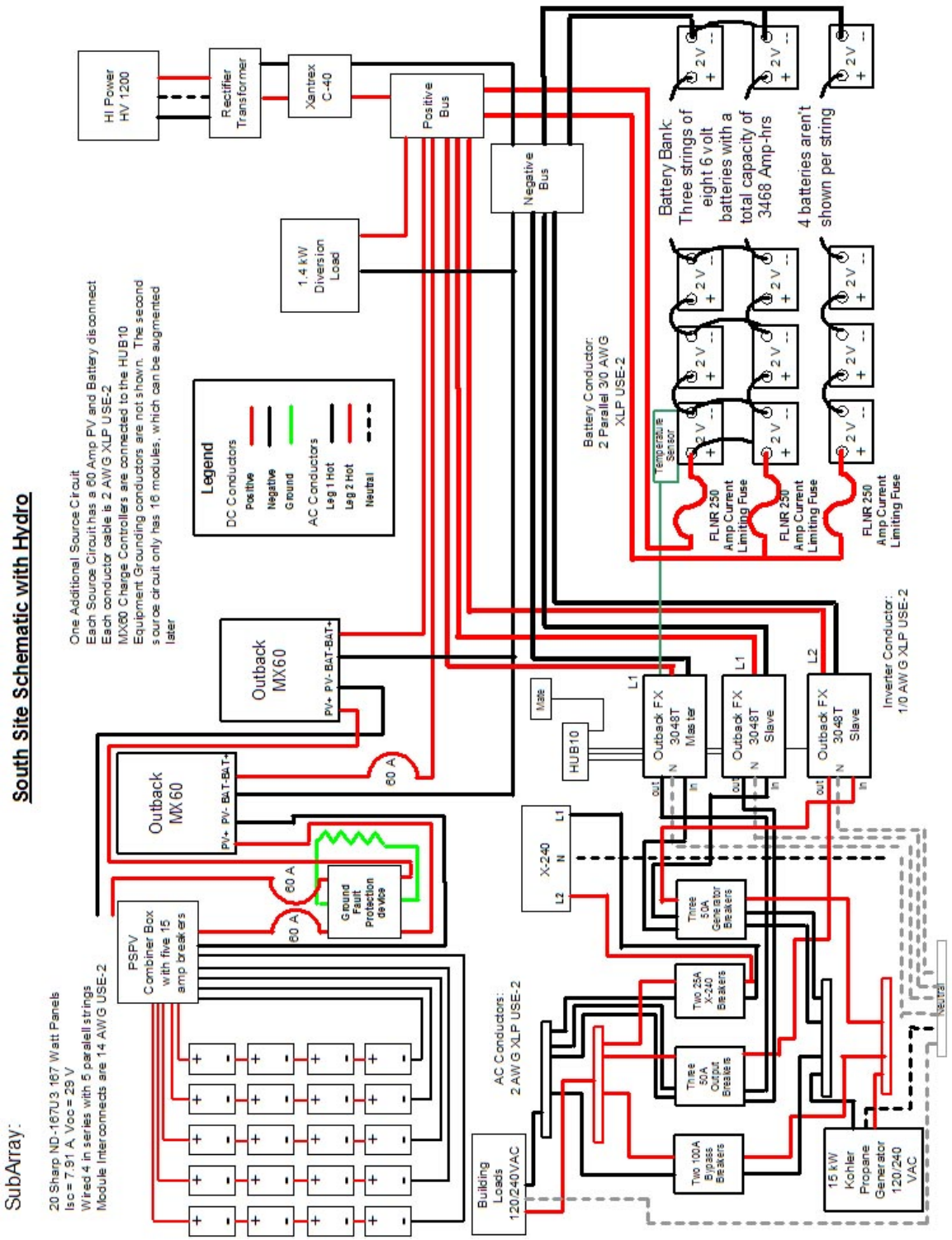
South Site Schematic with Hydro
SubArray:
20 Sharp ND-167U3 167 Watt Panels
Isc = 7.91 A, Voc = 29 V
Wired 4 in series with 5 parallell strings
Module Interconnects are 14 AWG USE-2
PSPV Combiner Box with five 15 amp breakers
Ground Fault Protection device
60 A
60 A
60 A
Outback MX60
PV+ PV- BAT-BAT+
Outback MX60
PV+ PV- BAT-BAT+
One Additional Source Circuit
Each Source Circuit has a 60 Amp PV and Battery disconnect
Each conductor cable is 2 AWG XLP USE-2
MX60 Charge Controllers are connected to the HUB10
Equipment Grounding conductors are not shown. The second source circuit only has 10 modules, which can be augmented later
Legend
DC Conductors
Positive
Negative
Ground
AC Conductors
Leg 1 Hot
Leg 2 Hot
Neutral
HI Power HV 1200
Rectifier Transformer
Xantrex C-40
Positive Bus
Negative Bus
1.4 kW Diversion Load
Battery Conductor: 2 Parallel 3/0 AWG XLP USE-2
Battery Bank: Three strings of eight 6 volt batteries with a total capacity of 3468 Amp-hrs
4 batteries aren't shown per string
2 V
Temperature Sensor
FLNR 250 Amp Current Limiting Fuse
FLNR 250 Amp Current Limiting Fuse
FLNR 250 Amp Current Limiting Fuse
Mate
HUB10
Outback FX 3048T Master
Outback FX 3048T Slave
Outback FX 3048T Slave
L1
L1
L2
Inverter Conductor: 1/0 AWG XLP USE-2
X-240
L1
N
L2
Three 50A Generator Breakers
Two 25A X-240 Breakers
Three 50A Output Breakers
Two 100A Bypass Breakers
AC Conductors: 2 AWG XLP USE-2
Building Loads 120/240VAC
15 kW Kohler Propane Generator 120/240 VAC
Neutral

Appendix G: Parts Lists

Shown below are the parts, conductors, and breaker lists for the Kipahulu system without hydro.

Table G 1: Parts List North without Hydro

Component	Quantity	Cost	Total Cost
Sharp ND-167U3	92	$ 576.69	$53,055.00
Outback MX 60 Controller	5	$ 431.55	$2,157.80
Outback FX3048T	4	$ 1,559.30	$6,237.20
Surrette 6-CS-25PS	32	$ 631.15	$20,197.00
Kohler 15RYG	1	$10,490.00	$10,490.00
FXA Adapter Kit (FX-DCC, FX-DCA, FX-ACA)	1	$ 85.78	$85.78
FX Turbo Kit	4	$ 85.78	$343.12
Remote Temperature Sensor	1	$ 19.28	$19.28
X-240 Auto Transformer	1	$ 192.84	$192.84
X-240 Fan Kit	1	$ 19.28	$19.28
MATE	1	$ 196.16	$196.16
HUB-10	1	$ 249.36	$249.36
CATV-6	1	$ 5.32	$5.32
Terminal bus Bars	3	$ 12.63	$37.89
Ground Bus bar	1	$ 9.63	$9.63
Outback Junction Box	5	$ 92.43	$462.15
Unirac Solar Mount PV Array Rack High Profile	92	$ -	$11,949.00
Installation Costs	0	$ -	$10,608.00
Totals			$116,314.81

Table G 2: Conductor List North without Hydro

Conductor	Length (ft)	Cost ($/ft)	Total Cost
XLP USE-2 Anixter 1 AWG 3BE-0101	69.638	$1.75	$121.87
XLP USE-2 Anixter 1 AWG 3BE-0101	87.75	$1.75	$153.56
XLP USE-2 Anixter 1 AWG 3BE-0101	44.183	$1.75	$77.32
XLP USE-2 Anixter 1 AWG 3BE-0101	62.294	$1.75	$109.02
XLP USE-2 Anixter 1 AWG 3BE-0101	18.728	$1.75	$32.77
XLP USE-2 Anixter 750 3BE-7501	48.667	$12.50	$608.33
XLP USE-2 Anixter 1/0 AWG 3BE-1011	12	$2.25	$27.00
XLP USE-2 Anixter 2 AWG 3BE-0201	12	$1.35	$16.20
XLP USE-2 Anixter 2 AWG 3BE-0201	12	$1.35	$16.20
			$1,162.27

Table G 3: Breaker List North without Hydro

Breaker	Quantity	Cost	Total Cost
OBPV-15	23	$7.98	$183.54
OBDC-60	2	$19.28	$38.56
OBDC-60	2	$19.28	$38.56
OBDC-60	2	$19.28	$38.56
OBDC-60	2	$19.28	$38.56
OBDC-60	2	$19.28	$38.56
Littlefuse FLNR300	4	$25.81	$103.24
Littlefuse FLNR150	1	$13.00	$13.00
Square-D Homeline 100	1	$112.00	$112.00
Square-D Homeline 100	1	$112.00	$112.00
Totals			$716.58

Table G 4: Parts List South without Hydro

Component	Quantity	Cost	Total Cost
Sharp ND-167U3	68	$576.69	$39,215.00
Outback MX 60 Controller	4	$431.55	$1,726.20
Outback FX3048T	3	$1,559.30	$4,677.90
Surrette 6-CS-25PS	24	$631.15	$15,148.00
Kohler 15RYG	1	$8,000.00	$8,000.00
FXA Adapter Kit (FX-DCC, FX-DCA, FX-ACA)	1	$85.78	$85.78
FX Turbo Kit	3	$85.78	$257.34
Remote Temperature Sensor	1	$19.28	$19.28
X-240 Auto Transformer	1	$192.84	$192.84
X-240 Fan Kit	1	$19.28	$19.28
MATE	1	$196.16	$196.16
Terminal bus Bars	3	$ 12.63	$37.89
Ground Bus bar	1	$ 9.63	$9.63
OBDC-GFP/2 Ground fault protection system	2	$85.78	$171.56
HUB-10	1	$249.36	$249.36
CATV-6	1	$5.32	$5.32
Outback Junction Box	4	$92.43	$369.72
Unirac Solar Mount PV Array Rack Flush Mounted	68	$0.00	$4,479.00
Structure to house power conditioning equipment and mount modules	1	$75,000.00	$75,000.00
Installation Costs	0	$0.00	$15,006.00
Totals			$164,866.26

Table G 5: Conductor List South without Hydro

Conductor	Length (ft)	Cost ($/ft)	Total Cost
XLP USE-2 Anixter 1	85.35	$1.75	$149.36

AWG 3BE-0101			
XLP USE-2 Anixter 1 AWG 3BE-0101	63.567	$1.75	$111.24
XLP USE-2 Anixter 1 AWG 3BE-0101	41.783	$1.75	$73.12
XLP USE-2 Anixter 1 AWG 3BE-0101	20	$1.75	$35.00
XLP USE-2 Anixter 500 3BE-5001	36.5	$9.50	$346.75
XLP USE-2 Anixter 1/0 AWG 3BE-1011	12	$27.00	$324.00
XLP USE-2 Anixter 2 AWG 3BE-0201	12	$16.20	$194.40
XLP USE-2 Anixter 6 AWG 3BE-0601	12	$7.44	$89.28
Totals			$1,039.47

Table G 6: Breaker List South without Hydro

Breaker	Quantity	Cost	Total Cost
OBPV-15	17	$7.98	$135.66
OBDC-60	2	$19.28	$38.56
OBDC-60	2	$19.28	$38.56
OBDC-60	2	$19.28	$38.56
OBDC-60	2	$19.28	$38.56
Square-D Homeline 40	4	$20.00	$80.00
Square-D Homeline 60	1	$13.00	$13.00
Square-D Homeline 100	1	$112.00	$112.00
Square-D Homeline 50	1	$40.30	$40.30
Totals			$382.90

Shown below are the parts, conductors, and breaker lists for the Kipahulu system without hydro.

Table G 7: Parts List North with Hydro

Component	Quantity	Cost	Total Cost
Sharp ND-167U3	60	$576.69	$34,601.00
Outback MX 60 Controller	3	$431.55	$1,294.70
Outback FX3048T	4	$1,559.30	$6,237.20
Surrette 6-CS-25PS	32	$631.15	$20,197.00
Kohler 15RYG	1	$10,490.00	$10,490.00
FXA Adapter Kit (FX-DCC, FX-DCA, FX-ACA)	1	$85.78	$85.78
FX Turbo Kit	4	$85.78	$343.12
Remote Temperature Sensor	1	$19.28	$19.28
X-240 Auto Transformer	1	$192.84	$192.84
X-240 Fan Kit	1	$19.28	$19.28
MATE	1	$196.16	$196.16
Terminal bus Bars	3	12.63	37.89
Ground Bus bar	1	9.63	9.63
HUB-10	1	$249.36	$249.36
CATV-6	1	$5.32	$5.32
Outback Junction Box	3	$92.43	$277.29
Unirac Solar Mount PV Array Rack High Profile	60	$0.00	$6,465.00
HV-1200 Turbine with necessary components	1	$0.00	$14,617.00
Installation Costs	0	$0.00	$9,575.20
Totals			$104,913.05

Table G 8: Conductor List North with Hydro

Conductor	Length (ft)	Cost ($/ft)	Total Cost
XLP USE-2 Anixter 1 AWG 3BE-0101	44.183	$1.75	$77.32
XLP USE-2 Anixter 1 AWG 3BE-0101	62.294	$1.75	$109.02
XLP USE-2 Anixter 1 AWG 3BE-0101	18.728	$1.75	$32.77
XLP USE-2 Anixter 3/0 AWG 3BE-3031	48.667	$3.75	$182.50
XLP USE-2 Anixter 1/0 AWG 3BE-1011	12	$2.25	$27.00
XLP USE-2 Anixter 2 AWG 3BE-0201	12	$1.35	$16.20
XLP USE-2 Anixter 2 AWG 3BE-0201	12	$1.35	$16.20
Totals			$461.01

Table G 9: Breaker List North with Hydro

Breaker	Quantity	Cost	Total Cost
OBPV-15	15	$7.98	$119.70

OBDC-60	2	$19.28	$38.56
OBDC-60	2	$19.28	$38.56
OBDC-60	2	$19.28	$38.56
Littlefuse FLNR200	4	$18.42	$73.68
Littlefuse FLNR150	1	$13.00	$13.00
Littlefuse FLNR90	1	$112.00	$112.00
Littlefuse FLNR90	1	$112.00	$112.00
Totals			$546.06

Table G 10: Parts List South with Hydro

Component	Quantity	Cost	Total Cost
Sharp ND-167U3	36	$576.69	$20,761.00
Outback MX 60 Controller	2	$431.55	$863.10
Outback FX3048T	3	$1,559.30	$4,677.90
Surrette 6-CS-25PS	24	$631.15	$15,148.00
Kohler 15RYG	1	$8,000.00	$8,000.00
FXA Adapter Kit (FX-DCC, FX-DCA, FX-ACA)	1	$85.78	$85.78
FX Turbo Kit	3	$85.78	$257.34
Remote Temperature Sensor	1	$19.28	$19.28
X-240 Auto Transformer	1	$192.84	$192.84
X-240 Fan Kit	1	$19.28	$19.28
MATE	1	$196.16	$196.16
HUB-10	1	$249.36	$249.36
CATV-6	1	$5.32	$5.32
Terminal bus Bars	3	$ 12.63	$37.89
Ground Bus bar	1	$ 9.63	$9.63
OBDC-GFP/2 Ground fault protection system	1	$85.78	$85.78
Outback Junction Box	2	$92.43	$184.86
Unirac Solar Mount PV Array Rack Flush Mounted	36	$0.00	$2,371.00
Structure to house power conditioning equipment and mount modules	1	$75,000.00	$75,000.00
HV-1200 Turbine with necessary components	1	$0.00	$10,163.00
Installation Costs	0	$0.00	$13,855.00
Totals			$152,182.52

Table G 11: Conductor List South with Hydro

Conductor	Length (ft)	Cost ($/ft)	Total Cost
XLP USE-2 Anixter 1	63.567	$1.75	$111.24

AWG 3BE-0101			
XLP USE-2 Anixter 1 AWG 3BE-0101	20	$1.75	$35.00
XLP USE-2 Anixter 3/0 AWG 3BE-3031	36.5	$3.75	$136.88
XLP USE-2 Anixter 1/0 AWG 3BE-1011	12	$27.00	$324.00
XLP USE-2 Anixter 2 AWG 3BE-0201	12	$16.20	$194.40
XLP USE-2 Anixter 6 AWG 3BE-0601	12	$7.44	$89.28
Totals			$890.80

Table G 12: Breaker List South with Hydro

Breaker	Quantity	Cost	Total Cost
OBPV-15	9	$7.98	$71.82
OBDC-60	2	$19.28	$38.56
OBDC-60	2	$19.28	$38.56
Littlefuse FLNR125	4	$10.00	$40.00
Littlefuse FLNR150	1	$13.00	$13.00
Square-D Homeline 100	1	$112.00	$112.00
Square-D Homeline 50	1	$40.30	$40.30
			$354.24